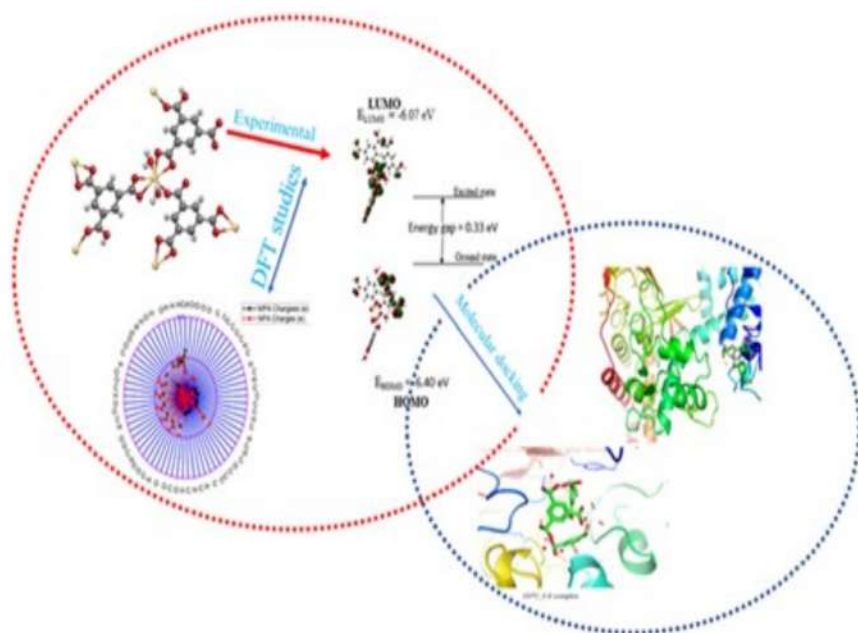


Eclética Química Journal

Volume 47 • number 4 • year 2022



Antimicrobial studies

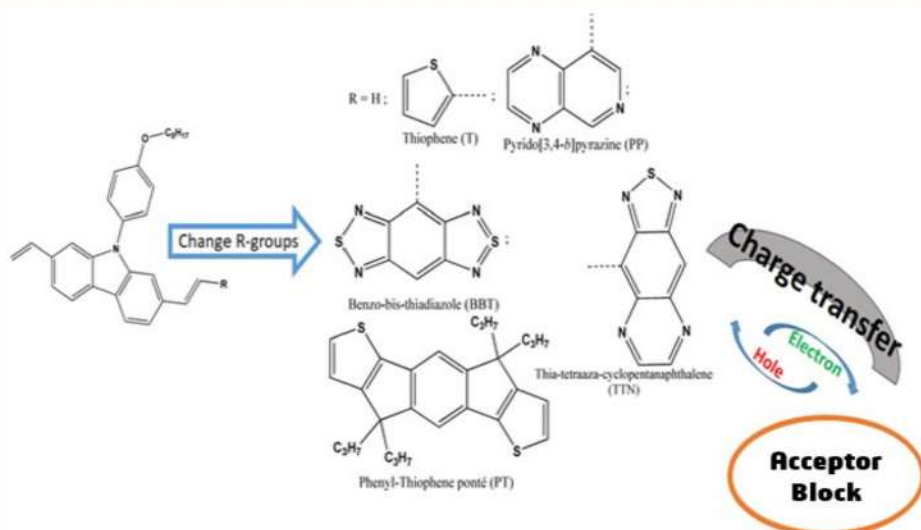
Experimental, DFT, molecular docking and *in silico* ADMET studies of cadmium-benzenetricarboxylates

Antioxidant activity

Secondary metabolites and pharmacological potential of *Thuja orientalis* and *T. occidentalis*: A short review

Phytochemicals

Biological evaluation of selected metronidazole derivatives as anti-nitroreductase via *in silico* approach



Computational study

Structural effect on the charge transfer and on the internal reorganization energy: Computational studies



UNIVERSIDADE ESTADUAL PAULISTA

Reitor

Pasqual Barretti

Vice-Reitora

Maysa Furlan

Pró-Reitora de Graduação

Celia Maria Giacheti

Pró-Reitora de Pós-Graduação

Maria Valnice Boldrin

Pró-Reitor de Pesquisa

Edson Cocchieri Botelho

Pró-Reitor de Extensão Universitária e Cultura

Raul Borges Guimarães

Pró-Reitor de Planejamento Estratégico e Gestão

Estevão Tomomitsu Kimpara



INSTITUTO DE QUÍMICA

Diretor

Sidney José Lima Ribeiro

Vice-Diretora

Denise Bevilaqua

Editorial Team

Editor-in-Chief

Prof. Assis Vicente Benedetti, São Paulo State University, Institute of Chemistry, Araraquara, Brazil

Associated Editors

Prof. Antonio Eduardo Mauro, São Paulo State University, Institute of Chemistry, Araraquara, Brazil

Prof. Horacio Heinzen, University of the Republic, Faculty of Chemistry, Montevideo, Uruguay

Prof. Marcos Carlos de Mattos, Federal University of Ceará, Center of Sciences, Fortaleza, Brazil

Prof. Maria Célia Bertolini, São Paulo State University, Institute of Chemistry, Araraquara, Brazil

Prof. Patrícia Hatsue Suegama, Federal University of Grande Dourados, Faculty of Exact and Technological Sciences, Dourados, Brazil

Prof. Paulo Clairmont Feitosa Lima Gomes, São Paulo State University, Institute of Chemistry, Araraquara, Brazil

Editorial Advisory Board

Prof. Adalgisa Rodrigues de Andrade, University of São Paulo, Faculty of Philosophy, Sciences and Literature, Ribeirão Preto, Brazil

Prof. Bayardo Baptista Torres, University of São Paulo, Institute of Chemistry, São Paulo, Brazil

Prof. Enric Brillas, University of Barcelona, Faculty of Chemistry, Barcelona, Spain

Prof. Ivano Gerardt Rolf Gutz, University of São Paulo, Institute of Chemistry, São Paulo, Brazil

Prof. Jairton Dupont, Federal University of Rio Grande do Sul, Institute of Chemistry, Porto Alegre, Brazil

Prof. José Antônio Maia Rodrigues, University of Porto, Faculty of Sciences, Porto, Portugal

Prof. Lauro Kubota, University of Campinas, Institute of Chemistry, São Paulo, Brazil

Prof. Marília Oliveira Fonseca Goulart, Federal University of Alagoas, Institute of Chemistry and Biotechnology, Maceió, Brazil

Prof. Massuo Jorge Kato, University of São Paulo, Institute of Chemistry, São Paulo, Brazil

Prof. Verónica Cortés de Zea Bermudez, University of Trás-os-Montes and Alto Douro, School of Life and Environmental Sciences, Vila Real, Portugal

EDITORIAL PRODUCTION

Ctrl K Produção Editorial – Araraquara, Brazil

digite@ctrlk.com.br

Editorial

It is a pleasure to announce the last issue of this 2022 year. Opens this issue a brief review showing recent phytochemical studies involving *T. orientalis* and *T. occidentalis*, as well as 40 constituents isolated from these species. Plants from Thuja genus in traditional medicine are used to treat cough, skin allergies, and asthma, and in Brazil are also used in the ornamentation of urban areas. Different parts of these plants displayed insecticidal, antitumor, and antioxidant activities, e.g., the essential oil of the leaves are constituted by monoterpenes and sesquiterpenes, with the flavonoids being the main substances found that have relevant biological activities. Computational chemistry is routinely used for the qualitative and quantitative evaluation of substances in almost every field of chemistry as in drug discovery/design activities. These tools were applied to study the effect of several substituents in the 1-(2-hydroxyethyl)-2-methyl-5-nitroimidazole, a powerful antibacterial and antiparasitic used alongside other drugs against *Helicobacter pylori* infection and on the interactions with the target nitroreductase RdxA protein. In the sequence, X-ray single-crystal crystallography was used to solve the structure of a coordination polymer having the formula $[\text{Cd}(\text{BTC})(\text{H}_2\text{O})_2]_n$. Furthermore, the complex's stability and overall reactivity were theoretically examined. The electron distribution in the complex's HOMO is concentrated in a small area, with no electrons distributed over the metallic center. Consequently, the electrons in the complex's LUMO were dispersed equally. The ADMET studies showed that the examined complex has important biological uses, notably for the treatment of microbial diseases. Closes this issue a theoretical study about the effects of addition of thiophene, bridged phenyl-thiophene, thia-tetra-azacyclopenta-naphthalene, benzo-bis-thiadiazole and pyrido(3,4-b)pyrazine to 9-(4-octyloxyphenyl)-2,7-divinylcabazole on the internal reorganization energies, electronic affinity and ionization potential. These compounds were characterized by their charge exchange potentials, donor-acceptor, which can be applied in energy conversion devices such as photovoltaic cells.

The editorial team of Eclética Química would like to gently tanks the enormous effort of all authors, reviewers and collaborators that made possible to conclude this year with highly promise results.

Assis Vicente Benedetti
Editor-in-Chief of EQJ

Citation databases: Eclética Quim. J. is indexed



*Click on the images to follow the links.

EBSCO has no link available. The address is for subscribers only.

INSTRUCTIONS FOR AUTHORS

BEFORE YOU SUBMIT

1. Check [Eclét. Quim. J.'s focus and scope](#)

Eclética Química Journal is a peer-reviewed quarterly publication of the Institute of Chemistry of São Paulo State University (UNESP). It publishes original researches as articles, reviews and short reviews in **all areas of Chemistry**.

2. Types of papers

- a. Original articles
- b. Reviews
- c. Short reviews
- d. Communications
- e. Technical notes
- f. Articles in education in chemistry and chemistry-related areas

Manuscripts submitted for publication as full articles and communications must contain original and unpublished results and should not have been submitted elsewhere either partially or whole.

a. Original articles

The manuscript must be organized in sections as follows:

1. Introduction
 2. Experimental
 3. Results and Discussion
 4. Conclusions
- References

Sections titles must be written in bold and sequentially numbered; only the first letter should be in uppercase letter. Subsections, numbered as exemplified, should be written in normal and italic letters; only the first letter should be in uppercase letter.

Example:

1. Introduction

1.1 History

2. Experimental

2.1 Surface characterization

2.1.1 Morphological analysis

b. Reviews

Review articles should be original and present state-of-the-art overviews in a coherent and concise form covering the

most relevant aspects of the topic that is being revised and indicate the likely future directions of the field. Therefore, before beginning the preparation of a Review manuscript, send a letter (one page maximum) to the Editor with the subject of interest and the main topics that would be covered in the Review manuscript. The Editor will communicate his decision in two weeks. Receiving this type of manuscript does not imply acceptance to be published in **Eclét. Quím. J.** It will be peer-reviewed.

c. Short reviews

Short reviews should present an overview of the state-of-the-art in a specific topic within the scope of the Journal and limited to 5,000 words. Consider a table or image as corresponding to 100 words. Before beginning the preparation of a Short Review manuscript, send a letter (one page maximum) to the Editor with the subject of interest and the main topics that would be covered in the Short Review manuscript.

d. Communications

Communications should cover relevant scientific results and are limited to 1,500 words or three pages of the Journal, not including the title, authors' names, figures, tables and references. However, Communications suggesting fragmentation of complete contributions are strongly discouraged by Editors.

e. Technical notes

Descriptions of methods, techniques, equipment or accessories developed in the authors' laboratory, as long as they present chemical content of interest. They should follow the usual form of presentation, according to the peculiarities of each work. They should have a maximum of 25 pages, including figures, tables, diagrams, etc.

f. Articles in education in chemistry and chemistry-correlated areas

Research manuscript related to undergraduate teaching in Chemistry and innovative experiences in undergraduate and graduate education. They should have a maximum of 25 pages, including figures, tables, diagrams, and other elements.

3. Special issues

Special issues with complete articles dedicated to Symposia and Congresses and to special themes or in honor of scientists with relevant contributions in Chemistry and correlate areas can be published by **Eclét. Quím. J.** under the condition that a previous agreement with Editors is established. All the guides of the journal must be followed by the authors.

4. Approval

Ensure all authors have seen and approved the final version of the article prior to submission. All authors must also approve the journal you are submitting to.

ETHICAL GUIDELINES

Before starting the submission process, please be sure that **all ethical aspects mentioned below were followed.** Violation of these ethical aspects may preclude authors from submitting or publishing articles in **Eclét. Quím. J.**

a. Coauthorship: The corresponding author is responsible for listing as coauthors only researchers who have really taken part in the work, for informing them about the entire manuscript content and for obtaining their permission to submit and publish it.

b. Nonauthors: Explicit permission of a nonauthor who has collaborated with personal communication or discussion to the manuscript being submitted to **Eclet. Quím. J.** must be obtained before being cited.

c. Unbiased research: Authors are responsible for carefully searching for all the scientific work relevant to their reasoning irrespective of whether they agree or not with the presented information.

d. Citation: Authors are responsible for correctly citing and crediting all data taken from other sources. This requirement is not necessary only when the information is a result of the research presented in the manuscript being submitted to **Eclet. Chem. J.**

e. Direct quotations: The word-for-word reproduction of data or sentences as long as placed between quotation marks and correctly cited is not considered ethical deviation when indispensable for the discussion of a specific set of data or a hypothesis.

f. Do not cite: Master's Degree dissertations and PhD theses are not accepted; instead, you must cite the publications resulted from them.

g. Plagiarism: Plagiarism, self-plagiarism, and the suggestion of novelty when the material was already published are unaccepted by **Eclet. Quím. J.** Before reviewing a manuscript, the **Turnitin antiplagiarism software** will be used to detect any ethical deviation.

h. Simultaneous submissions of the same manuscript to more than one journal is considered an ethical deviation and is conflicted to the declaration has been done below by the authors.

i. Studies with humans or other animals: Before submitting manuscripts involving human beings, materials from human or animals, the authors need to confirm that the procedures established, respectively, by the institutional committee on human experimentation and Helsinki's declaration, and the recommendations of the animal care institutional committee were followed. Editors may request complementary information on ethical aspects.

COPYRIGHT NOTICE

The corresponding author transfers the copyright of the submitted manuscript and all its versions to **Eclet. Quím. J.**, after having the consent of all authors, which ceases if the manuscript is rejected or withdrawn during the review process.

When a published manuscript in **Eclet. Quím. J.** is also published in other Journal, it will be immediately withdrawn from **Eclet. Quím. J.** and the authors informed of the Editor decision.

Self-archive to institutional, thematic repositories or personal webpage is permitted just after publication. The articles published by **Eclet. Quím. J.** are licensed under the [Creative Commons Attribution 4.0 International License](#).

PUBLICATION CHARGES

Eclética Química Journal is supported by the Institute of Chemistry/UNESP and publication is free of charge for authors.

MANUSCRIPT PREPARATION

COVER LETTER

We provide a template to help you prepare your cover letter. To download it, click [here](#).

The cover letter **MUST** include:

1. Identification of authors

- a. The authors' full names (they must be written in full and complete, separated by comma)

João M. José	Incorrect
J. M. José	Incorrect
João Maria José	Correct!

- b. E-mail addresses and affiliations (**neither more nor less than two instances**) of all authors;
c. ORCID ID links;
d. A plus sign (+) indicating the corresponding author.

Example:

Author Full Name¹⁺, Author Full Name²

1. University, Faculty or Institute, City, Country.
2. Company, Division or Sector or Laboratory, City, Country.

+ Author 1: address@mail.com, ORCID: <https://orcid.org/xxxx-xxxx-xxxx-xxxx>

Author 2: address@mail.com, ORCID: <https://orcid.org/xxxx-xxxx-xxxx-xxxx>

2. Authors' contribution

We request authors to include author contributions according to CRediT taxonomy standardized contribution descriptions. [CRediT \(Contributor Roles Taxonomy\)](#) is a high-level taxonomy, including 14 roles, that can be used to represent the roles typically played by contributors to scientific scholarly output. The roles describe each contributor's specific contribution to the scholarly output.

- a. Please, visit this link (<https://casrai.org/credit/>) to find out which role(s) the authors fit into;
- b. Do not modify the role names; do not write "all authors" in any role. Do not combine two or more roles in one line.**
- c. If there are any roles that no author has engaged in (such as funding in papers that were not funded), write "Not applicable" in front of the name of the role;
- d. Write the authors' names according to the [American Chemistry Society \(ACS\) citation style](#).

Example:

Conceptualization: Foster, J. C.; O'Reilly, R. K.

Data curation: Varlas, S.; Couturaud, B.; Coe, J.; O'Reilly, R. K.

Formal Analysis: Foster, J. C.; Varlas, S.

Funding acquisition: Not applicable.

Investigation: Foster, J. C.; O'Reilly, R. K.

Methodology: Coe, J.; O'Reilly, R. K.

Project administration: O'Reilly, R. K.

Resources: Coe, J.

Software: Not applicable.

Supervision: O'Reilly, R. K.

Validation: Varlas, S.; Couturaud, B.

Visualization: Foster, J. C.

Writing – original draft: Foster, J. C.; Varlas, S.; Couturaud, B.; Coe, J.; O'Reilly, R. K.

Writing – review & editing: Foster, J. C.; Varlas, S.; Couturaud, B.; Coe, J.; O'Reilly, R. K.

4. Indication of reviewers

We kindly ask the authors to suggest **five** suitable reviewers, providing full name, affiliation, and email.

5. Other information

- a. The authors must write one paragraph remarking the novelty and relevance of the work;
- b. The corresponding author must declare, on behalf of the other authors, that the manuscript being submitted is original and its content has not been published previously and is not under consideration for publication elsewhere;
- c. The authors must inform if there is any conflict of interest.

6. Acknowledgements and funding

Acknowledgements and funding information will be requested after the article is accepted for publication.

7. Data availability statement

A data availability statement informs the reader where the data associated with your published work is available, and under what conditions they can be accessed. Therefore, authors must inform if:

Data will be available upon request;

All dataset were generated or analyzed in the current study; or

Data sharing is not applicable.

MANUSCRIPT

We provide a template to help you prepare your manuscript. To download it, click [here](#).

1. General rules

Only manuscripts written in English will be accepted. British or American usage is acceptable, but they should not be mixed. Non-native English speakers are encouraged to have their manuscripts professionally revised before submission.

Manuscripts must be sent in editable files as *.doc, *.docx or *.odt. The text must be typed using font style Times New Roman and size 12. Space between lines should be 1.5 mm and paper size A4, top and bottom margins 2.5 cm, left and right margins 2.0 cm.

All contributions must include an **abstract** (170 words maximum), **three to five keywords** and a **graphical abstract** (8 cm wide × 8 cm high).

Supplementary information: all type of articles accepts supplementary information (SI) that aims at complementing the main text with material that, for any reason, cannot be included in the article.

TITLE

The title should be concise, explanatory and represent the content of the work. The title must have only the first letter of the sentence in uppercase. The following are not allowed: acronyms, abbreviations, geographical location of the research, en or em dashes (which must be replaced by a colon). Titles do not have full point.

ABSTRACT

Abstract is the summary of the article. The abstract must be written as a running text not as structured topics, but its content should present background, objectives, methods, results, and conclusion. It cannot contain citations. The text should be written in a single paragraph with a **maximum of 170 words**.

KEYWORDS

Keywords are intended to make it easier for readers to find the content of your text. As fundamental tools for database indexing, they act as a gateway to the text. The correct selection of keywords significantly increases the chances that a document will be found by researchers on the topic, and consequently helps to promote the visibility of an article within a myriad of publications.

FIGURES, TABLES AND EQUATIONS

Figures, tables and equations must be written with initial capital letter followed by their respective number and period, in bold, without adding zero “**Table 1**”, preceding an explanatory title. Tables, Figures and Equations should appear after the first citation and should be numbered according to the ascending order of appearance in the text (1, 2, 3...).

Figures, tables, schemes and photographs already published by the same or different authors in other publications may be reproduced in manuscripts of **Eclet. Quim. J.** only with permission from the editor house that holds the copyright.

Nomenclature, abbreviations, and symbols should follow IUPAC recommendations.

DATA AVAILABILITY STATEMENT

The data availability statement informs the reader where the data associated with your work is available, and under what conditions they can be accessed. They also include links (where applicable) to the data set.

- The data are available in a data repository (cite repository and the DOI of the deposited data);
- The data will be available upon request;
- All data sets were generated or analyzed in the current study;
- Data sharing is not applicable (in cases where no data sets have been generated or analyzed during the current study, it should be declared).

GRAPHICAL ABSTRACT

The graphical abstract must summarize the manuscript in an interesting way to catch the attention of the readers. As already stated, it must be designed with 8 cm wide × 8 cm high, and a 900-dpi resolution is mandatory for this journal. It must be submitted as *.jpg, *.jpeg, *.tif or *.ppt files as supplementary file.

We provide a template to help you prepare your GA. To download it, click [here](#).

SUPPLEMENTARY INFORMATION

When appropriate, important data to complement and a better comprehension of the article can be submitted as Supplementary File, which will be published online and will be made available as links in the original article. This might include additional figures, tables, text, equations, videos or other materials that are necessary to fully document the research contained in the paper or to facilitate the readers' ability to understand the work.

Supplementary material should be presented in appropriate .docx file for text, tables, figures and graphics. All supplementary figures, tables and videos should be referred in the manuscript body as "Table S1, S2...", "Fig. S1, S2..." and "Video S1, S2 ...".

At the end of the main text the authors must inform: This article has supplementary information.

Supplementary information will be located following the article with a different DOI number from that of the article, but easily related to it.

CITATION STYLE GUIDE

From 2021 on, the **Eclet. Quim. J.** will follow the [ACS citation style](#).

Indication of the sources is made by authorship and date. So, the reference list is organized alphabetically by author.

Each citation consists of two parts: the in-text citation, which provides brief identifying information within the text, and the reference list, a list of sources that provides full bibliographic information.

We encourage the citation of primary research over review articles, where appropriate, in order to give credit to those who first reported a finding. Find out more about our commitments to the principles of [San Francisco Declaration on Research Assessment \(DORA\)](#).

What information you must cite?

- a. Exact wording taken from any source, including freely available websites;
- b. Paraphrases of passages;
- c. Summaries of another person's work;
- d. Indebtedness to another person for an idea;
- e. Use of another researchers' work;
- f. Use of your own previous work.

You do not need to cite **common knowledge**.

Example:

Water is a tasteless and odorless liquid at room temperature (common knowledge, no citation needed)

In-text citations

You can choose to cite your references within or at the end of the phrase, as showed below.

Within the cited information:

One author: Finnegan states that the primary structure of this enzyme has also been determined (2004).

Two authors: Finnegan and Roman state that the structure of this enzyme has also been determined (2004).

Three or more authors: Finnegan *et al.* state that the structure of this enzyme has also been determined (2004).

At the end of the cited information:

One author: The primary structure of this enzyme has also been determined (Finnegan, 2004).

Two authors: The primary structure of this enzyme has also been determined (Finnegan and Roman, 2004).

Three or more authors: The primary structure of this enzyme has also been determined (Finnegan *et al.*, 2004).

If you need to cite more than one reference in the same brackets, separate them with semicolon and write them in alphabetic order:

The primary structure of this enzyme was determined (Abel *et al.*, 2011; Borges, 2004; Castro *et al.*, 2021).

Bibliographic references

Article from scientific journals

Foster, J. C.; Varlas, S.; Couturaud, B.; Coe, J.; O'Reilly, R. K. Getting into Shape: Reflections on a New Generation of Cylindrical Nanostructures' Self-Assembly Using Polymer Building Block. *J. Am. Chem. Soc.* **2019**, *141* (7), 2742–2753. <https://doi/10.1021/jacs.8b08648>

Book

Hammond, C. *The Basics of Crystallography and Diffraction*, 4th ed.; International Union of Crystallography Texts on Crystallography, Vol. 21; Oxford University Press, 2015.

Book chapter

Hammond, C. Crystal Symmetry. In *The Basics of Crystallography and Diffraction*, 4th ed.; International Union of Crystallography Texts on Crystallography, Vol. 21; Oxford University Press, 2015; pp 99–134.

Book with editors

Mom the Chemistry Professor: Personal Accounts and Advice from Chemistry Professors Who Are Mothers, 2nd ed.; Wozniak, K., Charlebois, A., Cole, R. S., Marzabadi, C. H., Webster, G., Eds.; Springer, 2018.

Website

ACS Publications Home Page. <https://pubs.acs.org/> (accessed 2019-02-21).

Document from a website

American Chemical Society, Committee on Chemical Safety, Task Force for Safety Education Guidelines. *Guidelines for Chemical Laboratory Safety in Academic Institutions*. American Chemical Society, 2016. <https://www.acs.org/content/dam/acsorg/about/governance/committees/chemicalsafety/publications/acs-safety-guidelines-academic.pdf> (accessed 2019-02-21).

Conference proceedings

Nilsson, A.; Petersson, F.; Persson, H. W.; Jönsson, H. Manipulation of Suspended Particles in a Laminar Flow. In *Micro Total Analysis Systems 2002, Proceedings of the μ TAS 2002 Symposium*, Nara, Japan, November 3–7, 2002; The Netherlands, 2002; pp 751–753. https://doi.org/10.1007/978-94-010-0504-3_50

Governmental and legislation information

Department of Commerce, United States Patent and Trademark Office. Section 706.02 Rejection of Prior Art [R-

07.2015]. *Manual of Patent Examining Procedure (MPEP)*, 9th ed., rev. 08.2017, last revised January 2018. <https://www.uspto.gov/web/offices/pac/mpep/s706.html#d0e58220> (accessed 2019-03-20).

Patent

Lois-Caballe, C.; Baltimore, D.; Qin, X.-F. Method for Expression of Small RNA Molecules within a Cell. US 7 732 193 B2, 2010.

Streaming data

American Chemical Society. Game of Thrones Science: Sword Making and Valyrian Steel. *Reactions*. YouTube, April 15, 2015. <https://www.youtube.com/watch?v=cHRcGoje4j4> (accessed 2019-02-28).

For more information, you can access the [ACS Style Quick Guide](#) and the [Williams College LibGuides](#).

SUBMITTING YOUR MANUSCRIPT

The corresponding author should submit the manuscript online by clicking [here](#). If you are a user, register by clicking [here](#).

At the **User home** page, click in **New submission**.

In Step 1, select a section for your manuscript, verify one more time if you followed all these rules in **Submission checklist**, add Comments for the Editor if you want to, and click Save and continue.

In Step 2, you will **upload your manuscript**. Remember it will pass through a double-blind review process. So, do not provide any information on the authorship.

In Step 3, enter **submission's metadata**: authors' full names, valid e-mail addresses and ORCID ID links (with "http" not "https"). Add title, abstract, contributors and supporting agencies, and the list of references.

In Step 4, upload the **cover letter**, the **graphical abstract** and other **supplementary material** you want to include in your manuscript.

In Step 5, you will be able to check all submitted documents in the **File summary**. If you are certain that you have followed all the rules until here, click in **Finish submission**.

REVIEW PROCESS

The time elapsed between the submission and the first response of the reviewers is around three months. The average time elapsed between submission and publication is around seven months.

Resubmission (manuscripts "rejected in the present form" or subjected to "revision") must contain a letter with the responses to the comments/criticism and suggestions of reviewers/editors should accompany the revised manuscript. All modifications made to the original manuscript must be highlighted.

If you want to check our Editorial process, click [here](#).

EDITOR'S REQUIREMENTS

Authors who have a manuscript accepted in **Eclet. Quim. J.** may be invited to act as reviewers.

Only the authors are responsible for the correctness of all information, data and content of the manuscript submitted to **Eclet. Quim. J.** Thus, the Editors and the Editorial Board cannot accept responsibility for the correctness of the material published in **Eclet. Quim. J.**

Proofs

After accepting the manuscript, **Eclet. Quim. J.** technical assistants will contact you regarding your manuscript page proofs to correct printing errors only, i.e., other corrections or content improvement are not permitted. The proofs shall be returned in three working days (72 h) via email.

Appeal

Authors may only appeal once about the decision regarding a manuscript. To appeal against the Editorial decision on your manuscript, the corresponding author can send a rebuttal letter to the editor, including a detailed response to any comments made by the reviewers/editor. The editor will consider the rebuttal letter, and if deemed appropriate, the manuscript will be sent to a new reviewer. The Editor decision is final.

Contact

If you have any question, please contact our team:

Prof. Assis Vicente Benedetti
Editor-in-Chief
ecletica.iq@unesp.br

Letícia Amanda Miguel
Technical support
ecletica@ctrlk.com.br

SUMMARY

EDITORIAL BOARD.....	3
EDITORIAL.....	4
DATABASE.....	5
INSTRUCTIONS FOR AUTHORS	6

SHORT REVIEW

Secondary metabolites and pharmacological potential of <i>Thuja orientalis</i> and <i>T. occidentalis</i> : A short review	17
<i>Maria Eduarda Tech, Cássia Gonçalves Magalhães, Sidney Augusto Vieira Filho</i>	

ORIGINAL ARTICLES

Biological evaluation of selected metronidazole derivatives as anti-nitroreductase via <i>in silico</i> approach.....	27
<i>Moriam Dasola Adeoye, Abel Kolawole Oyebamiji, Mojeed Ayoola Ashiru, Rasheed Adewale Adigun, Olabisi Hadijat Olalere, Banjo Semire</i>	
Experimental, DFT, molecular docking and <i>in silico</i> ADMET studies of cadmium- benzenetricarboxylates	37
<i>Enyi Inah Basse, Terkumbur Emmanuel Gber, Edison Esther Ekpenyong, Henry Okon Edet, Innocent Benjamin, Imabasi Tom Ita</i>	
Structural effect on the charge transfer and on the internal reorganization energy: Computational study.....	55
<i>Mohamed Jabha, Abdelah El Alaoui, Abdellah Jarid, El Houssine Mabrouk</i>	

Secondary metabolites and pharmacological potential of *Thuja orientalis* and *T. occidentalis*: A short review

Maria Eduarda Tech¹, Cássia Gonçalves Magalhães¹⁺, Sidney Augusto Vieira Filho²

1. State University of Ponta Grossa, Department of Chemistry, Ponta Grossa, Brazil.

2. Federal University of Ouro Preto, Department of Pharmacy, Ouro Preto, Brazil.

+Corresponding author: Cássia Gonçalves Magalhães, **Phone:** +55 4232203062, **Email address:** cgmagalhaes@uepg.br

ARTICLE INFO

Article history:

Received: June 01, 2022

Accepted: October 10, 2022

Published: October 28, 2022

Keywords:

1. Cupressaceae
2. flavonoids
3. terpenes
4. antimicrobial potential
5. antioxidant activity

Section Editors: Marcos Carlos de Mattos

ABSTRACT: Species from *Thuja* genus (Cupressaceae) are found in Brazil, North America and Asia. In the traditional medicine, these plants are used in the treatment of cough, skin allergies, and asthma. In Brazil, *Thuja* species are also used in the ornamentation of urban areas. Different parts of these plants displayed insecticidal, antitumor, and antioxidant activities. The essential oil of the leaves from *Thuja* spp. are constituted by monoterpenes and sesquiterpenes. The main substances found in the extracts of these species are flavonoids, which display relevant biological activities. This brief review shows recent phytochemical studies involving *T. orientalis* and *T. occidentalis*, as well as 40 constituents isolated from these species. The existing pharmacological potential justifies the growing scientific interest in this genus.



Thuja orientalis



Thuja occidentalis

Forty isolated constituents:

Monoterpenes
Sesquiterpenes
Flavonoids
Tropolones

Pharmacological potential

Antipyretic Diuretic
Gastroprotection
Skin burns treatment
Adstringent Antioxydant
Antimicrobial

CONTENTS

1. Introduction
2. Methodology
3. Chemical composition
4. Pharmacological potential of *T. orientalis* and *T. occidentalis*
5. Concluding remarks

Authors' contribution
Data availability statement
Funding
Acknowledgments
References

1. Introduction

Scientific interest for plants is growing, mainly due to the accelerated loss of the biodiversity (Singh *et al.*, 2021). The world market of phytotherapeutics has attracted a growing number of people who seek cheaper medicines with fewer side effects, when compared to synthetic pharmaceuticals (Silva *et al.*, 2021). The diversified potential of natural products has been widely explored, and the resulting data are considered an important key for the development of new drugs (Atanasov *et al.*, 2021). Additionally, the development of green semisynthesis of metal nanoparticles (Gour and Jain, 2019) and biosensors (Kumar and Arora, 2020) highlighting the variety of application of plants. Within the plant biodiversity, species of the Cupressaceae family stand out.

Cupressaceae trees comprise important classes of organic compounds, especially terpenes and terpenoids, both of which have intense and often pleasant odors. These compounds are mainly present in heartwood, bark and leaves of Cupressaceae trees (Bhardwaj *et al.*, 2021). The most known terpenoids found in conifers are sesquiterpenoids, diterpenes, and tropolones. Some sesquiterpenoids, e.g., bisabolanes, cubenanes, guaianes, ylanganes, himachalanes, longifolanes, longibornanes, longipinanes, cedranes, thujopsanes, are also present in the Pinaceae, Podocarpaceae (Pereira *et al.*, 2020) and Taxodiaceae (Jiang *et al.*, 2018) families. However, tropolone derivatives, such as nootkatin, chanootin, and hinokitiol, are particularly characteristic in Cupressaceae (Park *et al.*, 2021; Yattoo *et al.*, 2018).

In this context, species from the *Thuja* genus (Cupressaceae family) represent a relevant object of study, considering its use in the traditional medicine for the treatment of scurvy and rheumatism. It is endemic in Asia and is cultivated in Northern Europe and Brazil as an ornamental shrub (Pradhan *et al.*, 2021; Viezzer *et al.*, 2018). Species of the genus *Thuja*, similar to various other conifers, are evergreen trees that grow from 3 to 60 meters tall, with stringy-textured reddish-brown bark. There are five species belonging to this genus of which *T. orientalis* and *T. occidentalis* L. are well characterized (Gupta and Sharma, 2021). These species are monoecious and large evergreen shrub or small to medium sized trees (Jain and Sharma, 2017). The main secondary metabolites associated to the therapeutic potential of *Thuja* spp. are flavonoids, terpenes, and coumarins (Bhardwaj *et al.*, 2021; Gupta and Sharma, 2021).

Thuja orientalis is a synonym of *Platyclusus orientalis* (L.) Franco, an accepted name in the genus *Platyclusus* (Cupressaceae family). All parts of

T. orientalis, popularly known as *tuia*, are used for several objectives. Extracts from leaves have antipyretic, diuretic, and astringent properties, while the root bark extracts are used to treat skin burns. The leaves extract of *T. orientalis* also shows relevant antimicrobial activity (Burange *et al.*, 2021). Extracts from stems are used against parasites of the skin, dysentery, and constipation. *T. orientalis* extracts can be also used for dermatological treatments, renal, and gastrointestinal disorders (Gupta and Sharma, 2021). Also, the significant occurrence of phenolic compounds in the polar extracts from this species is related to its antioxidant activity (Moawad and Amin, 2019).

Thuja occidentalis L., commonly known as white cedar, is used in traditional medicine to treat bronchial catarrh, enuresis, psoriasis, uterine carcinomas, amenorrhea, and other diseases (Gupta and Sharma, 2021). The tincture from this species is used in the treatment of warts, papillomas, and condylomas related to human papilloma virus (Aguilar-Velázquez *et al.*, 2018). *T. occidentalis* also present pharmacological properties, such as antioxidant, gastroprotective, antimicrobial, antitumor, antidiabetic, and anti-atherosclerotic activities (Gupta and Sharma, 2021; Stan *et al.*, 2019).

Due to the scientific importance of this species, the aim of this work was to provide a short review related to chemical constitution and biotechnological potential of *T. orientalis* and *T. occidentalis* reported in the last five years.

2. Methodology

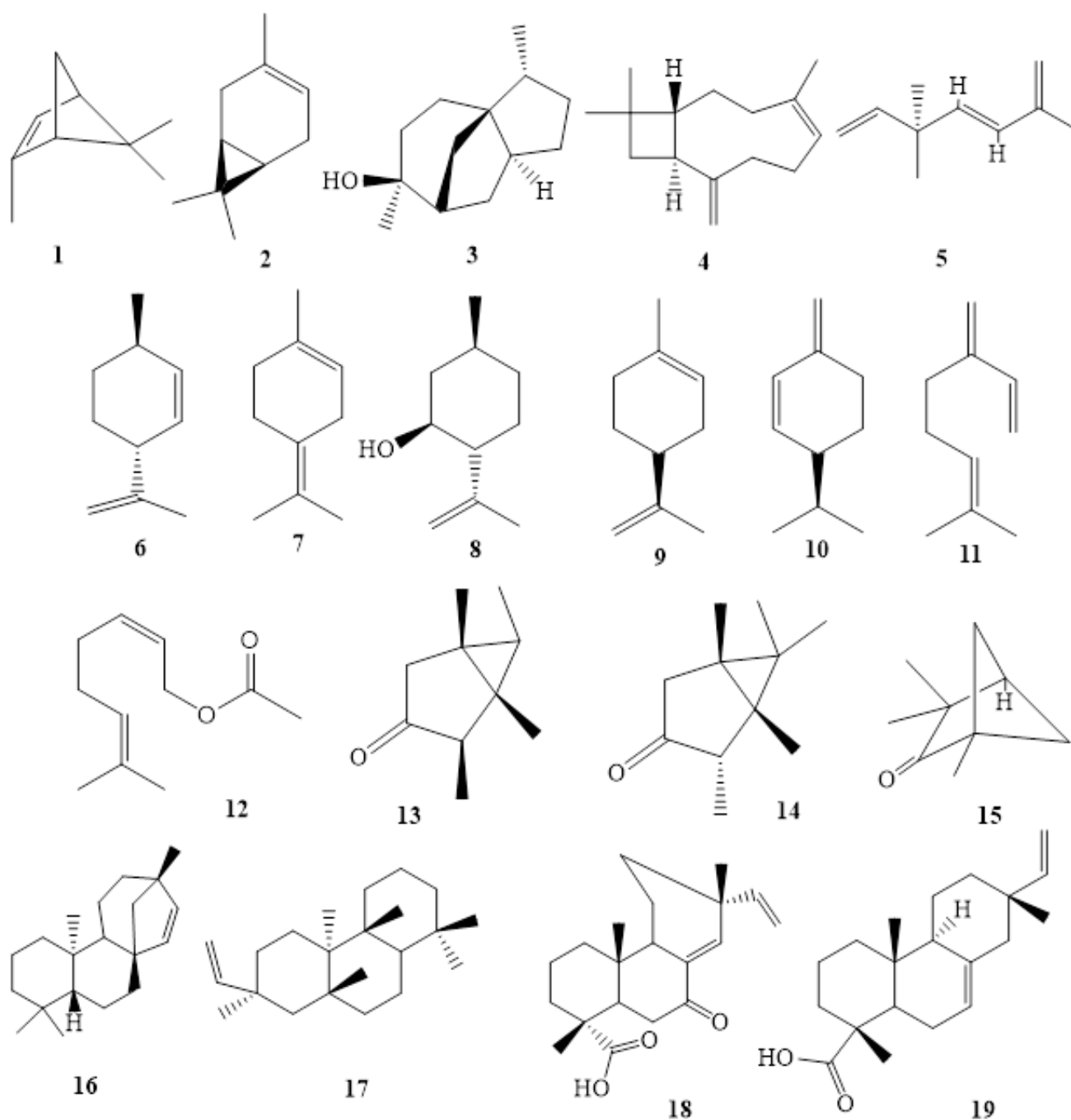
Data relating to *T. orientalis* and *T. occidentalis* were obtained through PubMed and Google Scholar published in the last five years. The following exclusion criteria were adopted: (i) article whose full text was not accessible in the database; (ii) publications that did not include the search phrases in the abstract or title; (iii) articles in other languages; and (iv) articles in which the phytochemicals used in the biological activity assays were not isolated from these species, but were acquired from industries. The chemical structures of compounds from these species were drawn using ChemDrawn 12.0 software.

3. Chemical composition

Essential oils from *T. orientalis* and *T. occidentalis* leaves are mainly constituted by terpenes **1** to **21** (Fig. 1). The major compounds found in the oil from *T. orientalis* collected in India are α -pinene (**1**, 29.2%), δ -3-carene

(**2**, 20.1%), and the sesquiterpene alcohol α -cedrol (**3**, 9.8%) (Bhardwaj *et al.*, 2021). A similar profile was reported for an oil sample of *T. orientalis* collected in Iran (Sanei-Dehkordi *et al.*, 2018). Terpenes **1** to **3**, and β -caryophyllene (**4**) are the major compounds found in essential oil from Chinese populations of *T. orientalis* (Bae *et al.*, 2021). A comparison of the chemical composition of essential oils extracted from wild and planted *T. orientalis* leaves in Korea was carried out (Seo *et al.*, 2019). The main compounds found in these essential oils were artemisiatriene (**5**, 17.7%), *trans*-

isolimonene (**6**, 17.2%), terpinolene (**7**, 5.2%), and isopulegol (**8**, 4.8%). The main constituents of essential oil from *T. orientalis* cultivated in Tokat, Turkey, were d-limonene (**9**, 36.7%), β -phellandrene (**10**, 36.7%), and β -myrcene (**11**, 15.3%). The quantitative and qualitative characteristics of secondary metabolites variation observed in these essential oils occur due to the existence of different chemotypes of a same species (Seo *et al.*, 2019) and mainly by the influence of environmental conditions (Li *et al.*, 2022).



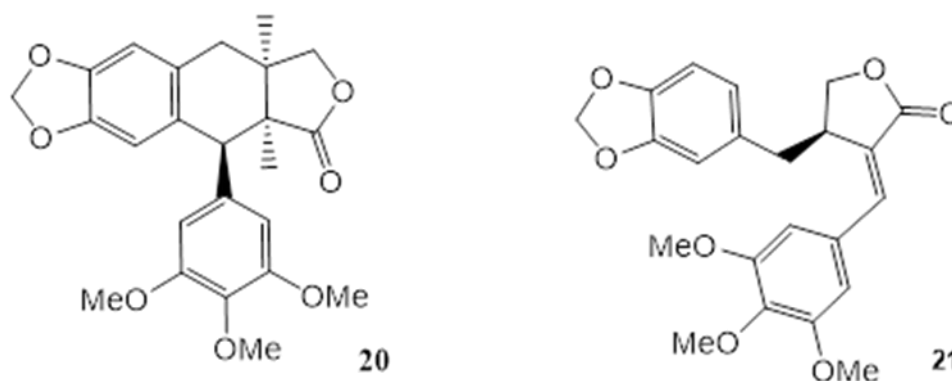


Figure 1. Chemical structure of compounds **1** to **21** found in *T. orientalis* and *T. occidentalis* essential oils.

Gas chromatography coupled to mass spectrometry (GC-MS) analysis of the essential oil from leaves of *T. orientalis* cultivated in Egypt and Saudi Arabian showed a similar profile considering the major compounds (α -cedrol and β -caryophyllene). In contrast, limonene was present in the Saudi Arabian *T. orientalis* essential oil, while caryophyllene oxide and vellerdiol were found in the Egyptian sample (Elsharkawy *et al.*, 2017). In general, the chemical constitution of essential oils is determined by GC-MS. However, the use of high-performance counter current chromatography, allowed to the isolation of α -cedrol (**3**) from essential oil of *T. orientalis* leaves (Rehman *et al.*, 2022).

The analysis of fruit oil from *T. orientalis* grown in Egypt revealed the occurrence of sesquiterpenes α -pinene (**1**, 11.3%), α -cedrol (**3**, 11.2%), β -myrcene (**11**, 9.6%), geranyl acetate (**12**, 9.0%) and β -caryophyllene (**4**, 8.9%) (Moawad and Amin, 2019). A comparison between the essential oil from Egyptian *T. orientalis* leaves with the one cultivated in Saudi Arabia was performed, being **3** and **4** the main terpenes found in the two oil samples. However, the third major compound, d-limonene (**9**), found in the Saudi sample, was absent in the Egyptian oil, probably due to influence from the severe environmental conditions of this country (Moawad and Amin, 2019).

The main compounds found in the essential oil from *T. occidentalis* L. leaves, known as cedar oil, are α -thujone (**13**, 65%), isothujone (**14**, 8%), and fenchone (**15**, 8%) (Caruntu *et al.*, 2020). Besides compound (**13**, 57%), the diterpenes hibaene (**16**, 7.3%) and rimuene (**17**, 5%) were detected in expressive amount in the essential oil from Chinese cultivar for this species (Bai *et al.*, 2020). The constituents of the essential oil from leaves and cones of *T. occidentalis* collected in Tunisia was described (Bellili *et al.*, 2018). Interestingly, the

chemical profile of the essential oil of *T. occidentalis* leaves was similar to that of *T. orientalis* essential oil collected in India.

A bioassay-guided fractionation of *T. occidentalis* extract carried out by Nakano *et al.* (2021) led to the isolation of the compounds (+)-7-oxo-13-*epi*-pimara-14,15-dien-18-oic acid (**18**), (+)-isopimaric acid (**19**), isopicrodeoxypodophyllotoxin (**20**), and (-)-deoxypodorhizone (**21**) (Fig. 1).

Phytochemical methods applied to study extracts of *T. orientalis* showed that it is a source of flavonoids and diterpenes, which are considered the majority compounds found in this species. From methanolic extract of *T. orientalis* fruits, the metabolites cupressuflavone (**22**), amentoflavone (**23**), robustaflavone (**24**), (+)-catechin (**25**), kaempferol-3-rhamnoside (afzelin) (**26**), quercitrin (**27**), 3-glucosylquercetin (isoquercitrin) (**28**), and myricitrin (**29**), quercetin (**30**), rutin (**31**), luteolin (**32**), and naringenin (**33**), (Fig. 2) were isolated (Bai *et al.*, 2019; Chakraborty *et al.*, 2018; Darwish *et al.*, 2021).

Quercitrin (**27**), isocupressic acid (**34**), *trans*-communic acid (**35**), isopimara-7,15-dien-3 β -ol (**36**), abietatriene-3 β -ol (**36**), and 15-isopimaren-3 β ,8 β -diol (**37**) (Fig. 2) were isolated from methanolic extract of leaves and stems of *T. orientalis* (Bae *et al.*, 2021). In this context, extracts from *T. occidentalis* also were considered a source of the flavonoids afzelin (**26**), quercitrin (**27**), isoquercitrin (**28**), and coumarins (Caruntu *et al.*, 2020).

The above data demonstrate the significant variety of secondary metabolites in *T. orientalis* and *T. occidentalis* species, and their potential to be applied mainly in pharmacological areas.

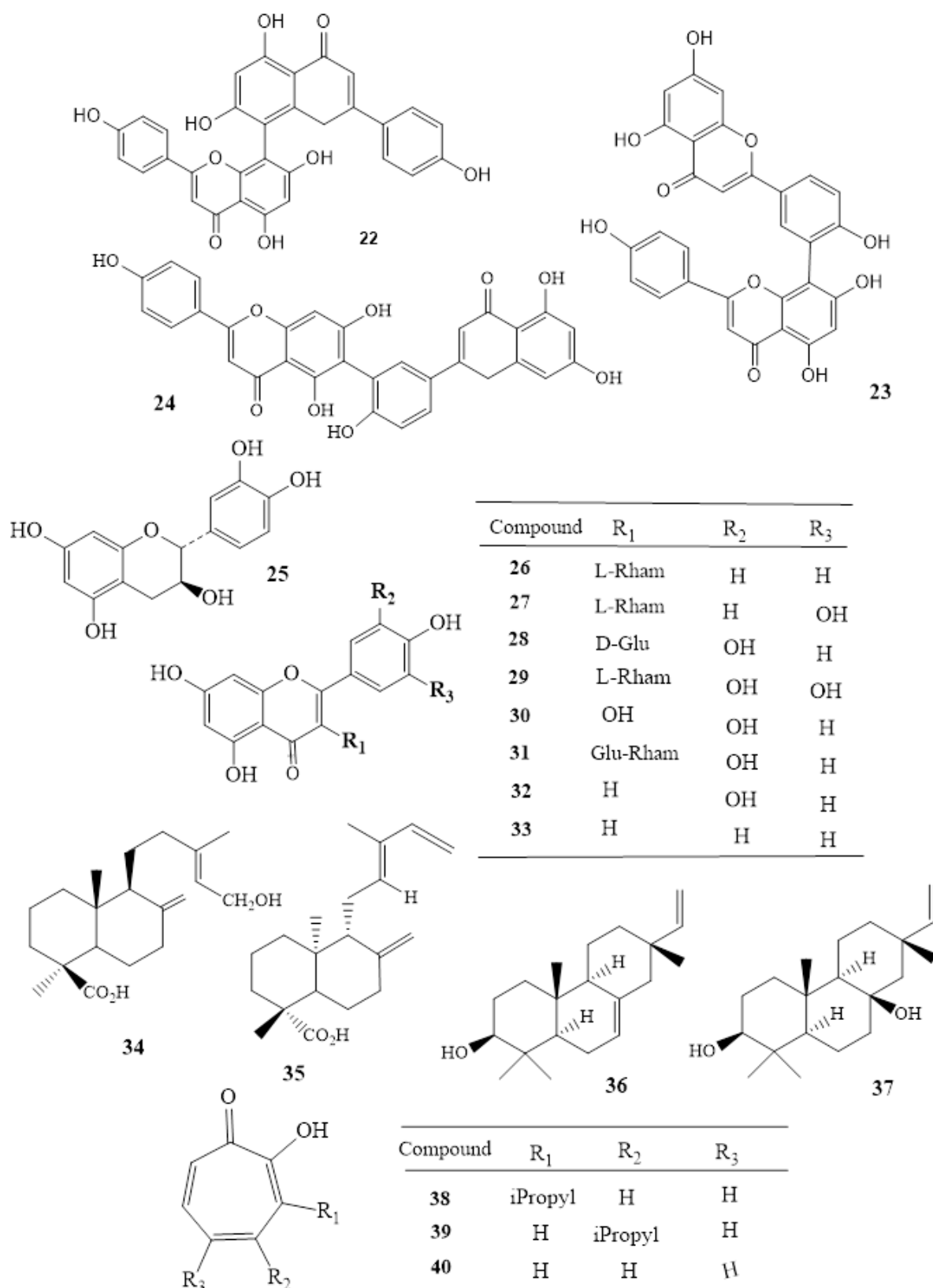


Figure 2. Chemical structure of compounds 22 to 40 found in *T. orientalis* and *T. occidentalis* essential oils or extracts. Glu = D-glucosyl, Rham = L-rhamnosyl.

4. Pharmacological potential of *T. orientalis* and *T. occidentalis*

T. orientalis and *T. occidentalis* are used for the treatment of different diseases and symptoms, such as cough, asthma, cutaneous affections, bacterial dysentery, and premature blindness. Its leaves also show astringent, diuretic, antipyretic, and emmenagogue properties (Gupta and Sharma, 2021). The seeds of these two species have sedative effects and their barks are used to treat skin burns (Caruntu *et al.*, 2020; Srivastava *et al.*, 2022). There are a large number of research papers that support the traditional use of these plants, as is described in the sequence.

The essential oil from *T. orientalis* exhibits antimicrobial activity. For instance, the inhibition of the growth of *Salmonella mutans* and *S. typhimurium* was attributed to three naturally occurring monocyclic tropolones: α -thujaplicin (38), β -thujaplicin (39) and γ -thujaplicin (40) (Fig. 2), which act as chelating agents in the bacterial wall cell (Jain and Sharma, 2017).

The antimicrobial potential of *T. orientalis* and *T. occidentalis* has been reported. The antimicrobial property of *T. occidentalis* leaves extract obtained with methanol inhibited the growth of *Bacillus cereus* and *Candida albicans* (Caruntu *et al.*, 2020). A synergism between *Psidium guajava* and *T. orientalis* leaves extracts was observed when they were evaluated against methicillin-resistant *Staphylococcus aureus*. This synergism was probably due to the combined inhibitory effect of phenolics present in the leaf extracts, *i.e.*, quercetin and gallic acid and catechin (Chakraborty *et al.*, 2018).

Extracts from leaves and cones from *T. orientalis* grown in Tunisia were assayed against foodborne microorganisms, such as *Listeria monocytogenes* ATCC 7644, *S. aureus* ATCC 29213, *Escherichia coli* ATCC 8739, *Pseudomonas aeruginosa* ATCC 27853, *S. typhimurium* NCTC 6017, *Aspergillus flavus* (foodborne isolate), and *Aspergillus niger* CTM 10099. The highest antimicrobial activities by disk diffusion assay were observed for *T. orientalis* essential oil from leaves. The most potent antimicrobial activity was recorded against *E. coli* and *S. typhimurium*, highlighting the potential of this essential oil as a natural preservative against foodborne pathogens (Bellili *et al.*, 2018).

T. orientalis is appointed as a relevant alternative to improve the immunity, considering the infections caused by viruses, with emphasis on SARS-CoV-2 (Srivastava *et al.*, 2022). Considering the cytotoxic activity of these two species of the Cupressaceae family, *T. occidentalis* extracts also showed antiproliferative and proapoptotic

activity against the A549 lung cancer cell line, and *T. orientalis* was active against breast cancer and leukemia cells (Srivastava *et al.*, 2022). Based on teratogenic assays, the *T. orientalis* extract revealed low therapeutic index (TI = 0.808) with and median lethal concentration (LC₅₀ = 0.703 mg mL⁻¹) after a period of 24 h that is within the desirable value (below 1) for drug administration (Breeta *et al.*, 2018).

The presence of phenolic compounds in *Thuja* spp. evidence their antioxidant potential. The mother tincture of *T. orientalis* showed higher inhibitory activity against the generation of the 1,1-diphenyl-2-picryl-hydrazyl (DPPH) radical, and effective oxygen radical absorbance capacity (Stan *et al.*, 2019). The antioxidant activity of *T. orientalis* extracts obtained using solvents of different polarities was tested in erythrocytes from a healthy donor. The ethyl acetate extract showed the higher reduction of reactive oxidant species (Alamdari *et al.*, 2018).

The antidiabetic activity of hydroalcoholic extract from *T. orientalis* aerial parts, collected from three different regions of India, showed an expressive activity when compared to glibenclamide, used as positive control (Pradhan and Sarangdevot, 2020). This antidiabetic effect was attributed to the presence of flavonoids such as quercetin (27), rutin (31), luteolin (32), and naringenin (33), previously reported as potential antidiabetic drugs (Bai *et al.*, 2019).

The administration of methanolic extracts of *T. occidentalis* twigs in alloxan-induced rats significantly increased glucose homeostasis and alleviate kidney and liver functions. The twigs of this species could be a potential source of the new oral antidiabetic drug (Tyagi *et al.*, 2019). To flavonoids 27, 31–33 was also attributed the potential phytotherapeutic of a mother tincture from a mixture of branches and leaves of *T. occidentalis*. This sample inhibited the inflammation of colitis induced by 2,4,6-trinitrobenzenesulfonic acid (Stan *et al.*, 2019). The efficacy of the gastroprotective effect induced by the methanolic extract of *T. occidentalis* was similar to that produced by omeprazole, a proton pump inhibitor that decreases the amount of acid produced in the stomach (Caruntu *et al.*, 2020).

The anti-inflammatory activity of the aqueous extract and of a polysaccharide rich fraction of *T. occidentalis*, both at 300 mg kg⁻¹, did not induce gastric toxicity in experimental models of acute inflammation. The effect of these samples was attributed to mechanisms involving mediators such as histamine, serotonin, prostaglandin E₂, and bradykinin, as well as reduction of the vascular permeability and neutrophil migration to the damaged site. In addition, both of the samples reduced

the production of proinflammatory cytokines (TNF- and IL-6), decreased immunostaining of COX-2 and iNOS, and inhibited oxidative stress (Silva *et al.*, 2017). The successful anti-inflammatory property of *T. occidentalis* was also proved considering the decreasing of the gene expression of the inflammation markers (interleukin-6 and tumor necrosis factor- α) induced by the administration of 2,4,6-trinitrobenzenesulfonic acid after the application of the mother tincture from this plant (Stan *et al.*, 2019).

The antioxidant potential of the essential oil from cones and leaves of *T. occidentalis* grown in Tunisia was assayed by DPPH free-radical scavenging activity method. All essential oils tested showed better antioxidant activity than trolox against DPPH radical scavenging. However, the essential oil from leaves exhibited the highest total antioxidant activity (Bellili *et al.*, 2018). The cytotoxic effect of α -thujone, the major compound of *T. occidentalis* essential oil, was evaluated against glioblastoma multiforme (GBM) cells, with special emphasis on the mechanisms of its effect on cell viability and invasiveness (Nakano *et al.*, 2021; Pudelek *et al.*, 2019). An attenuating effect on the viability and proliferation of GBM cells was observed when α -thujone was administered at doses varying from 660 to 3.2 mmol L⁻¹. This effect was correlated with the induction of apoptosis in GBM cells and with considerable inhibition of GBM cells motility. Mechanistic analyses demonstrated the induction of oxidative stress and autophagy in α -thujone-treated tumor cells. It was demonstrated that α -thujone exerts pro-apoptotic and anti-invasive effects on GBM cells, confirming the potential of this monoterpene for the treatment of glioblastoma multiforme. Other reports demonstrate the potential of *T. occidentalis* for the treatment of polycystic ovary syndrome (Ahmad and Safuan, 2019; Nakano *et al.*, 2021; Parveen and Das, 2021) and inform that there is no contraindication in the administration of *T. occidentalis* mother tincture in the sycosis secondary to cancer treatments (Bagot, 2020).

Besides the relevant biological potential of species from *Thuja* genus, *T. orientalis* extract is a very important bioresource for synthesis of metal nanoparticles with silver (Bandyopadhyay *et al.*, 2017; Burange *et al.*, 2021), gold (Dong *et al.*, 2020) and copper (García-Hernández *et al.*, 2021). The aqueous leaves extract of *T. orientalis* was also efficient in the green synthesis of silica nanoparticles (SiO₂NPs) through magnetic stirrer method and using cold plasma. The biofilm inhibition of SiO₂NPs were evaluated against *S. aureus* and *E. coli*. The SiO₂NPs synthesized by cold plasma method showed the highest antimicrobial effect (Al-Azawi *et al.*, 2019).

The dried leaves of *T. orientalis* was evaluated as an adsorbent and showed an effective result in the remotion of Remazol Brilliant Blue R dye from aqueous solution (Arya *et al.*, 2020). Other important application reported for *T. orientalis* seeds extract is related to its use as a green reductant of graphene oxide. The analysis through GC-MS confirmed that α -tocopherol present in *T. orientalis* seeds extract was most likely responsible for the reduction of graphene oxide to reduced graphene oxide (Kumar *et al.*, 2021). Besides, the leaves extract of *T. orientalis* was capable of retard the oxidation of soybean biodiesel (Devi *et al.*, 2019).

The above data showed the versatile application of *Thuja* genus species and demonstrated the scientific potential of these plants.

5. Concluding remarks

Forty constituents have been identified from *T. orientalis* or *T. occidentalis*. Due to its diversified chemical structures, important pharmacological properties are attributed to these species, a part of their application in different areas within an industry context. The effective biotechnological potential of these species stimulates the research of new applications for these plants, which can improve the economic value of this natural resource and its sustainable management.

Authors' contribution

Conceptualization: Tech, M. E.; Magalhães, C. G.

Data curation: Tech, M. E.

Formal Analysis: Magalhães, C. G.; Vieira Filho, S. A.

Funding acquisition: Not applicable.

Investigation: Tech, M. E.

Methodology: Tech, M. E.

Project administration: Magalhães, C. G.

Resources: Not applicable.

Software: Not applicable.

Supervision: Magalhães, C. G.; Vieira Filho, S. A.

Validation: Not applicable.

Visualization: Not applicable.

Writing – original draft: Tech, M. E.

Writing – review & editing: Magalhães, C. G.; Vieira Filho, S. A.

Data availability statement

Data sharing is not applicable.

Funding

Not applicable

Acknowledgments

PIBIC-UEPG.

References

- Aguilar-Velázquez, G.; Espinosa, D.; Ordaz-Pichardo, C. Effects of Homeopathic Dilutions of *Echinacea angustifolia* and *Thuja occidentalis* on Cervical Cancer Cells. *Homeopathy*. **2018**, *107* (S1), 55–78. <https://doi.org/10.1055/s-0037-1608960>
- Ahmad, F.; Safuan, S. Assessing the Effectiveness of Plant Extracts in Polycystic Ovarian Syndrome: A Systematic Review. *Mal. J. Med. Health Sci.* **2019**, *15* (2), 120–129.
- Alamdari, D. H.; Aghasizadeh-Sharbat, M.; Mohadjerani, M.; Ferns, G. A.; Avan, A. Prooxidant-Antioxidant Balance and Antioxidant Properties of *Thuja orientalis* L: A Potential Therapeutic Approach for Diabetes Mellitus. *Curr. Mol. Pharmacol.* **2018**, *11* (2), 109–112. <https://doi.org/10.2174/1874467210666170404112211>
- Al-Azawi, M. T.; Hadi, S. M.; Mohammed, C. H. Synthesis of silica nanoparticles via green approach by using hot aqueous extract of *Thuja orientalis* leaf and their effect on biofilm formation. *Iraqi J. Agric. Sci.* **2019**, *50* (Special Issue), 245–255. <https://doi.org/10.36103/ijas.v50iSpecial.196>
- Arya, M. C.; Bafila, P. S.; Mishra, D.; Negi, K.; Kumar, R.; Bughani, A. Adsorptive removal of Remazol Brilliant Blue R dye from its aqueous solution by activated charcoal of *Thuja orientalis* leaves: an eco-friendly approach. *SN Appl. Sci.* **2020**, *2* (2), 265. <https://doi.org/10.1007/s42452-020-2063-2>
- Atanasov, A. G.; Zotchev, S. B.; Dirsch, V. M.; Supuran, C. T. Natural products in drug discovery: advances and opportunities. *Nat. Rev. Drug Discov.* **2021**, *20* (3), 200–216. <https://doi.org/10.1038/s41573-020-00114-z>
- Bae, S.; Han, J. W.; Dang, Q. L.; Kim, H.; Choi, G. J. Plant Disease Control Efficacy of *Platyclusus orientalis* and Its Antifungal Compounds. *Plants*. **2021**, *10* (8), 1496. <https://doi.org/10.3390/plants10081496>
- Bagot, J.-L. How to prescribe *Thuja occidentalis* in oncology? Analysis of the literature, study of practices and personal experience. *Rev. Homeopath.* **2020**, *11* (3), e26–e32. <https://doi.org/10.1016/j.revhom.2020.07.001>
- Bai, L.; Li, X.; He, L.; Zheng, Y.; Lu, H.; Li, J.; Zhong, L.; Tong, R. Antidiabetic Potential of Flavonoids from Traditional Chinese medicine: A Review. *Am. J. Chinese Med.* **2019**, *47* (5), 933–957. <https://doi.org/10.1142/S0192415X19500496>
- Bai, L.; Wang, W.; Hua, J.; Guo, Z.; Luo, S. Defensive functions of volatile organic compounds and essential oils from northern white-cedar in China. *BMC Plant Biol.* **2020**, *20* (1), 500. <https://doi.org/10.1186/s12870-020-02716-6>
- Bandyopadhyay, A.; Banerjee, P. P.; Shaw, P.; Mondal, M. K.; Das, V. K.; Chowdhury, P.; Karak, N.; Bhattacharya, S.; Chattopadhyay, A. Cytotoxic and Mutagenic Effects of *Thuja occidentalis* Mediated Silver Nanoparticles on Human Peripheral Blood Lymphocytes. *Mater. Focus*. **2017**, *6* (3), 290–296. <https://doi.org/10.1166/mat.2017.1405>
- Bellili, S.; Aouadhi, C.; Dhifi, W.; Ghazghazi, H.; Jlassi, C.; Sadaka, C.; El Beyrouthy, M.; Maaroufi, A.; Cherif, A.; Mnif, W. The Influence of Organs on Biochemical Properties of Tunisian *Thuja occidentalis* Essential Oils. *Symmetry*. **2018**, *10* (11), 649. <https://doi.org/10.3390/sym10110649>
- Bhardwaj, K.; Silva, A. S.; Atanassova, M.; Sharma, R.; Nepovimova, E.; Musilek, K.; Sharma, R.; Alghuthaymi, M. A.; Dhanjal, D. S.; Nicoletti, M.; Sharma, B.; Upadhyay, N. K.; Cruz-Martins, N.; Bhardwaj, P.; Kuča, K. Conifers Phytochemicals: A Valuable Forest with Therapeutic Potential. *Molecules*. **2021**, *26* (10), 3005. <https://doi.org/10.3390/molecules26103005>
- Breeta, R. E.; Jesubatham, P. D.; Grace, V. M. B.; Viswanathan, S.; Srividya, S. Non-toxic and non-teratogenic extract of *Thuja orientalis* L. inhibited angiogenesis in zebra fish and suppressed the growth of human lung cancer cell line. *Biomed. Pharmacother.* **2018**, *106*, 699–706. <https://doi.org/10.1016/j.biopha.2018.07.010>
- Burange, P. J.; Tawar, M. G.; Bairagi, R. A.; Malviya, V. R.; Sahu, V. K.; Shewatkar, S. N.; Sawarkar, R. A.; Mamurkar, R. R. Synthesis of silver nanoparticles by using *Aloe vera* and *Thuja orientalis* leaves extract and their biological activity: a comprehensive review. *Bull. Nat. Res. Centre.* **2021**, *45* (1), 181. <https://doi.org/10.1186/s42269-021-00639-2>
- Caruntu, S.; Ciceu, A.; Olah, N. K.; Don, I.; Hermenean, A.; Cotoraci, C. *Thuja occidentalis* L. (Cupressaceae): Ethnobotany, phytochemistry and biological activity. *Molecules*. **2020**, *25* (22), 5416. <https://doi.org/10.3390/molecules25225416>
- Chakraborty, S.; Afaq, N.; Singh, N.; Majumdar, S. Antimicrobial activity of Cannabis sativa, Thuja orientalis and Psidium guajava leaf extracts against methicillin-resistant Staphylococcus aureus. *J. Integr. Med.* **2018**, *16* (5), 350–357. <https://doi.org/10.1016/j.joim.2018.07.005>
- Darwish, R. S.; Hammada, H. M.; Ghareeb, D. A.; Abdelhamid, A. S. A.; Harraz, F. M.; Shawky, E. Seasonal dynamics of the phenolic constituents of the cones and leaves of oriental Thuja (*Platyclusus orientalis* L.) reveal their anti-

- inflammatory biomarkers. *RSC Adv.* 2021, 11 (40), 24624–24635. <https://doi.org/10.1039/D1RA01681D>
- Devi, A.; Das, V. K.; Deka, D. A green approach for enhancing oxidation stability including long storage periods of biodiesel via *Thuja orientalis* L. as an antioxidant additive. *Fuel.* 2019, 253, 1264–1273. <https://doi.org/10.1016/j.fuel.2019.05.127>
- Dong, Y.; Hu, X.-M.; Cao, Y.-F.; Wang, Y.-C.; Li, L.-Z.; Lu, J.-Y.; Li, X.-X. *Thuja occidentalis* mediated AuNPs as wound dressing agents for abdominal wound healing in nursing care after surgery. *Appl. Nanosci.* 2020, 10 (9), 3577–3584. <https://doi.org/10.1007/s13204-020-01459-y>
- Elsharkawy, E. R.; Aljohar, H.; Donia, A. E. R. M. Comparative study of antioxidant and Saudi Arabia. *J. Pharm. Res. Int.* 2017, 15 (5), 1–9. <https://doi.org/10.9734/BJPR/2017/32387>
- García-Hernández, L.; Flores-Saldivar, J. A.; Ortega, P. R.; Guerrero, M. U. F. Synthesis of colloidal CuNPs using the extract of *Thuja orientalis*. *ECS Trans.* 2021, 101 (1), 131. <https://doi.org/10.1149/10101.0131ecst>
- Gour, A.; Jain, N. K. Advances in green synthesis of nanoparticles. *Artif. Cells Nanomed. Biotechnol.* 2019, 47 (1), 844–851. <https://doi.org/10.1080/21691401.2019.1577878>
- Gupta, M.; Sharma, K. A Review of Phyto-Chemical Constituent and Pharmacological Activity of *Thuja* Species. *Int. J. Pharm. Res. Appl.* 2021, 6 (1), 85–95.
- Jain, N.; Sharma, M. Ethanobotany, Phytochemical and Pharmacological Aspects of *Thuja orientalis*: A Review. *Int. J. Pure App. Biosci.* 2017, 5 (4), 73–83. <https://doi.org/10.18782/2320-7051.2976>
- Jiang, L.; George, S. C. Biomarker signatures of Upper Cretaceous Latrobe Group hydrocarbon source rocks, Gippsland Basin, Australia: distribution and palaeoenvironment significance of aliphatic hydrocarbons. *Int. J. Coal Geol.* 2018, 196, 29–42. <https://doi.org/10.1016/j.coal.2018.06.025>
- Kumar, V.; Arora, K. Trends in nano-inspired biosensors for plants. *Mat. Sci. Energy Technol.* 2020, 3, 255–273. <https://doi.org/10.1016/j.mset.2019.10.004>
- Kumar, P.; Andersson, G.; Subhedar, K. M.; Dhimi, H. S.; Gupta, G.; Mukhopadhyay, A. K.; Joshi, R. P. Utilization of green reductant *Thuja orientalis* for reduction of GO to RGO. *Ceramics Int.* 2021, 47 (10 – Part B), 14862–14878. <https://doi.org/10.1016/j.ceramint.2020.08.063>
- Li, R. W.; Smith, P. N.; Lin, G. D. Variation of biomolecules in plant species. In *Herbal Biomolecules in Healthcare Applications*. Academic Press, 2022; pp 81–99. <https://doi.org/10.1016/B978-0-323-85852-6.00028-7>
- Moawad, A.; Amin, E. Comparative antioxidant activity and volatile oil composition of leaves and fruits of *Thuja orientalis* Growing in Egypt. *Wal. J. Sci. Technol. (WJST)* 2019, 16 (11), 823–830. <https://doi.org/10.48048/wjst.2019.3269>
- Nakano, D.; Ishitsuka, K.; Ishihara, M.; Tsuchihashi, R.; Okawa, M.; Tamura, K.; Kinjo, J. Screening of promising chemotherapeutic candidates from plants against Human adult T-Cell Leukemia/Lymphoma (VII): active principles from *Thuja occidentalis* L. *Molecules.* 2021, 26 (24), 7619. <https://doi.org/10.3390/molecules26247619>
- Park, J. S.; Ko, K.; Kim, S.-H.; Lee, J. K.; Park, J.-S.; Park, K.; Kim, M. R.; Kang, K.; Oh, D.-C.; Kim, S. Y.; Yumnam, S.; Kwon, H. C.; Shin, J. Tropolone-Bearing Sesquiterpenes from *Juniperus chinensis*: structures, photochemistry and bioactivity. *J. Nat. Prod.* 2021, 84 (7), 2020–2027. <https://doi.org/10.1021/acs.jnatprod.1c00321>
- Parveen, S.; Das, S. Homeopathic treatment in patients with polycystic ovarian syndrome: a case series. *Homeopathy.* 2021, 110 (3), 186–193. <https://doi.org/10.1055/s-0041-1725039>
- Pereira, R.; Lima, F. J.; Simbras, F. M.; Bittar, S. M. B.; Kellner, A. W. A.; Saraiva, A. Á. F.; Bantim, R. A. M.; Sayão, J. M.; Oliveira, G. R. Biomarker signatures of Cretaceous Gondwana amber from Ipubi Formation (Araripe Basin, Brazil) and their palaeobotanical significance. *J. S. Am. Earth Sci.* 2020, 98, 102413. <https://doi.org/10.1016/j.jsames.2019.102413>
- Pradhan, P.; Sarangdevot, Y. S. Evaluation of antidiabetic activity of aerial parts of *Thuja occidentalis*. *Plant Arch.* 2020, 20 (Suppl. 1), 957–962.
- Pradhan, P.; Sarangdevot, Y. S.; Vyas, B. Quantitative estimation of total phenols and flavonoids content in *Thuja orientalis*. *J. Pharmacogn. Phytochem.* 2021, 10 (1), 687–689.
- Pudelek, M.; Catapano, J.; Kochanowski, P.; Mrowiec, K.; Janik-Olchawa, N.; Czyż, J.; Ryszawy, D. Therapeutic potential of monoterpene α -thujone, the main compound of *Thuja occidentalis* L. essential oil, against malignant glioblastoma multiforme cells in vitro. *Fitoterapia.* 2019, 134, 172–181. <https://doi.org/10.1016/j.fitote.2019.02.020>
- Rehman, R.; Zubair, M.; Bano, A.; Hewitson, P.; Ignatova, S. Isolation of industrially valuable α -Cedrol from essential oil of *Platycladus orientalis* (*Thuja orientalis*) leaves using linear gradient counter current chromatography. *Ind. Crops Prod.* 2022, 176, 114297. <https://doi.org/10.1016/j.indcrop.2021.114297>
- Sanei-Dehkordi, A.; Gholami, S.; Abai, M. R.; Sedaghat, M. M. Essential oil composition and larvicidal evaluation of

Platycladus orientalis against two mosquito vectors, Anopheles stephensi and Culex pipiens. J. Arthropod Borne Dis. 2018, 12 (2), 101–107. <https://doi.org/10.18502/jad.v12i2.35>

Seo, K.-S.; Lee, B.; Yun, K. W. Chemical composition and antibacterial activity of essential oils extracted from wild and planted Thuja orientalis leaves in Korea. J. Essent. Oil-Bear. Plants. 2019, 22 (5), 1407–1415. <https://doi.org/10.1080/0972060X.2019.1689177>

Silva, I. S.; Nicolau, L. A. D.; Sousa, F. B. M.; Araújo, S.; Oliveira, A. P.; Araújo, T. S. L.; Souza, L. K. M.; Martins, C. S.; Aquino, P. E. A.; Carvalho, L. L.; Silva, R. O.; Rolim-Neto, P. J.; Medeiros, J. V. R. Evaluation of anti-inflammatory potential of aqueous extract and polysaccharide fraction of Thuja occidentalis Linn. in mice. Int. J. Biol. Macromol. 2017, 105 (Part 1), 1105–1116. <https://doi.org/10.1016/j.ijbiomac.2017.07.142>

Silva, P. E. S.; Furtado, C. O.; Damasceno, C. A. Utilização de plantas medicinais e medicamentos fitoterápicos no Sistema Público de Saúde Brasileiro nos últimos 15 anos: uma revisão integrativa. Braz. J. Dev. 2021, 7 (12), 116235–116255. <https://doi.org/10.34117/bjdv7n12-402>

Singh, V.; Shukla, S.; Singh, A. The principal factors responsible for biodiversity loss. Open J. Plant Sci. 2021, 6 (1), 11–14. <https://doi.org/10.17352/ojps.000026>

Srivastava, A.; Jit, B. P.; Dash, R.; Srivastava, R.; Srivastava S. Thuja Occidentalis: an unexplored phytomedicine with therapeutic applications. Comb. Chem. High Throughput Screen. 2022, 25, 1537–1548. <https://doi.org/10.2174/1386207325666220308153732>

Stan, M. S.; Voicu, S. N.; Caruntu, S.; Nica, I. C.; Olah, N.-K.; Burtescu, R.; Balta, C.; Rosu, M.; Herman, H.; Hermenean, A.; Dinischiotu, A. Antioxidant and anti-inflammatory properties of a Thuja occidentalis Mother tincture for the treatment of ulcerative colitis. Antioxidants. 2019, 8 (9), 416–435. <https://doi.org/10.3390/antiox8090416>

Tyagi, C. K.; Porwal, P.; Mishra, N.; Sharma, A.; Chandekar, A.; Punekar, R.; Punniyakoyi, V. T.; Kumar, A.; Anghore, D. Antidiabetic activity of the methanolic extracts of Thuja occidentalis Twigs in Alloxan-induced Rats. Curr. Tradit. Med. 2019, 5 (2), 138–143. <https://doi.org/10.2174/2215083805666190312153743>

Viezzler, J.; Biondi, D.; Martini, A.; Grise, M. M. A vegetação no paisagismo das praças de Curitiba-PR. Cienc. Florest. 2018, 28 (1), 369–383. <https://doi.org/10.5902/1980509831608>

Yatoo, M. I.; Gopalakrishnan, A.; Saxena, A.; Parray, O. R.; Tufani, N. A.; Chakraborty, S.; Tiwari R.; Dhama, K.; Iqbal, H. M. N. Anti-inflammatory drugs and herbs with special emphasis on herbal medicines for countering inflammatory

diseases and disorders - a review. Recent Pat. Inflamm. Allergy Drug Discov. 2018, 12 (1), 39–58. <https://doi.org/10.2174/1872213X12666180115153635>

Biological evaluation of selected metronidazole derivatives as anti-nitroreductase via *in silico* approach

Moriam Dasola Adeoye¹, Abel Kolawole Oyebamiji²⁺, Mojeed Ayoola Ashiru¹, Rasheed Adewale Adigun¹, Olabisi Hadijat Olalere¹, Banjo Semire³

1. Fountain University, Faculty of Science, Osogbo, Osun State, Nigeria.
2. Bowen University, Department of Chemistry and Industrial Chemistry, Iwo, Nigeria.
3. Ladoke Akintola University of Technology, Faculty of Pure and Applied Science, Ogbomosho, Nigeria.

+Corresponding author: Abel Kolawole Oyebamiji, **Phone:** +2348032493676, **Email address:** abeloyebamiji@gmail.com

ARTICLE INFO

Article history:

Received: February 27, 2022

Accepted: July 11, 2022

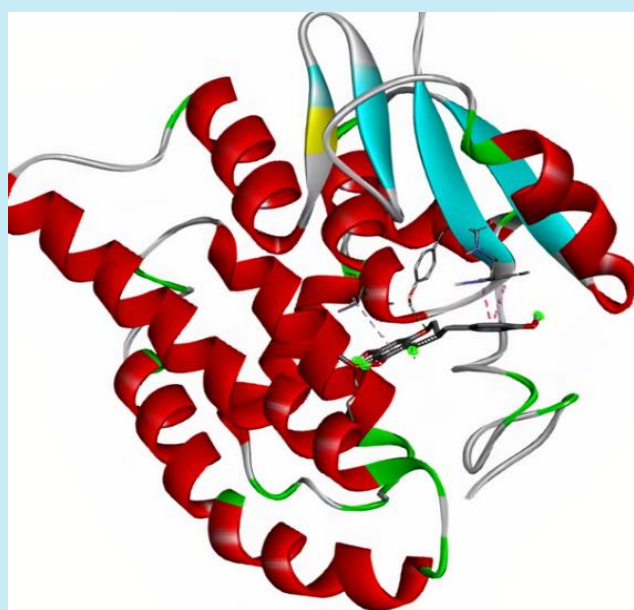
Published: October 28, 2022

Keywords:

1. ligand
2. antibacterial
3. gastric
4. phytochemicals
5. ADME

Section Editors: Assis Vicente Benedetti

ABSTRACT: The 1-(2-hydroxyethyl)-2-methyl-5-nitroimidazole (2HMN) is a powerful antibacterial and antiparasitic drug used alongside other drugs against *Helicobacter pylori* infection and was investigated the effects of substituents: -OH (A), H (B), -SPh (C), -COOH (D), -NO₂ (E) and -OCH₃ (F) on the interactions of 2HMN with the target nitroreductase RdxA protein for the treatment of the infection. Spartan 14 (optimization), PyMOL 1.7.4.4 (to treat downloaded protein), Autodock Tool (locate protein binding site), Autodock vina 1.1.2 (docking calculation) were used to discover the nonbonding interaction between docked complexes using SWISSADME and Pre-ADMET software. The band gaps order for the studied compounds were C < A < F < B < D < E, a probability of highest charge distribution and activity for SPh substituted derivatives and the ligands conformed to the Lipinski's rule of five. Compounds D and E are noninhibitors and nonsubstrate for cytochrome P450 2C9, P450 2D6, P450 2C19 with the same efficient calculated binding affinity (-21.3 kJ mol⁻¹) and inhibition constant (7.8) comparable to the standard compound A.



1. Introduction

Helicobacter pylori (*H. pylori*), a microaerophilic gram-negative bacterium, has been described as the first formally recognized carcinogenic bacterial, and one of the most successful human pathogens which is believed to be transmitted from person to person through closed contact and exposure to fecal matters or vomit (Fig. 1) (Bürgers *et al.*, 2008; Kayali *et al.*, 2018). These bacteria are typically found in the mucous layer that covers and protects the stomach and small intestine's tissues (Houghton and Wang, 2005). Its infection, by inflaming the stomach's inner layer, which is a complicated interplay between the bacterial, the host, and environmental factors, has been established to be the key factor with various gastric diseases such as chronic gastritis, peptic ulcers, and gastric mucosa-associated lymphoid tissue (MALT) lymphoma (Jemilohun and Otegbayo, 2016; Wu *et al.*, 2009). Although, many other factors, such as the persistent use of anti-inflammatory pain relievers, including aspirin, are responsible for peptic ulcer diseases (Bürgers *et al.*, 2008).

The clinical use of many 5-nitroimidazoles derivatives, especially metronidazole [1-(2-hydroxyethyl)-2-methyl-5-nitroimidazole] (2HMN) as antibiotic for the effective treatment of patients with *H. pylori* linked gastritis and peptic ulcer ailment, has been listed and approved by the World Health Organization. Metronidazole (A) (Fig. 2) has also been used in combination with other antibiotics such as tetracycline, amoxicillin and clarithromycin to treat ulcer. However, it is uncommon to find both bacteria and protozoa to cause ulcer (Houghton and Wang, 2005). Some studies (Ghotaslou *et al.*, 2015; Kim *et al.*, 2020) in the last few years have reported that *H. pylori* is exhibiting an increasing double resistance to metronidazole and this has drawn the attention many researchers to study physiological and pharmacological significance of some metronidazole and its derivatives (Alawadi *et al.*, 2015). To contribute to this ongoing area of research, this study investigates the relative substituents' effects on the interactions of some nitroimidazole derivatives on the target; nitroreductase RdxA proteins (PDB ID: 3qdl).

The roles of computational chemistry for the qualitative and quantitative evaluation of substances and in almost every field of chemistry cannot be overstated. Of recent, it is routinely used to accelerate the long and costly drug discovery/design activities, from drug target identification, commonly a receptor or an enzyme, to the design and optimization of new drug-like compounds. Thus, each computational chemistry method can impact and accelerate a given phase of the drug discovery

process, from structure-based drug design technique molecular docking (stimulation of molecular interaction and generation of potent inhibitory ability, i.e., binding affinity), molecular dynamics for hit identification and lead generation to quantitative structure-activity relationship (QSAR) (Adejoro *et al.*, 2016).

The quantum mechanically derived molecular descriptors and physicochemical variables also dictate the pharmacokinetics of any studied compounds (Venkatesh and Aravinda, 2017). These calculated descriptors affect their drug-likeness and, ultimately, their absorption, distribution, metabolism, excretion and toxicity (ADMET) properties, which are the key factors to be optimized to generate drug candidate in clinical trials (Palermo and Vivo, 2015). ADMET properties influence the drug levels and the kinetics of drug exposures to the tissues, and, hence, the performance and pharmacological activities of compounds as drugs (Patil, 2016). This study, therefore, determines the ADME properties of the studied 2HMN and some other derivatives of nitroimidazole to investigate their oral-bioavailability and drug-likeness properties.

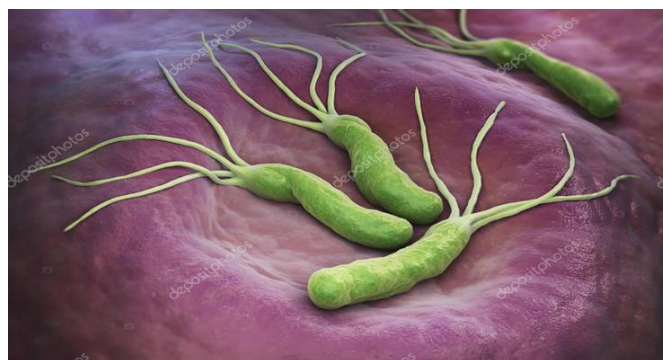


Figure 1. Pictorial view of *H. pylori*.
Source: Bürgers *et al.* (2008).

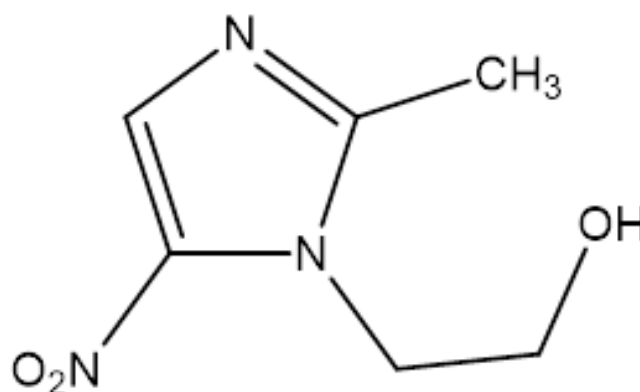


Figure 2. Structure of metronidazole [A].

2. Materials and Methods

2.1 Ligand Preparation

The ligands preparation and computational analyses of the studied compounds were carried out with Spartan-14 software package at DFT/B3LYP/6-311G** level of theory. Using molecular editor builder of Spartan 14, the equilibrium geometries of each of these compound A–F (Tab. 1), were modeled, and their structures were minimized. The compounds were fully optimized (Fig. 3) using equilibrium geometry at ground state, with the features in the personal computer Spartan 14 software at HF-DFT self-consistent field level of theory, to estimate the physicochemical properties; dipole moment, polarizability, solvation energy, partition coefficient (log P), a measure of lipophilicity/ hydrophobicity, frontier orbital energies (E_{HOMO} and E_{LUMO}) of the studied compounds. Following their geometry optimization, their energy gaps ($E_{\text{HOMO}}-E_{\text{LUMO}}$) were computed. The E_{HOMO} and E_{LUMO} of the modeled molecules were related to the ionization potential (IP), the electron affinity (EA), and the global hardness (η), using Koopman's theorem (1–3) (Adeoye *et al.*, 2019). These descriptors help to predict, on theoretical basis, the chemical activities of these compounds.

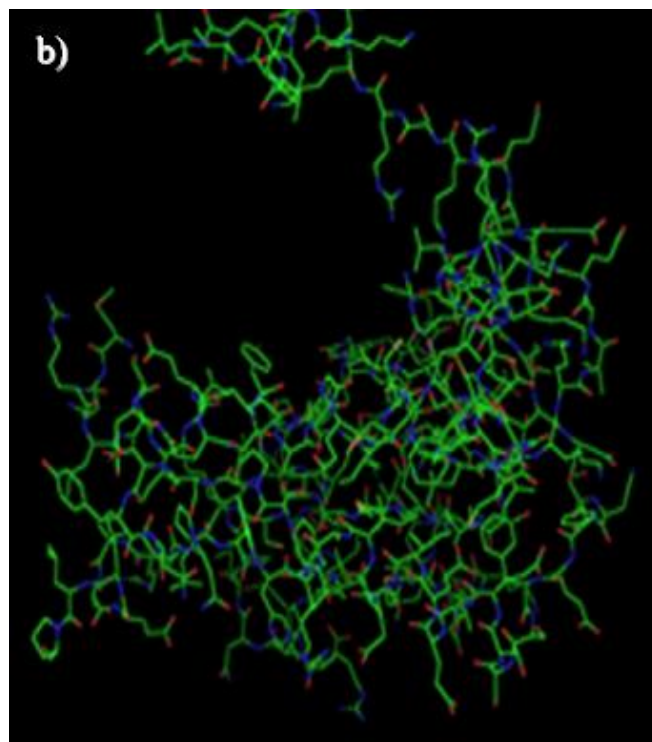


Figure 3. Structures of (a) [raw protein (3dql)] and (b) [cleaned protein].

Source: Martínez-Júlvez *et al.* (2012).

Table 1. Two-dimensional (2D) structures of the studied compounds.

	R ₁	Name
A	OH	1-(2-hydroxyethyl)-2-methyl-5-nitroimidazole
B	H	N-ethyl-2-methyl-5-nitroimidazole
C	SPh	1-(2-thiophenylethyl)-2-methyl-5-nitroimidazole
D	COOH	1-(2-carboxylethyl)-2-methyl-5-nitroimidazole
E	NO ₂	1-(2-nitroethyl)-2-methyl-5-nitroimidazole
F	OCH ₃	1-(2-methoxyethyl)-2-methyl-5-nitroimidazole

2.2 Preparation of the Studied Receptor (Protein)

The target protein for this study was nitroreductase Rdx protein (PDB ID: 3QDL) (Martínez-Júlvez *et al.*, 2012). The 3D structure (X-ray diffraction) was obtained from the protein data bank and treated with PyMOL 1.7.4.4 for the removal of water molecules and any other residues apart from the desired molecule. Schrödinger (Maestro 12.7) (Morakinyo *et al.*, 2022) and the

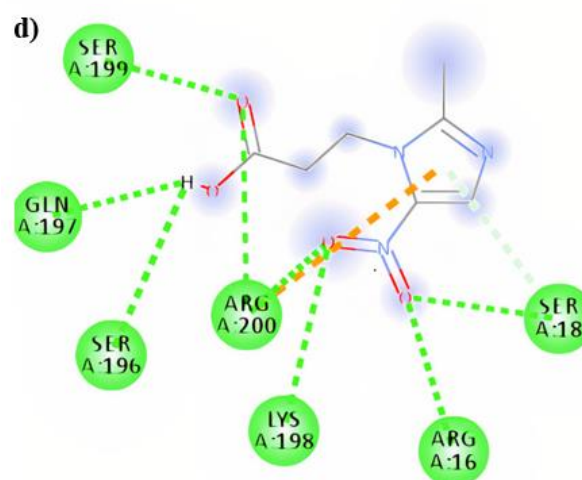
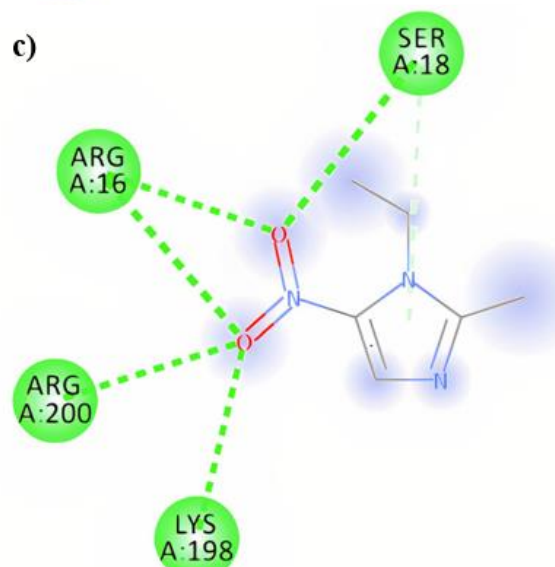
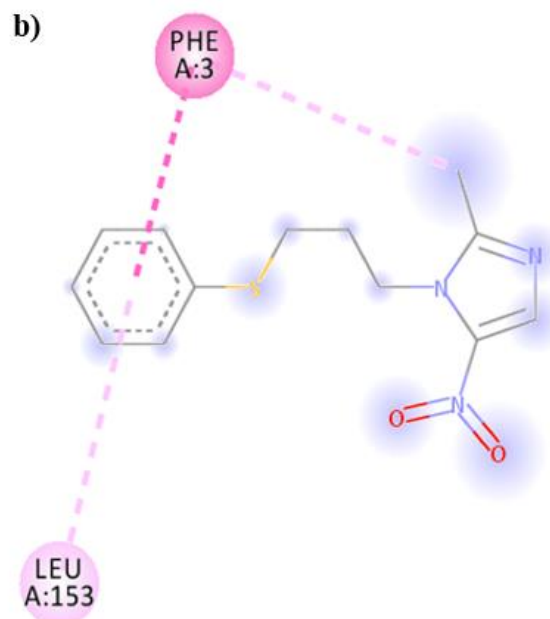
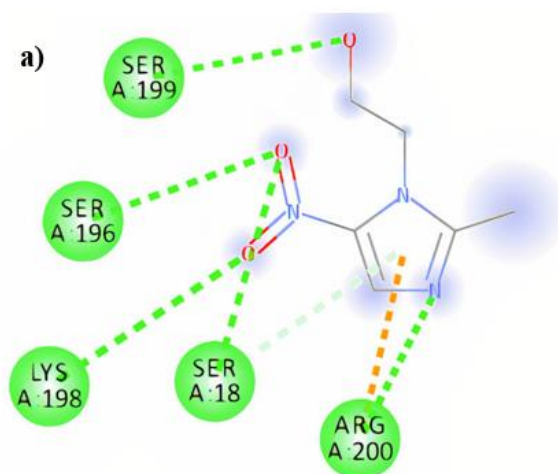
references therein attached journals were used to determine the target protein's active site, in preparation for site specific docking. The structure of the raw protein (3dql) from the data bank and the cleaned protein are as presented in Figs. 4a and b.

2.3 Molecular Docking Analysis

The optimized compounds were docked into the active pockets of the target *H. pylori* protease; nitroreductase RdxA protein (PDB ID: 3QDL), using two softwares with different algorithm profiles (Autodock Vina and Discovery studio) to predict their binding abilities with the studied receptor (Forli *et al.*, 2016; Roche *et al.*, 2015). The docking process mainly involves spatial matching and energy matching (Meng *et al.*, 2011) between the ligand and the receptor (cleaned protein) for optimal conformation. The grid center (X = 16.082, Y = 4.657, Z = 10.976) and box size (X = 84, Y = 94, Z = 46) were used. And the spacing was set to be 1.00 Å.

2.4 ADMET Prediction

The absorption, distribution, metabolism, excretion and toxicology of a substance in and through the human body are dealt with by ADMET characteristics (Balani *et al.*, 2005). The modeled ligands (A–F) were evaluated for their ADME properties using SwissADME software (Daina *et al.*, 2017; Oyebamiji *et al.*, 2022) for accessing their oral-bioavailability and drug-likeness features. These assist in studying the ligands' pharmacokinetics and pharmacodynamics properties (Iwaloye *et al.*, 2021). Molecular weight, hydrogen bond donor (HBD), hydrogen bond acceptor (HBA), blood–brain barrier (BBB), human intestinal absorption (HIA) are all predicted significant ADME properties.



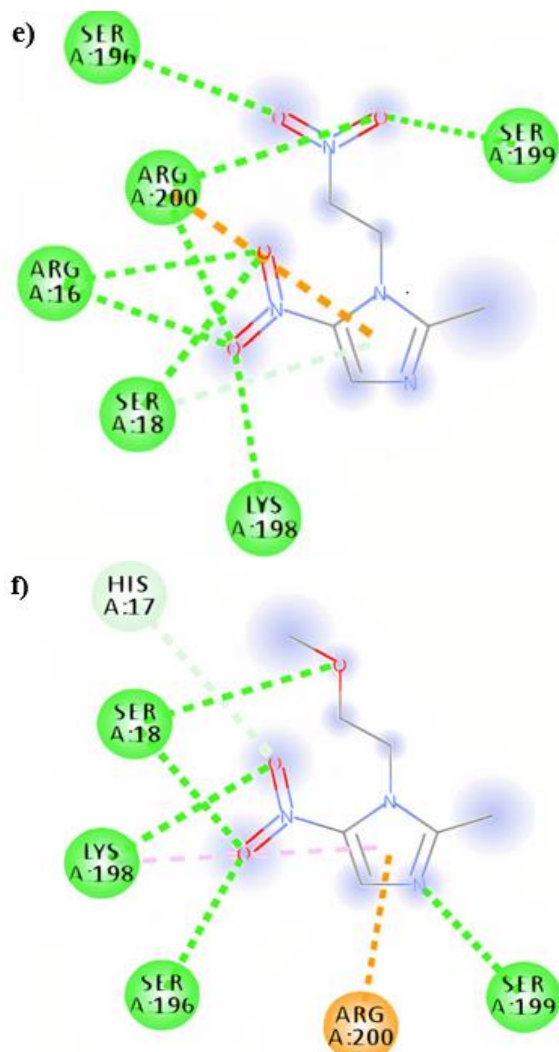


Figure 4. 2D structure of interaction between compound (a–f) and nitroreductase RdxA protein (PDB ID: 3QDL).

3. Results and Discussion

3.1 Calculated Descriptors

The frontier orbital electron densities of atoms in a molecule can be used to analyze the electron donor acceptor interaction (Akintelu *et al.*, 2021). The 2D structures for the studied compounds are as shown on Tab. 1. The frontier molecular orbital energies (E_{HOMO} and E_{LUMO}) are used to determine how a molecule interacts with the other species. The E_{HOMO} orbital energy donates electron, since it is the outermost (highest energy) orbital containing electrons. In contrast, the E_{LUMO} orbital accepts electrons since it is the innermost (lowest energy) orbital that can accept electrons (Raj *et al.*, 2015). According to the frontier molecular orbital theory, the interaction between the

HOMO and LUMO of reactants formed the transition state.

The E_{HOMO} and E_{LUMO} are directly related to the IP and EA respectively (Eqs. 1 and 2). Higher E_{HOMO} signify that the compound has stronger ability to donate electron(s) to the neighboring compound, the better ability of its drug-likeness properties, as well as the ability of such compound to inhibit receptor (Gao *et al.*, 2010). The band gap ($E_g/E_{HOMO}-E_{LUMO}$) is also an important parameter that reflects the chemical activity of the molecules. The E_g and associated molecular/physicochemical properties are as presented in Tab. 2. More so, the HOMO π -electrons are delocalized on the 5-nitroimidazole ring in compounds A, B, D and E, delocalized on the entire molecules in compound F, but localized on thiophenylethyl substituent of compound C. However, the LUMO π -electrons are more localized on the nitro (NO_2) group substituent of the nitroimidazole ring in compounds A, B, D, E and F, but are more localized on the 5-nitroimidazole ring in compound C. This attests to studied compounds' intramolecular charge transfer characteristic properties (Kulhánek *et al.*, 2012). The lowest and highest E_g values were recorded for compound C (3.94 eV) and E (4.63 eV) respectively; a strong indication of highest distribution of charges, and hence, the probability of higher chemical activity of compound C ($R = SPh_3$) compared with the other compounds (Oyebamiji *et al.*, 2021a).

$$IP = E_{HOMO} \quad (1)$$

$$EA = E_{LUMO} \quad (2)$$

The partition coefficient (lipophilicity / log P) plays important roles in drugs design (Méndez-Lucio *et al.*, 2017). It has been described as the main physicochemical determinant that influences the bioavailability, permeability, and penetrability of pharmacophore in biological membranes, and toxicity of the compounds. Their values are therefore used as determinants in some industrial processes, such as agricultural chemistry, drug formulation and flavoring of finished products (Lipinski *et al.*, 2020; Oyebamiji *et al.*, 2021b). According to the Lipinski's rule of 5 (MW \leq 500 amu, LogP [octanol-water partition coefficient] \leq 5, HDB [total number of N–H and O–H bonds] \leq 5 and HBA [total number of N and O atoms] \leq 10) (Erazua *et al.*, 2021), problem is likely to be encountered in the oral usage of this drug-like compound if log P value is higher than 5 (Stefaniu and Pintilie, 2018). The log P for all the studied compounds (Tab. 2) were within the acceptable range, which therefore showed that the compounds can be taken

orally. Compounds D, E, F have their log P values (0.59–0.7) less than 1, being closer to that of the standard—metronidazole (0.42). Furthermore, for compounds to be useful in drug formulation targeted at central nervous

system, and intestinal absorption, their log P should fall in the range; 1.35–1.8 (Adegoke *et al.*, 2020). This was observed for compounds B (1.28), while the log P for compound C is slightly greater than 3 (Tab. 2).

Table 2. Calculated descriptors for the studied compounds.

Mol		A	B	C	D	E	F
MW (amu)	Molecular weight	171.15	155.15	277.34	199.16	200.15	185.18
DM (Debye)	Dipole moment	4.55	4.89	2.98	4.29	3.88	3.59
E_{HOMO} (eV)	Highest occupied molecular orbital	-6.80	-6.90	-6.26	-7.03	-7.35	-6.95
E_{LUMO} (eV)	Lowest unoccupied molecular orbital	-2.26	-2.29	-2.32	-2.41	-2.72	-2.39
Band Gap	Band gap	4.54	4.61	3.94	4.62	4.63	4.56
HBA	Hydrogen bond accept	5	4	5	5	5	5
HBD	Hydrogen bond donor	1	0	0	1	0	0
Log p	Lipophilicity	0.42	1.28	3.45	0.70	0.59	0.78
Ovality	Ovality	1.30	1.29	1.47	1.35	1.35	1.36
PSA (Å²)	Polar surface area	65.15	46.30	46.06	80.15	85.44	53.77
SE (KJ/mol)	Solvation energy	-37.24	-27.70	-45.09	-43.64	-34.32	-31.80

Note: Referenced drug = Compound A = metronidazole.

Solvation energy, a measure of interaction of solute with solvent that leads to stabilization of species in solution, is also highly significant in drugs development. The highest solvation energies recorded for compound C is an indication that its interaction with solvent will be more thermodynamically favored than other studied molecules (Choi *et al.*, 2013). The trends in the polar surface area of the compounds ($C < B < F < A < D < E$) differ from their volumes ($B < A < E < F < D < C$), and molecular weight ($B < A < F < D < E < C$) variations. Ovality is related to molecular surface area and van der Waal's volume; it increases with increasing structural linearity and deviate from spherical form, which is usually 1 for spherical shape molecules (Abdul-Hammed *et al.*, 2020). The reported trend in the ovality values of the studied compounds: $B (1.29) < A (1.30) < D (1.35) = E (1.35) < F (1.36) < C (1.49)$, suggests that compound C vary more greatly from spherical shape than the other compounds. The dipole moment and polarizability of molecule which measure the bond properties (induction polarization), charge densities and nonbonding interactions between ligand and receptor of molecules follow the trend: $B > A > D > E > F > C$. As reported by Adeoye *et al.* (2017) and Oyewole *et al.* (2020), the unpredictable properties of drug-like molecules may arise as a result of large dipole moment value, molecules with better charge distribution and increasing distance will have higher dipole moment and polarizability. Thus, the studied compounds may possibly have strong nonbonded connections with the target nitroreductase Rdx proteins (PDB ID: 3qdl).

3.2 Molecular Docking and ADME Studies

A docking study was used to predict the preferred orientation or correct conformation of the ligand in the active site of the protein. The binding energy measure of binding affinity is an important parameter generated from molecular docking to provide information on the strength of the interaction between the ligand and receptor. The interaction is spontaneous; the greater the binding affinity (in term of negativity), the better the inhibition (Adeoye *et al.*, 2022; Ibrahim *et al.*, 2019). Consequently, the five studied compounds (B–F) were docked against the target (PDB ID: 3qdl) to determine the nonbonding interactions present in the studied complex using metronidazole (A) as the standard. The calculated binding affinities for the compounds A–F were -18.8 , -18.0 , -17.2 , -21.3 , -21.3 and -18.4 kJ mol⁻¹, respectively. Compounds D and E have the same binding affinity (-21.3 kJ mol⁻¹) and inhibition constant (7.8) which were compared with the referenced drug (compound A [metronidazole]) (Tab. 3 and Fig. 4). It was observed that the addition of $-COOH$ and $-NO_2$ to the parent compound enhanced it inhibit activity. Also, as shown in Tab. 2, lower ability of compounds D and E to donate electron to target compounds as well as their greater capacity to receive from the nearby compounds enhanced it capability to inhibit nitroreductase Rdx proteins than others studied compound as well as the referenced drug (compound A).

Table 3. Calculated scoring, residues, inhibition constant and types of non-bonding interactions between 2HMN derivatives and Nitroreductase RdxA Protein (PDB ID: 3qdl).

Compounds	Binding Affinity (kJ mol ⁻¹)	Residue involved in the interaction	Inhibition constant K _i (nmol L ⁻¹)	Types of nonbonding interaction involved
A	-18.8	SER 199, SER 196, LYS 198, SER 18, ARG 200	6.1	Conventional hydrogen bond π-carbon, π-donor hydrogen bond
B	-18.0	ARG 16, LYS 198, ARG 200, SER 18	5.6	π- π stacked, π-alkyl C
C	-17.2	PHE 3, LEU 153	5.2	Conventional hydrogen bond, π-donor hydrogen bond
D	-21.3	ARG 16, GLN 17, SER 199, SER 196, LYS 198, SER 18, ARG 200	7.8	Conventional hydrogen bond, π-carbon π-donor hydrogen bond
E	-21.3	SER 199, SER 196, LYS 198, ARG 16, SER 18, ARG 200	7.8	Conventional hydrogen bond, π-carbon π-donor hydrogen bond
F	-18.4	HIS 17, SER 199, SER 196, LYS 198, SER 18, ARG 200	5.9	Conventional hydrogen bond, π-alkyl, π-cation carbon-hydrogen bond

Note: Referenced drug = Compound A = metronidazole.

These compounds proved to possess highest tendency to inhibit nitroreductase RdxA proteins (PDB ID: 3qdl) and may likely be more potent than other studied ligands. The amino acid residues involved in the interactions and the types of nonbonding interactions involved are as

displayed in Fig. 4 and Tab. 3. Furthermore, compounds D and E's ADME features with the best efficient calculated binding affinity were comparable with the standard metronidazole (Tab. 4).

Table 4. Drug-likeness prediction.

Compounds	Molecular weight	Log P	HBD	HBA	Violations
A	171.156	0.42	1	5	0
B	155.157	1.28	0	4	0
C	277.348	3.45	0	5	0
D	199.166	0.70	1	5	0
E	200.154	0.59	0	5	0
F	185.183	0.78	0	5	0

The higher the HIA, the better the compound's tendency to be absorbed upon oral administration (Oyebamiji *et al.*, 2020). As observed in Tab. 5, the values of HIA for the studied compounds are positive and correlated with the standard. This further proved that the selected compounds have capacities to be absorbed in the intestine. The ability to cross the BBB for compounds D and E are also closer to the existing standard drug (metronidazole), while the molar solubility in aqueous state (log S) values of the selected compounds and standards fall within the recommended range of 1 to 5 (Ibrahim *et al.*, 2018). The observed ADME factors indicate that the selected compounds and the standards

have better absorption and distribution properties. The Caco-2 permeability reveals the permeability on lipid absorption and metabolism of the studied compounds (Semire *et al.*, 2017). The probability of this was higher in compound D, but little lower than the standard in the ligand E. Also, in terms of metabolic activities of the selected ligands, compounds D and E are non-inhibitors and nonsubstrates for microsomal enzymes (CYP450 2C9, CYP450 2D6 and CYP450 2C19), similar to the standard. A noninhibitor of CYP450 means that the molecule will not hamper the biotransformation of the drugs metabolized by CYP450 enzyme (Nisha *et al.*, 2016).

Table 5. Predicted ADME properties of the studied compounds.

	Compound D		Compound E		Compound A (Metronidazole)	
	Result	Probability	Result	Probability	Result	Probability
Blood-Brain Barrier	BBB+	0.114253	BBB+	0.12801	BBB+	0.173454
Human Intestinal Absorption	HIA+	High	HIA+	High	HIA+	High
Caco-2 Permeability	Caco-2	High	Caco2+	High	Caco2+	High
Log S	ESOL	-0.67	ESOL	-0.86	ESOL	-1.00
Solubility (mg/ml)	Very soluble	4.32+01	Very soluble	2.76+01	Very soluble	1.72+01
Log S	Ali	-1.00	Ali	-1.49	Ali	-1.29
P-gp substrate	Substrate	No	Substrate	No	Substrate	No
Log p	ILOGP	0.77	ILOGP	0.59	ILOGP	1.16
Lipinski's rule		Yes		Yes		Yes
CYP450 2D6 Substrate	Noninhibitor	No	Substrate	No	Noninhibitor	No
CYP450 2C9 Inhibitor	Noninhibitor	No	Noninhibitor	No	Noninhibitor	No
CYP450 2D6 Inhibitor	Noninhibitor	No	Noninhibitor	No	Noninhibitor	No
CYP450 2C19 Inhibitor	Noninhibitor	No	Noninhibitor	No	Noninhibitor	No
CYP450 3A4 Inhibitor	Inhibitor	No	Inhibitor	No	Inhibitor	No
CYP450 3A4 Substrate	Substrate	No	Substrate	Substrate	Substrate	Substrate
Synthetic accessibility		2.23		2.53		2.30
Ghose		0		0		0
Vegar		0		0		0
Pain		0, Alert		0.12801		0, Alert

4. Conclusions

This study was carried out to determine the effects of substituents: -OH, H, -SPh, -COOH, -NO₂ and -OCH₃ on the chemical activities and interactions of six nitroimidazole derivatives on the target nitroreductase Rdx protein (PDB ID: 3qdl) for the treatment of *H. pylori* infection. The nonbonding interactions and the calculated binding affinities that exist between the six compounds and the nitroreductase Rdx protein were identified. The ADME features showed that substituted -COOH and -NO₂ nitroimidazole derivatives has the same binding energies (kJ mol⁻¹) and higher tendency to inhibit target nitroreductase Rdx protein (PDB ID: 3qdl) than the referenced drug despite their higher band gaps. The compounds are also noninhibitors and non-substrates for microsomal enzymes (CYP450 2C9, CYP450 2D6 and CYP450 2C19), with capacities to be absorbed in the intestine and ability to cross the BBB comparable with the standard.

Authors' contribution

Conceptualization: Adeoye, M. D.; Oyebamiji, A. K.

Data curation: Adeoye, M. D.; Oyebamiji, A. K.

Formal Analysis: Adeoye, M. D.; Oyebamiji, A. K.

Funding acquisition: Ashiru, M. J.; Adigun, R. A.

Investigation: Adeoye, M. D.

Methodology: Adeoye, M. D.

Project administration: Adeoye, M. D.

Resources: Olalere, O. H.

Software: Semire, B.

Supervision: Semire, B.

Validation: Oyebamiji, A. K.

Visualization: Adeoye, M. D.; Oyebamiji, A. K.

Writing – original draft: Adeoye, M. D.

Writing – review & editing: Oyebamiji, A. K.

Data availability statement

All data sets were generated or analyzed in the current study.

Funding

Not applicable

Acknowledgments

We are grateful to Computational Chemistry Research Laboratory, Chemical Sciences Department, Fountain University and Mrs. E. T. Oyebamiji as well as Miss Priscilla F. Oyebamiji for the assistance in the course of this study.

References







Abdul-Hammed, M.; Semire, B.; Adegboyega, S. A.; Oyebamiji, A. K.; Olowolafe, T. A. Inhibition of cyclooxygenase-2 and thymidylate synthase by dietary sphingomyelins: insights from DFT and molecular docking studies. *Phys. Chem. Res.* **2020**, *8* (2), 297–311. <https://doi.org/10.22036/pcr.2020.214026.1717>

Adegoke, R. O.; Oyebamiji, A. K.; Semire, B. Dataset on the DFT-QSAR, and docking approaches for anticancer activities of 1, 2, 3-triazole-pyrimidine derivatives against human

- esophageal carcinoma (EC-109). *Data Br.* **2020**, *31*, 105963. <https://doi.org/10.1016/j.dib.2020.105963>
- Adejoro, I. A.; Waheed, S. O.; Adeboye, O. O. Molecular docking studies of *Lonchocarpus cyanescens* triterpenoids as inhibitors for malaria. *J. Phys. Chem. Biophys.* **2016**, *6* (2), 1000213. <https://doi.org/10.4172/2161-0398.1000213>
- Adeoye, M. D.; Obi-Egbedi, N. O.; Iweibo, I. Solvent effect and photo-physical properties of 2, 3-diphenylcyclopropenone. *Arabian Journal of Chemistry* **2017**, *10* (Suppl 1), S134–S140. <https://doi.org/10.1016/j.arabjc.2012.06.019>
- Adeoye, M. D.; Abdulsalami, I. O.; Oyeleke, G. O.; Alabi, K. A. Theoretical studies of solvent effects on the electronic properties of 1, 3-bis [(furan-2-yl) methylene] urea and thiourea. *J. Phys. Theor. Chem. IAU, Iran.* **2019**, *15* (3–4), 115–125.
- Adeoye, M. D.; Olarinoye, E. F.; Oyebamiji, A. K.; Latona, D. F. Theoretical evaluation of potential anti-alanine dehydrogenase activities of acetamide derivatives. *Biointerface Res. Appl. Chem.* **2022**, *12* (6), 7469–7477 <https://doi.org/10.33263/BRIAC126.74697477>
- Akintelu, S. A.; Folorunso, A. S.; Oyebamiji, A. K. Phytochemical and antibacterial investigation of *Moringa oleifera* seed: Experimental and computational approaches. *Eclat. Quim. J.* **2021**, *46* (2), 17–25. <https://doi.org/10.26850/1678-4618eqj.v46.2.2021.p17-25>
- Alawadi, D. Y.; Saadeh, H. A.; Kaur, H.; Goyal, K.; Sehgal, R.; Hadda, T. B.; ElSawy, N. A.; Mubarak, M. S. Metronidazole derivatives as a new class of antiparasitic agents: synthesis, prediction of biological activity, and molecular properties. *Med. Chem. Res.* **2015**, *24* (9), 1196–1209. <https://doi.org/10.1007/s00044-014-1197-4>
- Balani, S.; Miwa, G. T.; Gan, L.-S.; Wu, J.-T.; Lee, F. W. Strategy of utilizing *in-vitro* and *in-vivo* ADME tools for lead optimization and drug candidate selection. *Curr. Top. Med. Chem.* **2005**, *5* (11), 1033–1038. <https://doi.org/10.2174/156802605774297038>
- Bürgers, R.; Schneider-Brachert, W.; Reischl, U.; Behr, A.; Hiller, K.-A.; Lehn, N.; Schmalz, G.; Ruhl, S. *Helicobacter pylori* in human oral cavity and stomach. *Eur. J. Oral. Sci.* **2008**, *116* (4), 297–304. <https://doi.org/10.1111/j.1600-0722.2008.00543.x>
- Choi, H.; Kang, H.; Park, H. New solvation free energy function comprising intermolecular solvation and intramolecular self-solvation terms. *J. Cheminformatics.* **2013**, *5*, 8. <https://doi.org/10.1186/1758-2946-5-8>
- Daina, A.; Michielin, O.; Zoete, V. Swiss ADME: A free web tool to evaluate pharmacokinetics, drug-likeness and medicinal chemistry friendliness of small molecules. *Sci. Rep.* **2017**, *7*, 42717. <https://doi.org/10.1038/srep42717>
- Erazua, E. A.; Akintelu, S. A.; Adelowo, J. M.; Odoemene, S. N.; Josiah, O. M.; Raheem, S. F.; Latona, D. F.; Adeoye, M. D.; Esan, A. O.; Oyebamiji, A. K. QSAR and molecular docking studies on nitro(triazole/imidazole)-based compounds as anti-tubercular agents. *Trop. J. Nat. Prod. Res.* **2021**, *5* (11), 2022–2029. <https://doi.org/10.26538/tjnpr/v5i11.22>
- Forli, S.; Huey, R.; Pique, M.; Sanner, M. F.; Goodsell, D. S.; Olson, A. Computational protein-ligand docking and virtual drug screening with the AutoDock suite. *Nat. Protoc.* **2016**, *11* (5), 905–919. <https://doi.org/10.1038/nprot.2016.051>
- Gao, Q.; Yang, L.; Zhu, Y. Pharmacophore based drug design approach as a practical process in drug discovery. *Curr. Comput.-Aided Drug Des.* **2010**, *6* (1), 37–49. <https://doi.org/10.2174/157340910790980151>
- Ghotaslou, R.; Leylabadlo, H. E.; Asl, Y. M. Prevalence of antibiotic resistance in *Helicobacter pylori*: A recent literature review. *World J. Methodol.* **2015**, *5* (3), 164–174. <https://doi.org/10.5662/wjm.v5.i3.164>
- Houghton, J. M.; Wang, T. C. *Helicobacter pylori* and gastric cancer: A new paradigm for inflammation-associated epithelial cancers. *Gastroenterology.* **2005**, *128* (6), 1567–1578. <https://doi.org/10.1053/j.gastro.2005.03.037>
- Ibrahim, A. O.; Oyebamiji, A. K.; Semire, B. Computational investigations on stability and equilibrium composition of (Z)-indol-3-ylidenemethanol: an enol-tautomer of 1H-indole-3-carbaldehyde via DFT Approach. *Curr. Phys. Chem.* **2018**, *8* (3), 194–210. <https://doi.org/10.2174/1877946809666181212113209>
- Ibrahim, A. O.; Oyebamiji, A. K.; Semire, B. Thermodynamics and kinetics of hydrogen transfer mechanism in 1-[(E)-1,3-benzothiazol-2-ylazo]naphthalen-2-ol tautomers in aqueous medium: Density functional theory. *Iraqi J. Sci.* **2019**, *60* (4), 677–687.
- Iwaloye, O.; Elekofehinti, O. O.; Kikiowo, B.; Fadipe, T. M.; Akinjiyan, M. O.; Ariyo, E. O.; Aiyeku, O. O.; Adewumi, N. A. Discovery of traditional Chinese medicine derived compounds as wild type and mutant *Plasmodium falciparum* dihydrofolate reductase inhibitors: Induced fit docking and ADME studies. *Curr. Drug Discov. Technol.* **2021**, *18* (4), 554–569. <https://doi.org/10.2174/1570163817999200729122753>
- Jemilohun, A. C. Otegbayo, J. A. *Helicobacter pylori* infection: Past, present and future. *Pan Afr. Med. J.* **2016**, *23*, 216. <https://doi.org/10.11604/pamj.2016.23.216.8852>
- Kayali, S.; Manfredi, M.; Gaiani, F.; Bianchi, L.; Bizzarri, B.; Leandro, G.; Di Mario, F.; de' Angelis, G. L. *Helicobacter pylori*, transmission routes and recurrence of infection: State of the art. *Acta. Biomed.* **2018**, *89* (8-S), 72–76. <https://doi.org/10.23750/abm.v89i8-S.7947>
- Kim, Y.; Lee, K. H.; Kim, J.-H.; Park, S. P.; Song, Y. G.; Jeon, S. Y.; Park, H. Is Only clarithromycin susceptibility important for the successful eradication of *Helicobacter pylori*? *Antibiotics* **2020**, *9* (9), 589. <https://doi.org/10.3390/antibiotics9090589>

- Kulhánek, J.; Bureš, F. Imidazole as a parent π -conjugated backbone in charge-transfer chromophores. *Beilstein J. Org. Chem.* **2012**, *8*, 25–49. <https://doi.org/10.3762/bjoc.8.4>
- Lipinski, C. A.; Lombardo, F.; Dominy, B. W.; Feeney, P. J. Experimental and computational approaches to estimate solubility and permeability in drug discovery and development settings. *Advanced Drug Delivery Reviews.* **2001**, *46*, 1–3, 3–26. [https://doi.org/10.1016/S0169-409X\(00\)00129-0](https://doi.org/10.1016/S0169-409X(00)00129-0)
- Martínez-Júlvez, M.; Rojas, A. L.; Olekhovich, I.; Angarica, V. E.; Hoffman, P. S.; Sancho, J. Structure of RdxA—an oxygen-insensitive nitroreductase essential for metronidazole activation in *Helicobacter pylori*. *FEBS J.* **2012**, *279*, 4306–4317. <https://doi.org/10.1111/febs.12020>
- Méndez-Lucio, O.; Medina-Franco, J. L. The many roles of molecular complexity in drug discovery. *Drug Discov. Today.* **2017**, *22* (1), 122–126. <https://doi.org/10.1016/j.drudis.2016.08.009>
- Meng, X.-Y.; Zhang, H.-X.; Mazei, M.; Cui, M. Molecular Docking: A powerful approach for structure-based drug discovery. *Curr. Comput.-Aided Drug Des.* **2011**, *7* (2), 146–157. <https://doi.org/10.2174/157340911795677602>
- Morakinyo, A. E.; Omoniyi, F. E.; Nzekwe, S. C.; Oyebamiji A. K.; Adelowo, J. M.; Lawal, S. A.; Olumade, A. A.; Olopade, E. O.; Oyedepo, T. A. Cardio-protective effect of *Hunteria umbellata* seed: Experimental and *in-silico* approaches. *Trop. J. Nat. Prod. Res.* **2022**, *6* (1), 87–94. <https://doi.org/10.26538/tjnpr/v6i1.16>
- Nisha, C. M.; Kumar, A.; Nair, P.; Gupta, N.; Silakari, C.; Tripathi, T.; Kumar, A. Molecular docking and *in silico* ADMET study reveals acylguanidine 7a as a potential inhibitor of β -secretase. *Adv. Bioinform.* **2016**, 2016, 9258578. <https://doi.org/10.1155/2016/9258578>
- Oyebamiji, A. K.; Tolufashe, G. F.; Oyawoye, O. M.; Oyedepo, T. A.; Semire, B. Biological activity of selected compounds from *Annona muricata* seed as antibreast cancer agents: Theoretical study. *J. Chem.* **2020**, 2020, 6735232. <https://doi.org/10.1155/2020/6735232>
- Oyebamiji, A. K.; Fadare, O. A.; Akintelu, S. A.; Semire, B. Biological studies on anthra[1,9-cd]pyrazol-6(2D)-one analogues as anti-vascular endothelial growth factor via *in silico* mechanisms. *Chemistry Africa.* **2021a**, *4* (4), 955–963. <https://doi.org/10.1007/s42250-021-00276-2>
- Oyebamiji, A. K.; Josiah O. M.; Akintelu, S. A.; Adeoye, M. D.; Sabitu, B. O.; Latona, D. F.; Esan, A. O.; Soetan, E. A.; Semire, B. Dataset on insightful bio-evaluation of 2-(quinoline-4-yloxy)acetamide analogues as potential anti-mycobacterium tuberculosis catalase-peroxidase agents via *in silico* mechanisms. *Data Br.* **2021b**, *38*, 107441. <https://doi.org/10.1016/j.dib.2021.107441>
- Oyebamiji, A. K.; Soetan, E. A.; Akintelu, S. A.; Ayeleso, A. O.; Mukwevho, E. Alpha-glucosidase activity of phytochemicals from *Phyllanthus amarus* leaves via *in-silico* approaches. *Pharmacological Research - Modern Chinese Medicine.* **2022**, *2*, 00054. <https://doi.org/10.1016/j.prmcm.2022.100054>
- Oyewole, R. O.; Oyebamiji, A. K.; Semire, B. Theoretical calculations of molecular descriptors for anticancer activities of 1, 2, 3-triazole-pyrimidine derivatives against gastric cancer cell line (MGC-803): DFT, QSAR and docking approaches. *Heliyon.* **2020**, *6* (5), e03926. <https://doi.org/10.1016/j.heliyon.2020.e03926>
- Palermo, G.; Vivo, M. Computational chemistry for drug discovery. In *Encyclopedia of Nanotechnology*. Springer Science, 2015; pp 1–15. https://doi.org/10.1007/978-94-007-6178-0_100975-1
- Patil, P. S. Drug discovery and ADMET process: A review. *Int. J. Adv. Res. Biol. Sci.* **2016**, *3* (7), 181–192. <http://s-o-i.org/1.15/ijarbs-2016-3-7-26>
- Raj, U.; Kumar, H.; Gupta, S.; Varadwaj, P. K. Novel DOT1L receptor natural inhibitors involved in mixed lineage leukemia: A virtual screening, molecular docking and dynamics simulation study. *Asian Pac. J. Cancer Prev.* **2015**, *16* (9), 3817–3825. <https://doi.org/10.7314/APJCP.2015.16.9.3817>
- Roche, D. B.; Brackenridge, D. A.; Guffin, L. J. Proteins and their interacting partners: An introduction to protein-ligand binding site prediction methods. *Int. J. Mol. Sci.* **2015**, *16* (12), 29829–29842. <https://doi.org/10.3390/ijms161226202>
- Semire, B.; Mutiu, O. A.; Oyebamiji, A. K. DFT and *ab initio* methods on NMR, IR and reactivity indices of indol-3-carboxylate and indazole-3-carboxylate derivatives of cannabinoids: comparative study. *J. Phys. Theor. Chem. IAU, Iran.* **2017**, *13* (4), 353–377.
- Stefaniu A.; Pintilie, L. Molecular descriptors and properties of organic molecules. In *Symmetry (group theory) and mathematical treatment in chemistry*. IntechOpen, 2018; pp 161–177. <https://doi.org/10.5772/intechopen.72840>
- Venkatesh, K.; Aravinda, P. Application of molecular descriptors in modern computational drug design—an overview. *Research J. Pharm. Tech.* **2017**, *10* (9), 3237–3241. <https://doi.org/10.5958/0974-360X.2017.00574.1>
- Wu, C.-Y.; Kuo, K. N.; Wu, M.-S.; Chen, Y.-J.; Wang, C.-B.; Lin, J.-T. Early *Helicobacter pylori* decreases patients with peptic ulcer diseases. *Gastroenterology.* **2009**, *137* (5), 1641–1648. <https://doi.org/10.1053/j.gastro.2009.07.060>

Experimental, DFT, molecular docking and *in silico* ADMET studies of cadmium-benzenetricarboxylates

Enyi Inah Bassey¹, Terkumbur Emmanuel Gber^{2,3+}, Edison Esther Ekpenyong¹, Henry Okon Edet³, Innocent Benjamin³, Imabasi Tom Ita^{2,3}

1. University of Calabar, Inorganic Materials Research Laboratory, Calabar, Nigeria.
2. University of Calabar, Department of Pure and Applied Chemistry, Calabar, Nigeria.
3. University of Calabar, Computational and Bio-Simulation Research Group, Calabar, Nigeria.

+Corresponding author: Terkumbur Emmanuel Gber, **Phone:** +2348059742439, **Email address:** gberterkumburemmanuel@gmail.com

ARTICLE INFO

Article history:

Received: February 27, 2022

Accepted: July 11, 2022

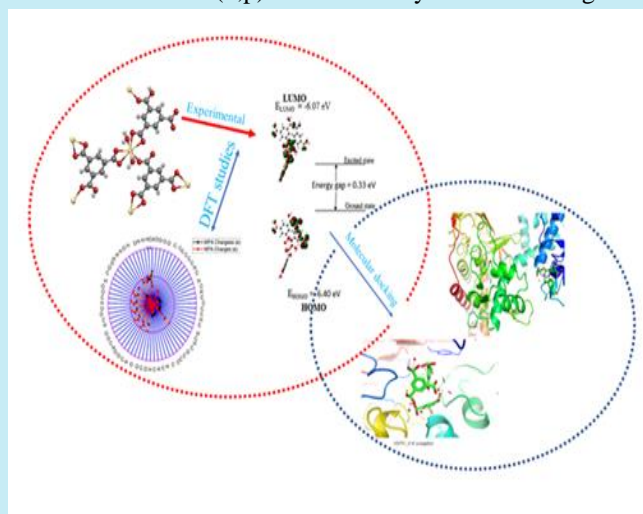
Published: October 28, 2022

Keywords:

1. synthesis
2. characterizations
3. antimicrobial studies
4. metal-organic frameworks

Section Editors: Assis Vicente Benedetti

ABSTRACT: The structure of the polymer $[\text{Cd}(\text{BTC})(\text{H}_2\text{O})_2]_n$ was identified by X-ray single-crystal crystallography. The complex's stability and overall reactivity were examined at the B3LYP/6-311++G (d,p) level of theory whereas the lighter elements (H, C, and O) were studied using the LanL2DZ basis set. The electron distribution in the complex's highest occupied molecular orbital is solely concentrated in a small area, with no electrons distributed over the cadmium. Consequently, the electrons in the complex's lowest unoccupied molecular orbital (LUMO) were dispersed equally. The Cd atom is partially obscured by charge delocalization in the LUMO. The natural bond orbital analysis supports the result for reactivity studies. The rate of absorption, distribution, metabolism, excretion, and toxicity (ADMET) of the complex evaluated by molecular docking in a bid allowed comprehend the biological applicability. The $[\text{Cd}(\text{BTC})(\text{H}_2\text{O})_2]_n$ exhibited excellent binding affinity with proteins 1D7U and 2XCS, while by ADMET it is suggested that cytotoxicity and carcinogenicity were inactive. It is clearly shown that the complex has strong biological uses, notably for the treatment of microbial diseases.



1. Introduction

Microbes are living creatures such as bacteria, fungus, viruses, and parasites that evolve through time. Their primary goals are to survive, reproduce and spread. They modify and adapt to their surroundings in order to survive (Gupta *et al.*, 2017; Reygaert, 2018). Genetic alterations may take place in the presence of an antimicrobial inhibitor to guarantee the bacteria's ongoing existence (Purssell, 2020). The mortality rate from infectious diseases brought on by resistant bacteria has increased as a result of antimicrobial drug resistance to certain antibiotics, such as quinolones (Balaban *et al.*, 2019; Odonkor and Addo, 2011). Therefore, it is necessary to create efficient microbial agents that are aimed at these issues.

Due to their highly porous nature and adaptable hybrid composition, metal organic frameworks (MOFs), which are porous coordination polymers, made of metal ions and organic ligands, have become new contenders in the search for novel dosage forms that may be used to enhance a patient's treatment and quality of life in general. Because of their superior encapsulation and physicochemical (releasing) capabilities, these solids, which were originally thought to be best suited for other uses including sensing (Sun *et al.*, 2013; Vikrant *et al.*, 2018), catalysis (Li *et al.*, 2019), gas storage (Cai *et al.*, 2020), and separation, have now been used in biological applications. A wide range of applications for MOFs in medication delivery are being investigated. These solids, which were first employed to transport medications in the form of tiny molecules, are currently a subject of increased research for the delivery of treatments of all types, including macromolecular cargos such proteins (Chuhadiya *et al.*, 2021; Lawson *et al.*, 2021; Pastore *et al.*, 2018), nucleic acids, cells (Kumar *et al.*, 2015).

To sufficiently explain how cadmium is employed in biological applications. Here, we report recent articles that expressly assert that cadmium exhibits substantial biological activity. In this context, density functional theory (DFT) has recently been applied to theoretically examine the bioactivity of cadmium complexes as promising antibacterial therapeutics. DFT studies, Hirschfeld surface analysis and antimicrobial activity were reported to be effective in biological application most significantly in the treatment of microbial diseases as reported by El-Gammal *et al.* (2014). Additionally, Hamdani and Amame (2019) carried out preparation, spectral, antibacterial, and anticancer molecular docking investigations of novel metal complexes $[M(\text{caffeine})_4](\text{PF}_6)_2$, where M was the chosen metal including cadmium. This finding demonstrated the cadmium complex's high calculated affinity for the protein P13K,

demonstrating the complex's potential as a therapeutic candidate to treat microbial infections. On the other hand, El-Gammal *et al.* (2014) conducted research on the synthesis, characterization, DFT, and biological investigations of isatinpicolinohydrazone interacted with Zn(II), Cd(II), and Hg(II), reporting that these metals demonstrated robust action in biological studies involving Cd(II). In a similar vein, Konakanchi *et al.* (2018) investigated the synthesis, structural, biological evaluation, molecular docking, and DFT properties of complexes containing heterocyclic thiosemicarbazones in Co(II), Ni(II), Cu(II), Zn(II), Cd(II), and Hg(II), and found that Cu(II) demonstrated excellent antibacterial and antifungal activities when compared to other studied metals.

In this investigation, a cadmium MOF was synthesized, described, and DFT studies were undertaken to ascertain the molecule's overall reactivity and stability. The atomic charges on the cadmium MOF have been researched and plotted together with the intercharge transfer inside the MOF by the natural bond orbital (NBO) analysis, and the molecular characteristics of the cadmium MOF have been reported. In order to better understand the binding activity, molecular docking was also carried out using the antimicrobial proteins 1D7U and 2XCS in combination with the cadmium MOF. However, in-silico absorption, distribution, metabolism, excretion, and toxicity (ADMET) research has been presented here to support the docking findings and take into account the bioactive molecule's position inside the MOF structure.

2. Materials and methods

2.1 Materials

Cadmium nitrate tetrahydrate (BDH Chemicals Ltd, 98%) – $\text{Cd}(\text{NO}_3)_2 \cdot 4\text{H}_2\text{O}$; ethanol (BDH Chemicals Ltd, 99%), benzene-1,3,5-tricarboxylic acid– H_2BTC , (Alfa Aesar, 99% purity) and deionized water (H_2O).

2.2 Experimental procedure

2.2.1 Synthesis of $[\text{Cd}(\text{BTC})(\text{H}_2\text{O})_2]_n$

The compound was synthesized from a solution mixture of cadmium nitrate tetrahydrate $\text{Cd}(\text{NO}_3)_2 \cdot 4\text{H}_2\text{O}$ (1.2003 g, 1.0 mmol) and 1,3,5-benzene tricarboxylic acid $\text{C}_9\text{H}_6\text{O}_6$ (0.8456 g, 1.0 mmol) using ethanol and deionized water as solvent in the ratio of 2:1 (5.2:2.6 cm^3). The reaction mixture was stirred for 20 min to obtain a complete miscible solution before transferring into an ace pressure glass tube and heated in an oven at a temperature of 120 °C for 24 h. A crop of colourless

crystalline material was obtained on cooling by filtration and washed with distilled water and air dried.

2.3 Crystal structure determination

2.3.1 Crystal structure determination of $[Cd(BTC)(H_2O)_2]_n$

A suitable crystal was selected and mounted on a GVA, PL13110002 diffractometer. The crystal was kept

at 120 K during data collection using Olex2 (Mason *et al.*, 2016), the structure was solved with the SHELXT (Sevvana *et al.*, 2019) structure solution program using intrinsic phasing and refined with the SHELXL (Shemchuk *et al.*, 2020) refinement package using least squares minimization. Crystal DATA for $[Cd(BTC)(H_2O)_2]_n$ is shown in Tab. 1.

Table 1. Crystal data and structure refinement for $[Cd(BTC)(H_2O)_2]_n$.

Identification code	CDJOOE
Empirical formula	C ₉ H ₈ CdO ₈
Formula weight	356.55
Temperature (K)	120(2)
Crystal system	Monoclinic
Space group	I2/a
A (Å)	13.1508(3)
B (Å)	9.1014(2)
C (Å)	17.8971(4)
A (°)	90
B (°)	103.455(2)
Γ (°)	90
Volume (Å ³)	2,083.32(8)
Z	8
Pcalcg (cm ³)	2.274
M (mm ⁻¹)	17.183
F(000)	1,392.0
Crystal size (mm ³)	0.521 × 0.159 × 0.149
Radiation	Cu Kα (λ = 1.54184)
2θ range for data collection (°)	10.164 to 144.642
Index ranges	-16 ≤ h ≤ 13, -7 ≤ k ≤ 11, -21 ≤ l ≤ 22
Reflections collected	3,976
Independent reflections	2005 [R _{int} = 0.0264, R _{sigma} = 0.0273]
Data/restraints/parameters	2005/0/166
Goodness-of-fit on F ²	1.123
Final R indexes [I ≥ 2σ (I)]	R ₁ = 0.0321, wR ₂ = 0.0894
Final R indexes [all data]	R ₁ = 0.0325, wR ₂ = 0.0899
Largest diff. peak/hole (e Å ⁻³)	0.90/-1.33

2.4 Computational method

All the Computational calculations in this work have been carried out using the Gaussian09W and GaussView 6.0.16 softwares (Dennington *et al.*, 2001; Frisch *et al.*, 2016) within the framework of DFT. The B3LYP functional which is a combination of Becke's three parameter exchange functional (B3) with the nonlocal correlation functional of Lee, Yang, and Parr (LYP) assigning the 6-311++G (d,p) and the LanL2DZ basis set was used for the lighter (H, C, O) and heavy elements respectively. The ground state optimization was carried out at singlet state with a positive charge +1. The NBO calculations were conducted using NBO 3.1 module

embedded in Gaussian09W (Bassej *et al.*, 2022). Highest occupied and lowest unoccupied molecular orbital (HOMO and LUMO) isosurface maps were plotted using Multiwfn 3.7 dev software (Isravel *et al.*, 2021). Origin 8.0 Pro was used for charge analysis. For molecular docking simulation, 3D structures of the protein complex (PDB code: 1D7U and 2XCS) were gotten from the Research Collaboratory for Structural Bioinformatics (RCSB) website (Deshpande *et al.*, 2005). The proteins were prepared using the BIOVIA Discovery Studio 4.5 software and docking was then performed using AutoDock Vina (Berman *et al.*, 2002; Trott and Olson, 2010). The 3D and 2D metal-ligand interaction as well as the H-bond interaction was

visualized using the BIOVIA Discovery Studio presented in [Supplementary Information](#) meanwhile the cadmium ligand and the standard drug levofloxacin docked with the receptor protein were visualized using PyMOL ([Seeliger and Groot, 2010](#)). SwissADME and pkCSM was used for the In-silico ADMET studies ([Kiran et al., 2020](#); [Sharbidre et al., 2021](#)).

3. Results and discussion

3.1 Structural parameters

The molecular structure as revealed by single crystal x-ray diffraction (SCXRD) technique shows that the Cd(II) ion is surrounded by seven oxygen atoms. Two of the oxygen atoms (O1W and O2W) are from two coordinated water molecules. The ORTEP drawing of $[\text{Cd}(\text{BTC})(\text{H}_2\text{O})_2]_n$ showing the coordination environment of the Cd(II) ion can be seen in [Fig. 1](#). Bond lengths of Cd–O1W and Cd–O2W are 2.305 and 2.380 Å respectively, and are slightly similar to the bond lengths of Cd–O1W (2.285 Å) and Cd–O2W (2.555 Å) reported by [Louis et al., \(2022\)](#). The other five oxygen atoms are coordinated from three BTC ligands. Two of the BTC molecules are bonded through (O3, O4, O5, and O6) oxygen atoms of the carboxylate group in a bidentate chelating fashion while the third BTC ligand coordinates to the Cd(II) ion in a monodentate manner by the carboxylic carbonyl oxygen (O7) atom. The Cd–O bond lengths vary in the range 2.291(3)–2.567(3) Å ([Fig. 1](#) and [Tabs. 2](#) and [3](#)).

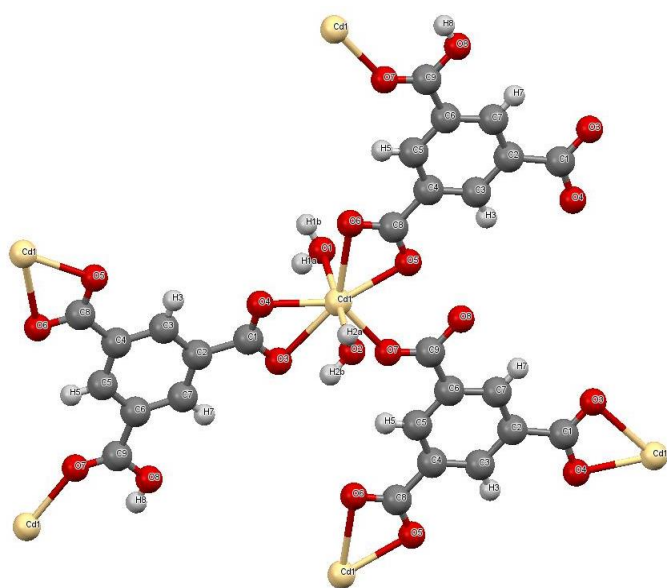


Figure 1. The ORTEP drawing of $[\text{Cd}(\text{BTC})(\text{H}_2\text{O})_2]_n$ showing the coordination environment of the Cd(II) ion.

The BTC ligands with μ_3 coordination mode bridged three adjacent Cd (II) ions to form a two-dimensional sheet structure which in turn as a result of the hydrogen bonding (O–H.....O) interaction from the coordinated water molecules (O1W and O2W) and the protonated carboxyl group of one of the ligands branched into a three-dimensional network of supramolecular structure.

3.2 Reactivity parameters

The frontier molecular orbital which comprises of the Highest occupied molecular orbital (HOMO) and the Lowest unoccupied molecular orbital (LUMO) are important parameters when considering the stability and chemical reactivity of a complex ([Agwupuye et al., 2021a](#); [2021b](#)). The energy gap is the difference in energy between the HOMO and LUMO orbitals. Interestingly, the energy gap is a critical parameter in describing a molecule's reactivity and stability ([Izuchukwu et al., 2022](#)). The HOMO and LUMO values are also useful when calculating the global quantum descriptors, which further explain a molecule's stability. The energy gap, as well as quantum descriptors such as chemical potential, chemical hardness, chemical softness, and electrophilicity, are calculated and presented in [Tab. 4](#) ([Udoikono et al., 2022](#); [Wu et al., 2012](#)). The low energy gap indicates higher chemical reactivity, polarizability, and low kinetic stability ([Unimuke et al., 2022](#)). This explains the intramolecular charge transfer within the complex and describes the bioactivity of the compound. Moreover, the chemical potential is the negative of electronegativity ([Eno et al., 2022](#); [Kavimani et al., 2018](#)). From our result, the Cd complex has a low chemical potential value of -6.23 eV. This is because the electrons in the fermi energy level regions are loosely bound. This is an indication that the complex has greater ability to accept electrons. The small energy gap (0.3322 eV) indicates possible excitation of electrons from HOMO to LUMO hence low stability of the complex. The chemical hardness value of 0.16 eV indicates a soft molecule and this corresponds with the softness value of 6.02 eV as softness is inversely proportional to hardness ([Gber et al., 2022](#)).

Table 2. Selected bond lengths (Å).

Atom set		Length (Å)	Atom set		Length (Å)
Cd1	O1	2.305(3)	O7	C9	1.228(5)
Cd1	O2	2.380(3)	O8	C9	1.312(5)
Cd1	O3	2.537(3)	C1	C2	1.496(5)
Cd1	O4	2.239(3)	C2	C3	1.397(5)
Cd1	O5 ¹	2.278(2)	C2	C7	1.400(5)
Cd1	O6 ¹	2.567(3)	C3	C4	1.393(5)

Table 3. Selected bond angles (°).

Atom set			Angle (°)	Atom set			Angle (°)
O1	Cd1	O2	175.92(9)	C1	O4	Cd1	98.4(2)
O1	Cd1	O3	88.31(10)	C8	O5	Cd1 ³	99.0(2)
O1	Cd1	O6 ¹	84.45(9)	C8	O6	Cd1 ³	86.1(2)
O1	Cd1	C1	88.37(10)	C9	O7	Cd1 ⁴	136.6(2)
O2	Cd1	O3	93.34(10)	O3	C1	Cd1	67.5(2)
O2	Cd1	O6 ¹	92.14(9)	O3	C1	O4	121.5(3)
O2	Cd1	C1	91.38(10)	O3	C1	C2	121.0(3)
O3	Cd1	O6 ¹	146.55(9)	O4	C1	Cd1	54.03(18)
O3	Cd1	C1	27.18(10)	O4	C1	C2	117.5(3)
O4	Cd1	O1	89.30(10)	C2	C1	Cd1	171.4(3)
O4	Cd1	O2	88.60(10)	C3	C2	C1	119.8(3)
O4	Cd1	O3	54.71(10)	C3	C2	C7	119.3(3)

Table 4. HOMO/LUMO, Energy gap and the quantum chemical reactivity parameters.

Chemical parameters	Charge (eV)
Chemical potential (μ)	-6.23
Hardness (η)	0.16
HOMO - 2	-6.46
HOMO - 1	-6.42
HOMO	-6.40
Ionization potential (IP)	6.40
Electron affinity (EA)	6.07
LUMO	-6.07
LUMO + 1	-5.91
LUMO + 2	-1.99
Energy gap Eg	0.33
Energy gap Eg 1	0.51
Energy gap Eg 2	4.47
Electrophilicity index (ω)	121.29
Electronegativity (χ)	6.23
Chemical softness (s)	6.02

Source: Elaborated by the authors using data from Bisong *et al.* (2020).

From Fig. 2, it is evident that electron distribution in the HOMO is only centred on a relative part of the Cd

atom of the MOF whereas in the LUMO electrons are evenly distributed among the Cd atom of the MOF complex and clouded with some percentage of charge delocalization.

3.3 NBO analysis

From the output of the NBO analysis, the total Lewis structure has 97.330% (core: 99.996%; valence Lewis: 95.997%) and the non-Lewis structure has 2.670% and Rydberg non-Lewis 0%. The NBO result (Tab. 5) showed that the σ (Cd1-O3) bond was formed from the $sp^{0.58}$ hybrid orbital on cadmium (36.51% p-character) interacting with $sp^{34.85}$ hybrid orbital on oxygen (97.21% p-character). The $sp^{2.84}$ hybrid on carbon atom (73.98% p-character) interacted with $sp^{2.33}$ hybrid atom of carbon (70.01% p-character) in sigma bond (C6-C8). Also, the transition between σ (C6-H63) with $sp^{2.71}$ hybrid on carbon (73.02% p-character) and on hydrogen (100% s-character). The $sp^{1.90}$ hybrid on carbon atom (65.53% p-character) interacted with $sp^{4.40}$ hybrid atom of carbon (81.49% p-character) in sigma bond (C6-C8).

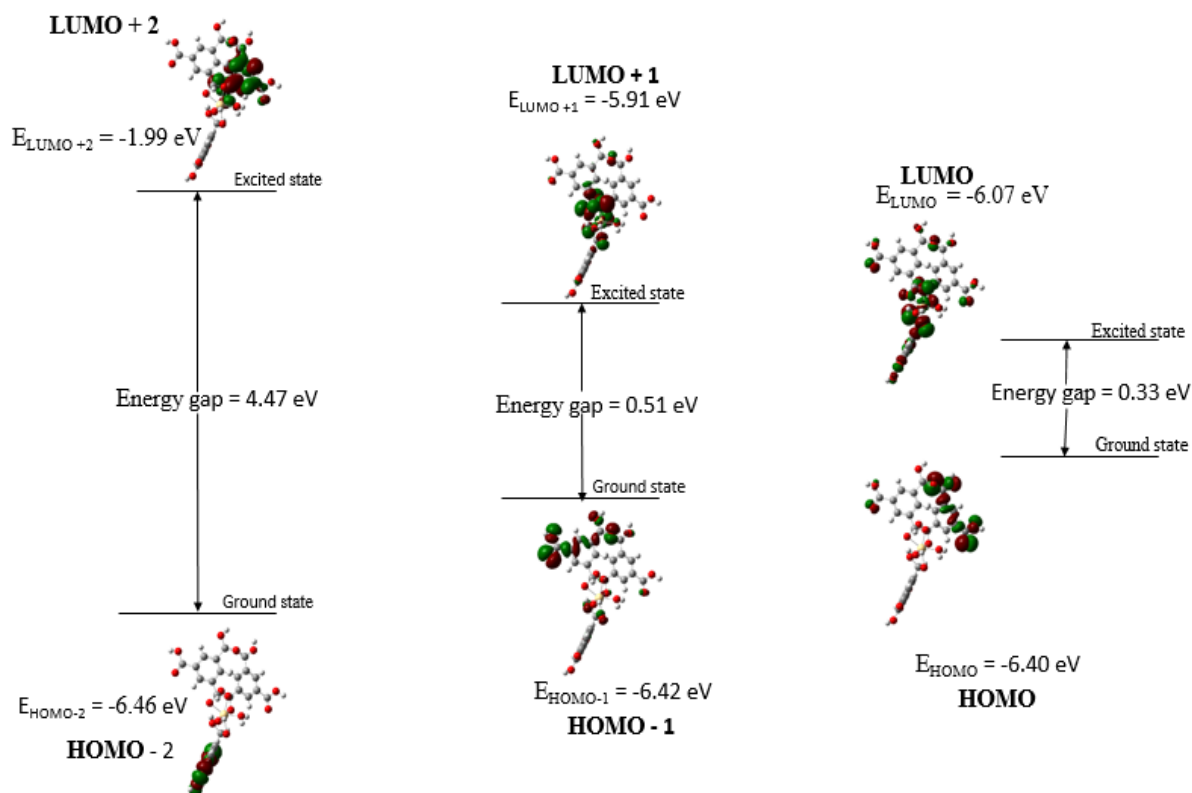


Figure 2. Pictorial representation of the molecular properties.

Table 5. NBO analysis, occupancies, hybrid, and atomic orbitals of the studied complex

Parameters	Occupancies	Hybrid	Atomic orbitals
σ Cd1 – O3	1.696	$sp^{0.58}$	s(63.28%)p(36.51%)d(0.22%)
σ C6 – C8	1.947	$sp^{2.33}$	s(29.99%)p(70.01%)
σ C6 – H63	1.946	$sp^{2.71}$	s(26.98%)p(73.02%)
σ C7 – C17	1.947	$sp^{2.91}$	s(25.60%)p(74.40%)
σ C7 – H62	1.932	$sp^{2.69}$	s(27.07%)p(72.93%)
LP (2)Cd1	1.999	spd^1	s(0.00%)p0.00(0.01%)d 1.00(99.99%)
LP*(6)Cd1	0.505	$sp^{1.83}$	s(35.29%)p(64.70%)d(0.01%)
LP (2) O2	1.868	$sp^{1.30}$	s(43.44%)p(56.56%)
σ^* Cd1 – O3	0.420	$sp^{0.58}$	s(63.28%)p(36.51%)d(0.22%)
σ^* C6 – C8	0.0705	$sp^{2.84}$	s(26.02%)p(73.98%)
σ^* C6 – H63	0.047	$sp^{2.71}$	s(26.98%)p(73.02%)
σ^* C7 – C17	0.070	$sp^{2.35}$	s(29.83%)p(70.17%)
σ^* C7 – H62	0.047	$sp^{2.69}$	s(27.07%)p(72.93%)

Source: Elaborated by the authors using data from Bisong *et al.* (2020).

The second order perturbation theory analysis of Fock matrix basis NBO analysis between donor and acceptor orbitals of the studied compound are represented in Tab. 6. The nature of the interaction between the donor and acceptor are determined by the value of the stabilization energy (Khan *et al.*, 2020). The stability of the system increases with increased electron delocalization associated with hyper-conjugation, thus a

high stabilization energy, the significant hyper-conjugative interactions and the value of their stabilization energies observed from the NBO analysis are: $\pi^*(C\ 38 - O\ 39) \rightarrow \pi^*(C\ 9 - C\ 11)$, 106.15 kcal mol⁻¹; $\pi^*(C\ 42 - O\ 43) \rightarrow \pi^*(C\ 13 - C\ 15)$, 87.31 kcal mol⁻¹; $\pi^*(C\ 58 - O\ 59) \rightarrow \pi^*(C\ 22 - C\ 24)$, 82.21 kcal mol⁻¹; LP*(Cd 1) \rightarrow $\sigma^*(Cd\ 1 - O\ 3)$, 95.04 kcal mol⁻¹; LP(O 66) \rightarrow LP*(Cd 1), 79.94 kcal mol⁻¹.

Table 6. Donor, acceptor, occupancy and the second order perturbation energies of Cd complex calculated at DFT/B3LYP.

Donor (i) (a.u.)	Occupancy (j) (a.u.)	Acceptor (j)	Occupancy (e)	E ² (kcal mol ⁻¹)	E(j) – E(i) (a.u.)
π^* C38 – O39	(0.233)	π^* C9 – C11	(0.346)	106.15	0.01
π^* C42 – O43	(0.233)	π^* C22 – C24	(0.337)	82.21	0.02
LP*(6) Cd 1	(0.505)	σ^* Cd1 – O3	(0.420)	95.04	0.04
π^* C42 – O43	(0.232)	π^* C13 – C15	(0.336)	87.31	0.01
LP(2) O4	(1.795)	LP*(8) Cd1	(0.358)	56.68	0.56
σ O2 – O37	(1.821)	LP*(6) Cd1	(0.505)	49.61	0.25
π C22 – C24	(1.628)	π^* C17 – C19	(0.341)	24.11	0.28
σ Cd1 – O3	(1.821)	π^* C26 – O27	(0.350)	28.91	0.29
π C28 – C30	(0.233)	π^* C29 – C31	(0.337)	23.32	0.07
LP (2) O66	(1.824)	LP*(6)Cd1	(0.505)	79.94	0.56
LP(2) O 4	(1.829)	σ^* Cd1 – O 3	(0.420)	43.95	0.51
LP (2) O66	(1.824)	LP*(7)Cd1	(0.394)	41.61	0.59

Source: Elaborated by the authors using data from Bisong *et al.* (2020).

3.4 Molecular docking

The crystal structure of the targeted proteins was obtained from the protein data bank (PDB IDs: 1D7U and 2XCS) for the evaluation of antimicrobial mechanism. The following properties are all part of the traditional drug design and development process: physical characteristic, substantiation, preclinical and clinical trials (Izuchukwu *et al.*, 2022; Udoikono *et al.*, 2022). Thus, the goal of the in-silico drug discovery (molecular docking) approach is to find small molecules that can modulate the function of a target protein, which is a recessed portion or a slight compartment of a protein where a ligand molecule binds to yield the required output (i.e., activation, inhibition, or modulation), the binding site, the right orientation, and the targeted protein ligand binding (Agwupuye *et al.*, 2021b). Furthermore, tiny compounds with useful pharmacokinetics and pharmacodynamics must be identified, as well as a series of sophisticated stages such as drug candidate discovery, candidate validation, pharmacokinetics, and preclinical toxicity evaluations (Andrade *et al.*, 2016; Lavé *et al.*, 2007). The title compound being an antimicrobial drug, the antimicrobial property of the drug is investigated further by docking the Cd MOF and the standard drug levofloxacin with some selected antimicrobial proteins 1D7U and 2XCS.

The 3D crystallographic structures of the receptor molecules chosen for docking studies were prepared by removing water molecule, adding explicit hydrogens, charges, and correction of deformation in amino acid sequence (Takaya *et al.*, 2020). The active sites of the receptor protein were predicted and defined based on the interaction of the crystallographic ligand with the receptor molecules respectively as visualized with the BIOVIA Discovery Studio visualizer and presented in

Fig. S1 and S2 of the Supplementary Information (Kar and Leszczynski, 2020). The binding score of the ligand docked with the proteins and the standard drug is presented in Tab. 6 and the average binding affinity has been generated based on the binding poses generated. From the binding score obtained from the AutoDock Vina tool, the inhibitory action and the binding strength was observed to be in the order 2XCS_Cd_complex > 1D7U_levofloxacin and 1D7U_Cd_complex > 1D7U_levofloxacin.

The score and the average are presented in Tab. 7. Interestingly, hydrogen bond interaction, which determines the activeness of a potential drug candidate, was observed, and other interactions, such as steric and hydrophilic, were carefully studied. [Cd(BTC)(H₂O)₂]_n showed its hydrogen interactions with the following amino residue when docked with 1D7U which were Ala 112, Ala 245, Arg 406, Asn 115, Asp 243, Gln 52, Gln 246, Glu 210, Glu 244, Gly 111, Gly 140, His 139, Lys 272, Met 141, Ser 214, Ser 215, Ser 271, and Trp 138. The standard levofloxacin displayed the following inhibitors when docked with 1D7U; Ala 112, Ala 245, Arg 406, Asn 115, Asp 243, Gln 52, Gln 246, Glu 210, Glu 244, Gly 111, Gly 140, His 139, Lys 272, Met 141, Ser 214, Ser 215, Ser 271, Trp 138, and Tyr: 20. Moreover, 11 interactions other than hydrogen occurred between the 1D7U protein binding site with the [Cd(BTC)(H₂O)₂]_n, which were Ala 152, Asn 394, Gln 397, Ile 212, Ile 395, Leu 398, Met 53, Ser 54, Ser 151, Thr 110, and Val 396. It is worthy to note that the only target molecule residue found in standard levofloxacin and not found in [Cd(BTC)(H₂O)₂]_n is Tyr 20. The standard levofloxacin inhibitor showed 4 hydrogen interactions for protein–ligand interactions: 2 donors from target protein Gln 246, and 2 donors from ligand (from oxygen atom in ligand to residue Trp 138), having

bond lengths ranging from 2.5–3.2 Å. However, [Cd(BTC)(H₂O)₂]_n showed 24 hydrogen interactions: 17 donors from target, 5 donors from ligand, and 2 donors from either target or ligand. The bond length ranges from 1.6–3.5 Å.

Hydrogen bonds in protein-ligand interactions are vital determinants for ligand binding affinity. The [Cd(BTC)(H₂O)₂]_n also showed some interactions with protein 2XCS which were 2XCS[B]: Arg 1069, Asp 1073, Gln 1056, Gly 1072, Lys 1065, Met 1058, 2XCS[D]: Arg 1069, Asp 1073, and Gly 1072. The standard levofloxacin inhibitor involves complex interaction with 15 active interaction sites of protein 2XCS, which were Arg 1069, Asp 1073, Gln 1056, Gly

1072, Lys 1065, Met 1058, 2XCS[D] Ala 1068, Arg 1069, Asp 1073, Gln 1056, Gly 1072, Ile 1070, Lys 1065, Lys 1066, and Met 1058. It is worthy to note that all interactions with the protein 2XCS[B] for levofloxacin and [Cd(BTC)(H₂O)₂]_n have the same number of residues ID. However, 11 more interactions occurred between the 2XCS protein binding site with the [Cd(BTC)(H₂O)₂]_n, which were 2XCS[B]: Gly 1052, Ile 1070, Leu 1053, Lys 1066, Ser 1063, Tyr 1064, Val 1074, 2XCS[D]: Asn 1153, Asp 1151, Glu 1154, and Lys 1077. The Epair energy for levofloxacin and [Cd(BTC)(H₂O)₂]_n is strongest for residue 2XCS[D] Arg 1069 (–28.3235) and 2XCS[B] Arg 1069 (–36.9925) respectively.

Table 7. The binding affinity values of different poses of the Cd_ complex and Levofloxacin with the receptor protein 1D7U and 2XCS predicted at Auto-dock Vina tool.

Modes	1D7U_[Cd(BTC)(H ₂ O) ₂] _n (kcal mol ⁻¹)	1D7U_Levofloxacin (kcal mol ⁻¹)	2XCS_[Cd(BTC)(H ₂ O) ₂] _n (kcal mol ⁻¹)	1D7U_Levofloxacin (kcal mol ⁻¹)
1	-7.0	-7.2	-11.5	-9.3
2	-6.7	-6.8	-11.2	-9.1
3	-6.6	-6.5	-11.2	-9.1
4	-6.6	-6.2	-11.2	-9.0
5	-6.6	-6.2	-11.1	-9.0
6	-6.6	-6.1	-11.1	-8.9
7	-6.6	-6.1	-11.1	-8.9
8	-6.5	-5.9	-11.1	-8.9
9	-6.4	-5.7	-11.0	-8.8
AVERAGE Binding affinity (kcal·mol ⁻¹)	-6.6	-6.3	-11.2	-9.0

The standard levofloxacin inhibitor showed 3 hydrogen bond interactions with target protein 2XCS and bond length between 2.62–2.69 Å. While, [Cd(BTC)(H₂O)₂]_n showed 11 hydrogen bond interactions: 5 donors from target, 5 donors from ligand and 1 donor from either target or ligand (Fig. 3). The bond lengths ranges from 2.6–3.5 Å. Analysis of high-resolution crystallographic structures for protein-ligand complexed revealed that the typical hydrogen bond distance between the donor and acceptor atom ranges from 2.5–3.4 Å. The graphical representation of intermolecular hydrogen bonds for protein-ligand complexes is of pivotal importance for the evaluation of

the residues responsible for ligand binding affinity, as presented in Fig. S1 and S2 of the Supplementary Information. Table 7 shows the energy overall descriptors for the interaction of 1D7U and 2XCS with standard levofloxacin and [Cd(BTC)(H₂O)₂]_n. The average binding score obtained and the number of hydrogen bond interactions found when [Cd(BTC)(H₂O)₂]_n was docked against the receptor proteins 1D7U and 2XCS showed that the proposed structure fits perfectly at the active site of proteins 1D7U and 2XCS which results to the high binding affinities observe compared to the commercial drug levofloxacin.

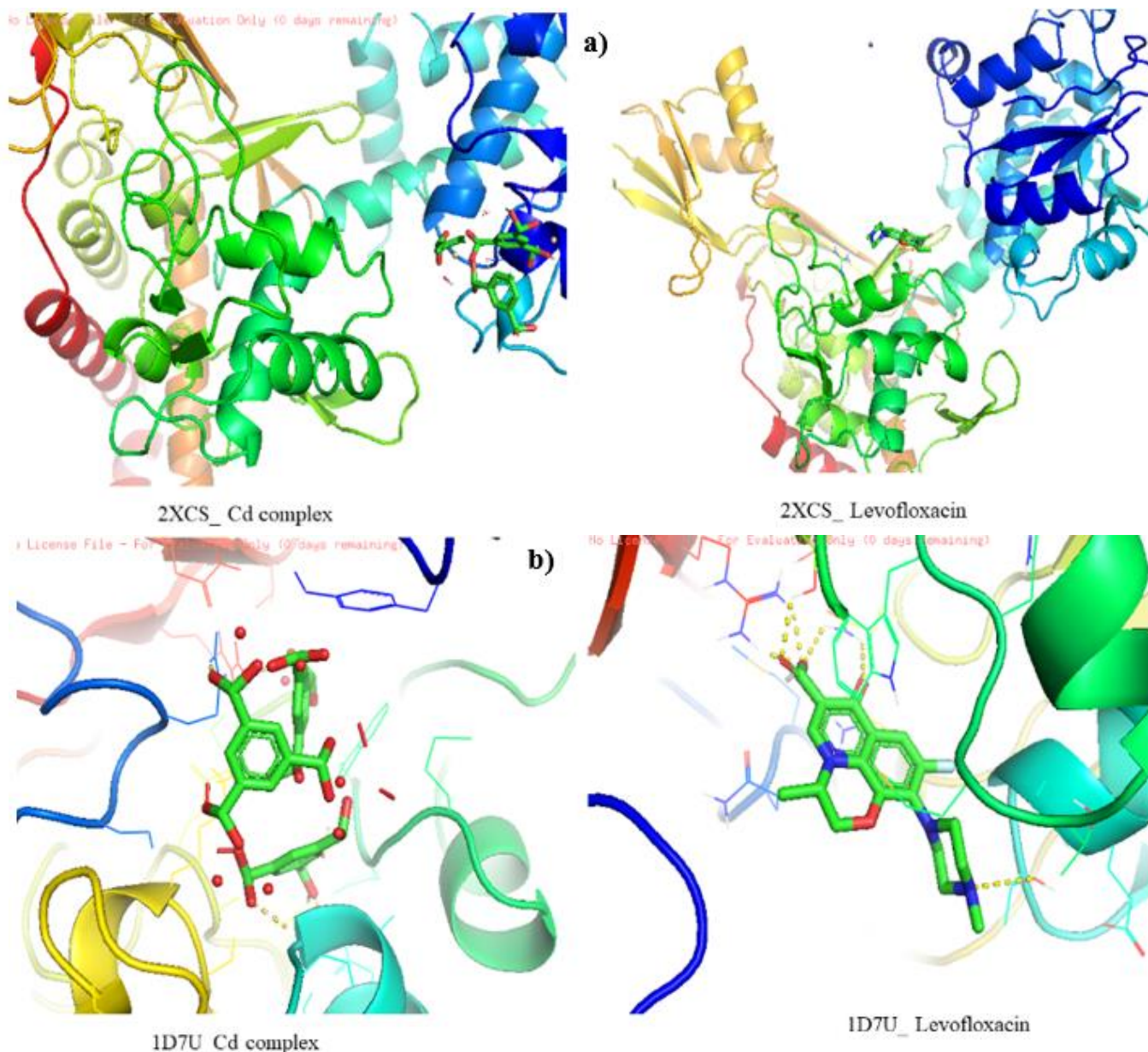


Figure 3. (a) PyMOL visualization for the interaction between protein (2XCS) with studied complex and levofloxacin (b) PyMOL visualization for the interaction between protein (1D7U) with the studied complex and levofloxacin

3.5 ADMET studies

To further support the result of docking studies, we also performed in-silico ADMET studies on the $[\text{Cd}(\text{BTC})(\text{H}_2\text{O})_2]_n$ and standard levofloxacin (reported in Tab. 8) as the interactions of inhibitor with a protein cannot promise its suitability as a drug. SwissADME and pkCSM are online platforms used to predict to a certain point the false-positive results commonly observed in the bioactive form of small compounds (Emori *et al.*, 2022).

The bioavailability radar plots (Fig. 4) gives a graphical picture of the drug-likeness parameters of the investigated compounds which describes the oral

availability of the bioactive molecules. Here, $[\text{Cd}(\text{BTC})(\text{H}_2\text{O})_2]_n$ presents only one off-shoot relative to unsaturation (INSATU) vertex, leading to suboptimal physiochemical properties for their oral bioavailability (Huxford *et al.*, 2010) while standard levofloxacin has been predicted as orally bioavailable.

In addition to the Lipinski rule of five (Jia *et al.*, 2020), another four drug-likeness rules named Ghose, Egan, Veber and Muegee (Daina *et al.*, 2017) were satisfied by levofloxacin. While $[\text{Cd}(\text{BTC})(\text{H}_2\text{O})_2]_n$ passed four of five drug-likeness rules, it violated Egan rule ($\text{TPSA} < 131.6 \text{ \AA}^2$) by having a topological surface area (TPSA) value of 133.52 \AA^2 . The brain or intestinal

estimated (BOILED) permeation predictive model (BOILED-Egg) is an extended and renewed version of the Edan-Egg model used to visually represent blood-brain barrier penetration (BBB) and human gastrointestinal absorption (HIA) relative to the distribution and absorption parameters, respectively. The analysis of Fig. 4 shows that both $[\text{Cd}(\text{BTC})(\text{H}_2\text{O})_2]_n$ and levofloxacin were passively absorbed by the gastrointestinal tract but were not BBB permeate.

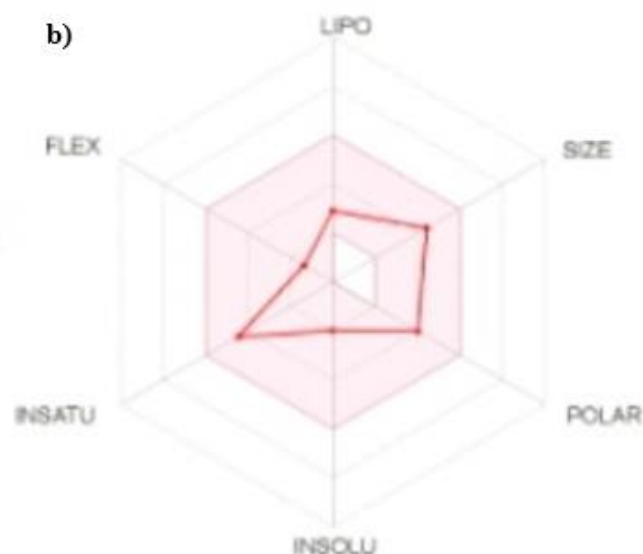
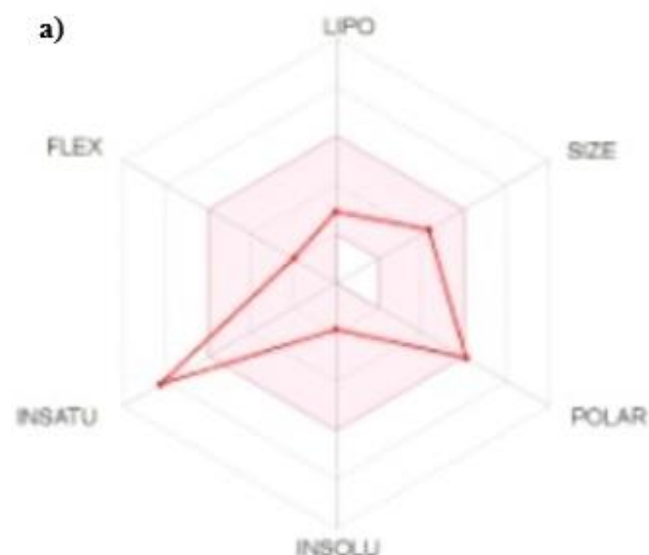


Figure 4. Radar plot of the six drug-likeness parameters used to predict the oral bioavailability of $[\text{Cd}(\text{BTC})(\text{H}_2\text{O})_2]_n$ and standard Levofloxacin.

Table 8. pkCSM results of $[\text{Cd}(\text{BTC})(\text{H}_2\text{O})_2]_n$ and levofloxacin.

Molecule ID		$[\text{Cd}(\text{BTC})(\text{H}_2\text{O})_2]_n$	Levofloxacin
Absorption	Caco-2 permeability	0.146	1.449
	Human intestinal absorption	23.874	96.053
	Skin permeability	-2.735	-2.735
Distribution	VD_{SS} (human)	-1.469	0.193
	Fraction unbound (human)	0.517	0.609
	CNS permeability	-3.574	-3.05
Excretion	Total clearance	1.187	0.317
	Renal OCT2 substrate	No	No
Toxicity	AMES toxicity	No	No
	Oral rat acute toxicity (LD_{50})	2.128	2.276
	Minnnow toxicity (LC_{50})	3.972	1.788

Semaphore flags: green = good, yellow = tolerable, and red = bad.

The absorption parameters using pkCSM online tool shows that levofloxacin is a more promising oral availability due to the optimal Caco-2-cell permeability (>0.9) and HIA ($>90\%$). Finally, $[\text{Cd}(\text{BTC})(\text{H}_2\text{O})_2]_n$ and levofloxacin are good skin permeable compounds ($\log K_p < -2.5$).

Regarding the distributions parameters, the two most important pharmacokinetic drug parameters are volume of distribution of steady state (VD_{SS}) and unbound fraction. VD_{SS} describes the extent of distribution of the drug and the unbound fraction describes the portion of

the free drug in plasma that may leak from the blood vessels or tube into the tissues around it (Tice, 2001). Values of $\text{VD}_{\text{SS}} > 0.45$ indicate that the drug will be distributed in tissue, whereas values < -0.15 indicate that the drug will be distributed in plasma. So, $[\text{Cd}(\text{BTC})(\text{H}_2\text{O})_2]_n$ has a VD_{SS} value of -1.469 and levofloxacin 0.193 and are within the unbound fraction of $0.5-0.6$. Both compounds do not penetrate the central nervous system.

The predicted values of total clearance, that measures the effectiveness of drug elimination from the body,

indicate that all compounds have a good renal elimination and are not substrates of the renal organic cation transporter 2 (OCT2). $[\text{Cd}(\text{BTC})(\text{H}_2\text{O})_2]_n$, unlike the standard levofloxacin, has high renal clearance. $[\text{Cd}(\text{BTC})(\text{H}_2\text{O})_2]_n$ did not pose any toxicity problems; levofloxacin, however, is hepatotoxic and may be associated with the interruption of normal functions of the liver.

4. Conclusions

Experimental and theoretical investigation of Cadmium complex of benzenetricarboxylates in monoclinic space group $12/a$ was observed to have lattice parameters $a = 13.1508(3) \text{ \AA}$, $b = 9.1014(2) \text{ \AA}$, $c = 17.8971(4) \text{ \AA}$, $\alpha = 90^\circ$, $\beta = 103.455(2)^\circ$ and $\gamma = 90^\circ$. The structural analysis revealed hydrogen bonding (O–H.....O) interaction from the coordinated water molecules (O1W and O2W) and the protonated carboxyl group of one of the ligands branched into a three-dimensional network of supramolecular structure. From the reactivity parameters, Cd complex of benzenetricarboxylates was observed to have a low chemical potential value of -6.23 eV , which could be accounted on the fact of the loosely bonded electron in the fermi energy level and, hence, was observed to have a greater electron accepting power. The small energy gap (0.3322 eV) indicates possible excitation of electrons from HOMO to LUMO, hence low stability of the complex. Three major transitions: $\pi^* \rightarrow \pi^*$, $\text{LP}^* \rightarrow \sigma^*$ and $\text{LP} \rightarrow \text{LP}^*$ were observed to have the major contribution in this study. From molecular docking analysis, the proposed complex $[\text{Cd}(\text{BTC})(\text{H}_2\text{O})_2]_n$ was observed to have better average binding score and interesting number of hydrogen bond, which determines the activeness of the proposed antimicrobial drug candidate. The complex $[\text{Cd}(\text{BTC})(\text{H}_2\text{O})_2]_n$ was docked with the receptor proteins 1D7U AND 2XCS and observation have it that the complex fits perfectly at the active site of proteins 1D7U and 2XCS hence shows the better binding affinity and efficacy of $[\text{Cd}(\text{BTC})(\text{H}_2\text{O})_2]_n$ as potent antimicrobial drug.

Authors' contribution

Conceptualization: Bassey, E. I.

Data curation: Ekpenyong, E. E.

Formal Analysis: Ekpenyong, E. E.

Funding acquisition: Not applicable

Investigation: Ita, I. T.

Methodology: Gber, T. E.

Project administration: Gber, T. E.

Resources: Benjamin, I.; Bassey, E. I.

Software: Not applicable

Supervision: Bassey, E. I.

Validation: Edet, H. O.

Visualization: Benjamin, I.

Writing – original draft: Ita, I. T.

Writing – review & editing: Edet, H. O.

Data availability statement

All data sets generated and analysed in the current study are presented in the manuscript.

Funding

Not applicable.

Acknowledgments

The center for high performance computing (CHPC), South Africa is gratefully acknowledged for providing computational resources for this project.

References

- Agwupuye, J. A.; Louis, H.; Unimuke, T. O.; David, P.; Ubana, E. I.; Moshood, Y. L. Electronic structure investigation of the stability, reactivity, NBO analysis, thermodynamics, and the nature of the interactions in methyl-substituted imidazolium-based ionic liquids. *J. Mol. Liq.* **2021a**, *337*, 116458. <https://doi.org/10.1016/j.molliq.2021.116458>
- Agwupuye, J. A.; Neji, P. A.; Louis, H.; Odey, J. O.; Unimuke, T. O.; Bisong, E. A.; Eno, E. A.; Utsu, P. M.; Ntui, T. N. Investigation on electronic structure, vibrational spectra, NBO analysis, and molecular docking studies of aflatoxins and selected emerging mycotoxins against wild-type androgen receptor. *Heliyon.* **2021b**, *7* (7), E07544. <https://doi.org/10.1016/j.heliyon.2021.e07544>
- Andrade, E. L.; Bento, A. F.; Cavalli, J.; Oliveira, S. K.; Schwanke, R. C.; Siqueira, J. M.; Freitas, C. S.; Marcon, R.; Calixto, J. B. Non-clinical studies in the process of new drug development-Part II: Good laboratory practice, metabolism, pharmacokinetics, safety and dose translation to clinical studies. *Braz. J. Med. Biol. Res.* **2016**, *49* (12), e5646. <https://doi.org/10.1590/1414-431x20165646>
- Balaban, N. Q.; Helaine, S.; Lewis, K.; Ackermann, M.; Aldridge, B.; Andersson, D. I.; Brynildsen, M. P.; Bumann, D.; Camilli, A.; Collins, J. J.; Dehio, C.; Fortune, S.; Ghigo, J.-M.; Hardt, W.-D.; Harms, A.; Heinemann, M.; Hung, D. T.; Jenal, U.; Levin, B. R.; Michiels, J.; Storz, G.; Tan, M.-W.; Tenson, T.; Van Melderen, L.; Zinkernagel, A. Definitions and guidelines for research on antibiotic persistence. *Nature Reviews Microbiology.* **2019**, *17* (7), 441–448. <https://doi.org/10.1038/s41579-019-0196-3>

- Bassey, V. M.; Apebende, C. G.; Idante, P. S.; Louis, H.; Emori, W.; Cheng, C.-R.; Agwupuye, J. A.; Unimuke, T. O.; Wei, K.; Asogwa, F. C. Vibrational Characterization and Molecular Electronic Investigations of 2-acetyl-5-methylfuran using FT-IR, FT-Raman, UV-VIS, NMR, and DFT Methods. *J. Fluoresc.* **2022**, *32* (3), 1005–1017. <https://doi.org/10.1007/s10895-022-02903-8>
- Berman, H. M.; Battistuz, T.; Bhat, T. N.; Bluhm, W. F.; Bourne, P. E.; Burkhardt, K.; Feng, Z.; Gilliland, G. L.; Iype, L.; Jain, S.; Fang, P.; Marvin, J.; Padilla, D.; Ravichandran, V.; Schneider, B.; Thanki, N.; Weissing, H.; Westbrook, D.; Zardecki, C. The Protein Data Bank. *Acta Cryst.* **2002**, *D58* (6), 899–907. <https://doi.org/10.1107/S0907444902003451>
- Bisong, E. A.; Louis, H.; Unimuke, T. O.; Odey, J. O.; Ubana, E. I.; Edim, M. M.; Edim, M. M.; Tizhe, F. T.; Agwupuye, J. A.; Utsu, P. M. Vibrational, electronic, spectroscopic properties, and NBO analysis of p-xylene, 3, 6-difluoro-p-xylene, 3, 6-dichloro-p-xylene and 3, 6-dibromo-p-xylene: DFT study. *Heliyon.* **2020**, *6* (12), E05783. <https://doi.org/10.1016/j.heliyon.2020.e05783>
- Cai, M.; Chen, G.; Qin, L.; Qu, C.; Dong, X.; Ni, J.; Yin, X. Metal Organic Frameworks as Drug Targeting Delivery Vehicles in the Treatment of Cancer. *Pharmaceutics.* **2020**, *12* (3), 232. <https://doi.org/10.3390/pharmaceutics12030232>
- Chuhadiya, S.; Suthar, H. D.; Patel, S. L.; Dhaka, M. S. Metal organic frameworks as hybrid porous materials for energy storage and conversion devices: A review. *Coord. Chem. Rev.* **2021**, *446*, 214115. <https://doi.org/10.1016/j.ccr.2021.214115>
- Daina, A.; Michielin, O.; Zoete, V. SwissADME: a free web tool to evaluate pharmacokinetics, drug-likeness and medicinal chemistry friendliness of small molecules. *Sci. Rep.* **2017**, *7* (1), 42717. <https://doi.org/10.1038/srep42717>
- Dennington, R.; Keith, T. A.; Millam, J. M. (2016). Gauss View 6.0. 16. Semichem Inc.: Missão Shawnee, KS, EUA. HyperChem, T. HyperChem 8.07, Programa Profissional HyperChem. Gainesville, Hipercubo. 2001.
- Deshpande, N.; Address, K. J.; Bluhm, W. F.; Merino-Ott, J. C.; Townsend-Merino, W.; Zhang, Q.; Knezevich, C.; Xie, L.; Chen, L.; Feng, Z.; Green, R. K.; Flippen-Anderson, J. L.; Westbrook, J.; Berman, H. M.; Bourne, P. E. The RCSB Protein Data Bank: a redesigned query system and relational database based on the mmCIF schema. *Nucleic Acids Res.* **2005**, *33* (Suppl 1), D233–D237. <https://doi.org/10.1093/nar/gki057>
- El-Gammal, O. A.; Rakha, T. H.; Metwally, H. M.; El-Reash, G. M. A. Synthesis, characterization, DFT and biological studies of isatinpicolinohydrazone and its Zn (II), Cd (II) and Hg (II) complexes. *Spectrochim. Acta A Mol. Biomol. Spectrosc.* **2014**, *127*, 144–156. <https://doi.org/10.1016/j.saa.2014.02.008>
- Emori, W.; Louis, H.; Adalikwu, S. A.; Timothy, R. A.; Cheng, C.-R.; Gber, T. E.; Agwamba, E. C.; Owen, A. E.; Ling, L.; Offiong, O. E.; Adeyinka, A. S. Molecular Modeling of the Spectroscopic, Structural, and Bioactive Potential of Tetrahydropalmatine: Insight from Experimental and Theoretical Approach. *Polycycl. Aromat. Compd.* **2022**, 1–18. <https://doi.org/10.1080/10406638.2022.2110908>
- Eno, E. A.; Louis, H.; Unimuke, T. O.; Gber, T. E.; Mbonu, I. J.; Ndubisi, C. J.; Adalikwu, S. A. Reactivity, stability, and thermodynamics of para-methylpyridinium-based ionic liquids: Insight from DFT, NCI, and QTAIM. *Journal of Ionic Liquids.* **2022**, *2* (1), 100030. <https://doi.org/10.1016/j.jil.2022.100030>
- Frisch, M. J.; Trucks, G. W.; Schlegel, H. B.; Scuseria, G. E.; Robb, M. A.; Cheeseman, J. R.; Scalmani, G.; Barone, V.; Petersson, G. A.; Nakatsuji, H. X.; Caricato, L. M.; Marenich, A. V.; Bloino, J.; Janesko, B. G.; Gomperts, R.; Mennucci, B.; Hratchian, H. P.; Ortiz, J. V.; Izmaylov, A. F.; Sonnenberg, J. L.; Williams-Yong, D.; Ding, F.; Lipparini, F. Egidi, F.; Goings, J.; Peng, B.; Petrone, A.; Henderson, T.; Ranasinghe, D.; Zakrzewski, V. G.; Gao, J.; Rega, N.; Zheng, G.; Liang, W.; Hada, M.; Ehara, M.; Toyota, K.; Fukuda, R.; Hasagawa, J.; Ishida, M.; Nakajima, T.; Honda, Y.; Kitao, O. Nakai, H.; Vreven, T. Throssell, K.; Montgomery, J. A.; Peralta, Jr, J. E.; Ogliaro, F.; Bearpark, M. J.; Heyd, J. J.; Brothers, E. N.; Kudin, K. N.; Staroverov, V. N.; Keith, T. A.; Kobayashi, R.; Normand, J.; Raghavachari, K.; Rendell, A. P. Burant, J. C.; Iyengar, S. S.; Tomasi, J.; Cossi, M.; Millam, J. M.; Klene, M.; Adamo, C.; Cammi, R.; Ochterski, J. W. Martin, R. L.; Morokuma, K. Farkas, O.; Foresman, J. B.; and Fox, D. J.; Gaussian, Inc., Wallingford CT, 2016.
- Gber, T. E.; Louis, H.; Owen, A. E.; Etinwa, B. E.; Benjamin, I.; Asogwa, F. C.; Orosun, M. M.; Eno, E. A. Heteroatoms (Si, B, N, and P) doped 2D monolayer MoS₂ for NH₃ gas detection. *RSC Advances.* **2022**, *12* (40), 25992–26010. <https://doi.org/10.1039/D2RA04028J>
- Gupta, A.; Gupta, R.; Singh, R. L. Microbes and Environment. In *Principles and Applications of Environmental Biotechnology for a Sustainable Future*. Springer, 2017; pp 43–48. https://doi.org/10.1007/978-981-10-1866-4_3
- Hamdani, H. E.; Amane, M. E. Preparation, spectral, antimicrobial properties and anticancer molecular docking studies of new metal complexes [M (caffeine)₄](PF₆)₂; M= Fe (II), Co (II), Mn (II), Cd (II), Zn (II), Cu (II), Ni (II). *J. Mol. Struct.* **2019**, *1184*, 262–270. <https://doi.org/10.1016/j.molstruc.2019.02.049>
- Huxford, R. C.; Della Rocca, J.; Lin, W. Metal-organic frameworks as potential drug carriers. *Curr. Opin. Chem. Biol.* **2010**, *14* (2), 262–268. <https://doi.org/10.1016/j.cbpa.2009.12.012>

- Isravel, A. D.; Jeyaraj, J. K.; Thangasamy, S.; John, W. J. DFT, NBO, HOMO-LUMO, NCI, stability, Fukui function and hole–Electron analyses of tolcapone. *Comput. Theor. Chem.* **2021**, *1202*, 113296. <https://doi.org/10.1016/j.comptc.2021.113296>
- Izuchukwu, U. D.; Asogwa, F. C.; Louis, H.; Uchenna, E. F.; Gber, T. E.; Chinasa, U. M.; Chinedum, N. J.; Eze, B. O.; Adeyinka, A. S.; Chris, O. U. Synthesis, vibrational analysis, molecular property investigation, and molecular docking of new benzenesulphonamide-based carboxamide derivatives against *Plasmodium falciparum*. *Journal of Molecular Structure.* **2022**, *1269*, 133796. <https://doi.org/10.1016/j.molstruc.2022.133796>
- Jia, C.-Y.; Li, J.-Y.; Hao, G.-F.; Yang, G.-F. A drug-likeness toolbox facilitates ADMET study in drug discovery. *Drug Discov. Today.* **2020**, *25* (1), 248–258. <https://doi.org/10.1016/j.drudis.2019.10.014>
- Kar, S.; Leszczynski, J. Open access in silico tools to predict the ADMET profiling of drug candidates. *Expert Opin. Drug Discov.* **2020**, *15* (12), 1473–1487. <https://doi.org/10.1080/17460441.2020.1798926>
- Kavimani, M.; Balachandran, V.; Narayana, B.; Vanasundari, K.; Revathi, B. Topological analysis (BCP) of vibrational spectroscopic studies, docking, RDG, DSSC, Fukui functions and chemical reactivity of 2-methylphenylacetic acid. *Spectrochim. Acta A Mol. Biomol. Spectrosc.* **2018**, *190*, 47–60. <https://doi.org/10.1016/j.saa.2017.09.005>
- Khan, E.; Khalid, M.; Gul, Z.; Shahzad, A.; Tahir, M. N.; Asif, H. M.; Asim, S.; Braga, A. C. Molecular structure of 1, 4-bis (substituted-carbonyl) benzene: a combined experimental and theoretical approach. *J. Mol. Struct.* **2020**, *1205*, 127633. <https://doi.org/10.1016/j.molstruc.2019.127633>
- Kiran, G.; Karthik, L.; Devi, M. S. S.; Sathiyarajeswaran, P.; Kanakavalli, K.; Kumar, K. M.; Kumar, D. R. In silico computational screening of *Kabasura Kudineer* - Official Siddha Formulation and JACOM against SARS-CoV-2 spike protein. *J. Ayurveda Integr. Med.* **2020**, *13* (1), 100324. <https://doi.org/10.1016/j.jaim.2020.05.009>
- Konakanchi, R.; Haribabu, J.; Prashanth, J.; Nishtala, V. B.; Mallela, R.; Manchala, S.; Gandamalla, D.; Karvembu, R.; Reddy, B. V.; Yellu, N. R.; Kotha, L. R. Synthesis, structural, Biological Evaluation, Molecular Docking and DFT Studies of Co (II), Ni (II), Cu (II), Zn (II), Cd (II) and Hg (II) Complexes bearing Heterocyclic Thiosemicarbazone ligand. *Appl. Organomet. Chem.* **2018**, *32* (8), e4415. <https://doi.org/10.1002/aoc.4415>
- Kumar, P.; Deep, A.; Kim, K.-H. Metal organic frameworks for sensing applications. *TrAC - Trends Anal. Chem.* **2015**, *73*, 39–53. <https://doi.org/10.1016/j.trac.2015.04.009>
- Lavé, T.; Parrott, N.; Grimm, H. P.; Fleury, A.; Reddy, M. Challenges and opportunities with modelling and simulation in drug discovery and drug development. *Xenobiotica.* **2007**, *37* (10–11), 1295–1310. <https://doi.org/10.1080/00498250701534885>
- Lawson, H. D.; Walton, S. P.; Chan, C. Metal–Organic Frameworks for Drug Delivery: A Design Perspective. *ACS Appl. Mater. Interfaces.* **2021**, *13* (6), 7004–7020. <https://doi.org/10.1021/acsami.1c01089>
- Li, H.; Li, L.; Lin, R.-B.; Zhou, W.; Zhang, Z.; Xiang, S.; Chen, B. Porous metal-organic frameworks for gas storage and separation: Status and challenges. *EnergyChem.* **2019**, *1* (1), 100006. <https://doi.org/10.1016/j.enchem.2019.100006>
- Louis, H.; Gber, T. E.; Asogwa, F. C.; Eno, E. A.; Unimuke, T. O.; Bassey, V. M.; Ita, B. I. Understanding the lithiation mechanisms of pyrenetetrone-based carbonyl compound as cathode material for lithium-ion battery: Insight from first principle density functional theory. *Mater. Chem. Phys.* **2022**, *278*, 125518. <https://doi.org/10.1016/j.matchemphys.2021.125518>
- Mason, H. E.; Li, W.; Carpenter, M. A.; Hamilton, M. L.; Howard, J. A.; Sparkes, H. A. Structural and spectroscopic characterisation of the spin crossover in [Fe(abpt)₂(NCS)₂] polymorph A. *New Journal of Chemistry.* **2016**, *40* (3), 2466–2478. <https://doi.org/10.1039/C5NJ02359A>
- Odonkor, S. T.; Addo, K. K. Bacteria Resistance to Antibiotics: Recent Trends and Challenges. *Int. J. Biol. Med. Res.* **2011**, *2* (4), 1204–1210.
- Pastore, V. J.; Cook, T. R.; Rzyayev, J. Polymer–MOF Hybrid Composites with High Porosity and Stability Through Surface-Selective Ligand Exchange. *Chem. Mater.* **2018**, *30* (23), 8639–8649. <https://doi.org/10.1021/acs.chemmater.8b03881>
- Pursell, E. Antimicrobials. In *Understanding Pharmacology in Nursing Practice*. Springer, 2020; pp 147–165. https://doi.org/10.1007/978-3-030-32004-1_6
- Reygaert, W. C. An overview of the antimicrobial resistance mechanisms of bacteria. *AIMS Microbiol.* **2018**, *4* (3), 482–501. <https://doi.org/10.3934/microbiol.2018.3.482>
- Seeliger, D.; Groot, B. L. Ligand docking and binding site analysis with PyMOL and Autodock/Vina. *J. Comput. Aided. Mol. Des.* **2010**, *24* (5), 417–422. <https://doi.org/10.1007/s10822-010-9352-6>
- Sevvana, M.; Ruf, M.; Usón, I.; Sheldrick, G. M.; Herbst-Irmer, R. Non-merohedral twinning: from minerals to proteins. *Acta Cryst.* **2019**, *D75* (12), 1040–1050. <https://doi.org/10.1107/S2059798319010179>

Sharbidre, A.; Dhage, P.; Duggal, H.; Meshram, R. *In silico* Investigation of *Tridax procumbens* Phyto-Constituents Against SARS-CoV-2 Infection. *Biointerface Res. Appl. Chem.* **2021**, *11* (4), 12120–12148. <https://doi.org/10.33263/BRIAC114.1212012148>

Theor. Chem. Acc. **2012**, *131* (3), 1138. <https://doi.org/10.1007/s00214-012-1138-6>

Shemchuk, O.; Song, L.; Tumanov, N.; Wouters, J.; Braga, D.; Grepioni, F.; Leyssens, T. Chiral Resolution of *RS*-Oxiracetam upon Cocrystallization with Pharmaceutically Acceptable Inorganic Salts. *Cryst. Growth Des.* **2020**, *20* (4), 2602–2607. <https://doi.org/10.1021/acs.cgd.9b01725>

Sun, C.-Y.; Qin, C.; Wang, X.-L.; Su, Z.-M. Metal-organic frameworks as potential drug delivery systems. *Expert Opin. Drug Deliv.* **2013**, *10* (1), 89–101. <https://doi.org/10.1517/17425247.2013.741583>

Takaya, D.; Niwa, H.; Mikuni, J.; Nakamura, K.; Handa, N.; Tanaka, A.; Yokoyama, S.; Honma, T. Protein ligand interaction analysis against new CaMKK2 inhibitors by use of X-ray crystallography and the fragment molecular orbital (FMO) method. *J. Mol. Graph.* **2020**, *99*, 107599. <https://doi.org/10.1016/j.jmgm.2020.107599>

Tice, C. M. Selecting the right compounds for screening: does Lipinski's Rule of 5 for pharmaceuticals apply to agrochemicals? *Pest Manag. Sci.* **2001**, *57* (1), 3–16. [https://doi.org/10.1002/1526-4998\(200101\)57:1<3::AID-PS269>3.0.CO;2-6](https://doi.org/10.1002/1526-4998(200101)57:1<3::AID-PS269>3.0.CO;2-6)

Trott, O.; Olson, A. J. AutoDock Vina: Improving the speed and accuracy of docking with a new scoring function, efficient optimization, and multithreading. *J. Comput. Chem.* **2010**, *31* (2), 455–461. <https://doi.org/10.1002/jcc.21334>







Udoikono, A. D.; Louis, H.; Eno, E. A.; Agwamba, E. C.; Unimuke, T. O.; Igbalagh, A. T.; Odey, J. O.; Adeyinka, A. S. Reactive azo compounds as a potential chemotherapy drugs in the treatment of malignant glioblastoma (GBM): Experimental and theoretical studies. *J. Photochem. Photobiol.* **2022**, *10*, 100116. <https://doi.org/10.1016/j.jpap.2022.100116>

Unimuke, T. O.; Louis, H.; Eno, E. A.; Agwamba, E. C.; Adeyinka, S. A. Meta-hybrid density functional prediction of the reactivity, stability, and IGM of azepane, oxepane, thiepane, and halogenated cycloheptane. *ACS Omega.* **2022**, *7* (16), 13704–13720. <https://doi.org/10.1021/acsomega.1c07361>

Vikrant, K.; Kumar, V.; Ok, Y. S.; Kim, K.-H.; Deep, A. Metal-organic framework (MOF)-based advanced sensing platforms for the detection of hydrogen sulfide. *TrAC - Trends Anal. Chem.* **2018**, *105*, 263–281. <https://doi.org/10.1016/j.trac.2018.05.013>

Wu, J. C.; Chattree, G.; Ren, P. Automation of AMOEBA polarizable force field parameterization for small molecules.

Experimental, DFT, molecular docking and *in silico* ADMET studies of cadmium-benzenetricarboxylates

Enya Inah Bassey¹, Terkumbur Emmanuel Gber^{2,3+}, Edison Esther Ekpenyong¹, Henry Okon Edet³, Innocent Benjamin³, Imabasi Tom Ita^{2,3}

1. University of Calabar, Inorganic Materials Research Laboratory, Calabar, Nigeria.
2. University of Calabar, Department of Pure and Applied Chemistry, Calabar, Nigeria.
3. University of Calabar, Computational and Bio-Simulation Research Group, Calabar, Nigeria.

+Corresponding author: Terkumbur Emmanuel Gber, **Phone:** +2348059742439, **Email address:** gberterkumburemanuel@gmail.com

ARTICLE INFO

Article history:

Received: February 27, 2022

Accepted: July 11, 2022

Published: October 28, 2022

Section Editors: Assis Vicente Benedetti

Keywords:

1. synthesis
2. characterizations
3. antimicrobial studies
4. metal-organic frameworks

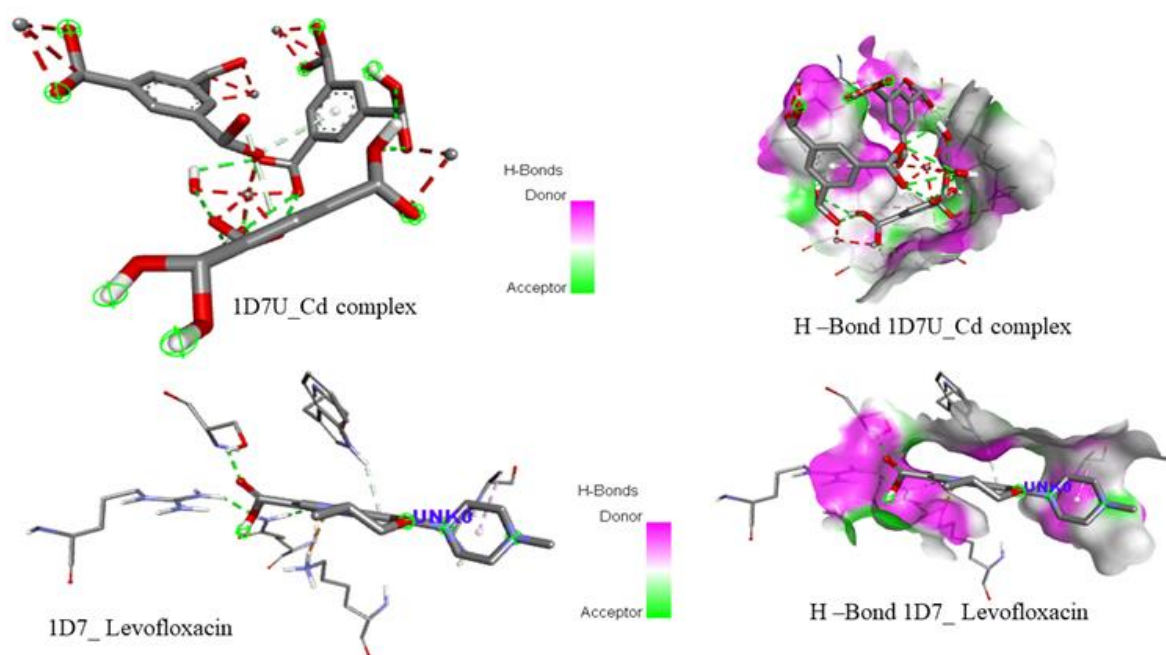


Figure S1. Interactions, H -Bond of the Cd complex and the standard drug with the receptor protein 2D7U.

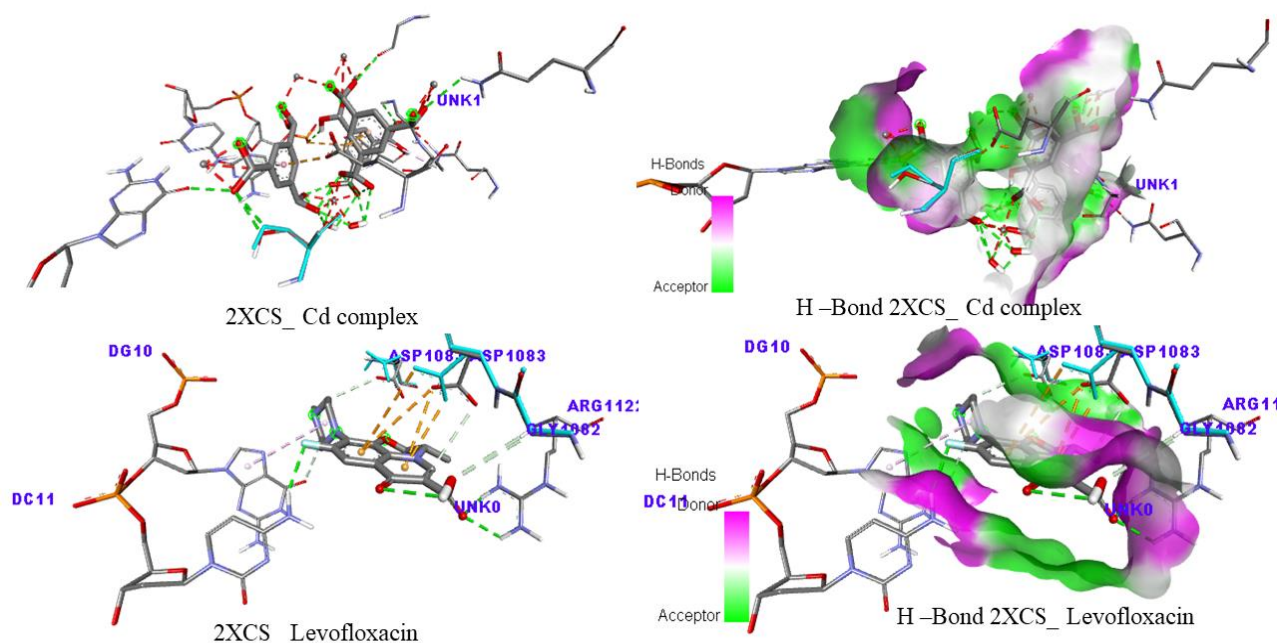


Figure S2. Interactions, H-bond of the Cd complex and the standard drug with the receptor protein 2XCS.

Table S1. Selected bond length (Å).

Atom	Atom	Length (Å)	Atom	Atom	Length (Å)
Cd1	O7 ²	2.291(3)	C4	C5	1.392(5)
Cd1	C1	2.737(4)	C4	C8	1.494(4)
O3	C1	1.254(5)	C5	C6	1.383(5)
O4	C1	1.279(5)	C6	C7	1.392(5)
O5	C8	1.270(4)	C6	C9	1.481(5)
O6	C8	1.249(4)			

Table S2. Selected bond angle (°).

Atom	Atom	Atom	Angle/°	Atom	Atom	Atom	Angle/°
O4	Cd1	O5 ¹	145.97(9)	C7	C2	C1	120.8(3)
O4	Cd1	O6 ¹	92.51(9)	C4	C3	C2	121.0(3)
O4	Cd1	O7 ²	133.61(10)	C3	C4	C8	121.6(3)
O4	Cd1	C1	27.53(10)	C5	C4	C3	119.1(3)
O5 ¹	Cd1	O1	88.82(10)	C5	C4	C8	119.4(3)
O5 ¹	Cd1	O2	90.96(10)	C6	C5	C4	120.3(3)
O5 ¹	Cd1	O3	159.07(9)	C5	C6	C7	120.8(3)
O5 ¹	Cd1	O6 ¹	53.50(9)	C5	C6	C9	116.3(3)
O5 ¹	Cd1	O7 ²	80.34(10)	C7	C6	C9	122.8(3)
O5 ¹	Cd1	C1	172.95(10)	C6	C7	C2	119.5(3)
O6 ¹	Cd1	C1	119.75(10)	O5	C8	C4	118.1(3)
O7 ²	Cd1	O1	96.08(11)	O6	C8	O5	121.4(3)
O7 ²	Cd1	O2	87.90(11)	O6	C8	C4	120.5(3)
O7 ²	Cd1	O3	79.36(10)	O7	C9	O8	124.6(3)
O7 ²	Cd1	O6 ¹	133.84(10)	O7	C9	C6	120.8(3)
O7 ²	Cd1	C1	106.38(10)	O8	C9	C6	114.6(3)
C1	O3	Cd1	85.3(2)				

Table S3. Atomic charges, Mulliken population analysis and natural population analysis.

Atoms	MPA	NPA
Cd	0.351858	0.19165
O	-0.160251	-0.15589
O	-0.197791	-0.21943
O	-0.129836	-0.11583
O	-0.169683	-0.16842
C	0.072627	0.15902
C	0.070250	0.15440
C	-0.001230	-0.00425
C	-0.067339	-0.03909
C	-0.068446	-0.04121
C	-0.006045	-0.02582
H	0.111999	0.07589
C	-0.005066	-0.02456
H	0.107752	0.07160
C	-0.064182	-0.03421
H	0.120903	0.08308
C	0.000951	0.00006
C	-0.069141	-0.04293
C	-0.070311	-0.04442
C	-0.004620	-0.02298
H	0.110747	0.07463
C	-0.005489	-0.02418
H	0.108542	0.07281
C	-0.064749	-0.03539
H	0.121100	0.08319
C	0.226919	0.30560
O	-0.122283	-0.13169
C	-0.011409	-0.03383
C	-0.065212	-0.03427
C	-0.062989	-0.03127
C	-0.005832	-0.02598
H	0.109237	0.07295
C	-0.004342	-0.02433
H	0.117572	0.07973
C	-0.060716	-0.02794
H	0.123710	0.08500
O	-0.109731	-0.09382
C	0.217715	0.28909
O	-0.185995	-0.20937
O	-0.242756	-0.26935
H	0.247392	0.25327
C	0.217902	0.28887
O	-0.183488	-0.20670
O	-0.242876	-0.26952
H	0.247830	0.25371
C	0.214235	0.28488
O	-0.193920	-0.21872
O	-0.246729	-0.27379
H	0.244788	0.25105
C	0.213358	0.28444
O	-0.196452	-0.22145
O	-0.246422	-0.27346
H	0.245099	0.25135
C	0.216048	0.28681
O	-0.187513	-0.21135

Continue...

O	-0.245395	-0.27236
H	0.246389	0.25250
C	0.217195	0.28877
O	-0.188226	-0.21202
O	-0.242992	-0.26973
H	0.246737	0.25266
H	0.091839	0.05796
H	0.113569	0.07441
O	-0.329324	-0.37112
H	0.258796	0.28798
O	-0.324794	-0.36555
H	0.249810	0.28012
H	0.272082	0.30149
H	0.268622	0.29725

Structural effect on the charge transfer and on the internal reorganization energy: Computational study

Mohamed Jabha^{1,2+}, Abdelah El Alaoui², Abdellah Jarid³, El Houssine Mabrouk^{1,4}

1. University of Moulay Ismail, Faculty of Sciences and Technics, Errachidia, Morocco.
2. University of Moulay Ismail, Faculty of Sciences, Meknes, Morocco.
3. University of Cadi Ayyad, Faculty of Sciences Semlalia, Marrakech, Morocco.
4. Sidi Mohamed Ben Abdellah University, Faculty of Sciences, Fez, Morocco.

+Corresponding author: Mohamed Jabha, **Phone:** +212614018410, **Email address:** m.jabha@edu.umi.ac.ma

ARTICLE INFO

Article history:

Received: July 26, 2022

Accepted: October 10, 2022

Published: October 28, 2022

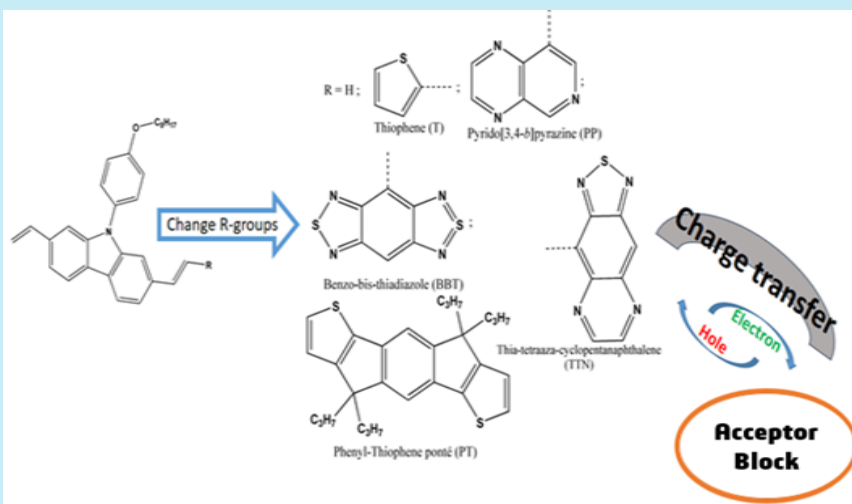
Keywords:

1. 2,7-Divinylcarbazole
2. Benzo-bis-thiadiazole
3. photovoltaic cell
4. DFT
5. charge transfer

Section Editors: Assis Vicente Benedetti

ABSTRACT: The effects of addition of thiophene, bridged phenyl-thiophene, thia-tetra-azacyclopenta-naphthalene, benzo-bis-thiadiazole, and pyrido(3,4-b)pyrazine to 9-(4-octyloxyphenyl)-2,7-divinylcabazole on the internal reorganization energies, electronic affinity, and ionization potential were studied using density functional theory (DFT). These compounds are characterized by their charge exchange potentials (donor-acceptor), which can be applied in energy conversion devices such as photovoltaic cells. The so-called internal reorganization concerns, above all, the positions of holes and points of high electron density on the molecular skeleton.

Thus, valuable information is provided by the knowledge of the structure, the length of the desired oligomer and the nature of the radicals attached to the oligomer. Considering the available data, 2,7-divinylcarbazole (CrV-H) is the basic oligomer to carry out this theoretical study by extending the choice of ligands and length order to other oligomers while setting charge mobility as the major objective. The λ^+ of all the oligomers studied was lower than their λ^- except for the CrV-BBT oligomer, indicating a lower hole transfer cost than electron transfer cost with changes in molecular geometry during this process.



1. Introduction

The advent of organic electronics is deeply related to the development of new oligomers with high performance and reproducible properties (Muth *et al.*, 2013; Rodríguez-Monge and Larsson, 1995). Thus, the design of new oligomer architectures is a task usually accompanied by difficulties, especially the molecular stability that should generate the reproducible properties.

Oligomers based on 2,7-divinylcarbazole have been the subject of much experimental and theoretical work (Huixia *et al.*, 2017; Jabha *et al.*, 2018; 2021; Leclerc *et al.*, 2006). They have been qualified as promising compounds. Thus, taking into account the available data of this nanostructure, a theoretical approach would allow to widen the field of stakes for applications in electronics, optoelectronics and light energy-electric energy conversion. Thus, a quantum treatment by means of the density functional theory (DFT) seems to be a good way to understand the relationship between the structures and the electronic properties mentioned above.

Studies such as the one realized by Aly (2009) show that carbazole units have properties (high thermal stability, excellent physicochemical, and charge hole transport properties). Similarly, derivatives of carbazole have been analyzed by chemical modification (Jabha *et al.*, 2018).

In general, oligomers and conjugated organic polymers (Jabha *et al.*, 2021) have the same mechanism of charge transfer, their rate of hole and electron transfer mainly depends on the reorganization energy due to the geometrical relaxation that accompanies this transfer (André and Brédas, 2002). The reorganization energy is usually expressed as the sum of the internal and external contributions. The internal reorganization energy comes from the change in the equilibrium geometry of the donor and acceptor sites due to charge gain/loss during an electron transfer. The external reorganization energy comes from the electronic and nuclear polarization/decay of a surrounding medium.

In this manuscript, the strategy is the theoretical study of the structural properties of a carbazole-based oligomers series, in order to reveal the charge transfer and electronic properties of organic semiconductor materials of different natures. The effect of substitution and nature of substituent grouping on the reorganization energy for hole and electron transfer (λ^+ and λ^-) and electron affinity and ionization potential are also investigated (Schwenn *et al.*, 2011).

2. Computational details

All calculations were performed using the Gaussian 09 series (Bally *et al.*, 1991; Frisch *et al.*, 1984; Green *et al.*, 2005; Rassolov *et al.*, 2001). The ground state structure of all oligomers was fully optimized at the level of DFT theory and B3LYP functional by choosing 6-31G (d,p) basis set (Baker *et al.*, 1995; Ochterski *et al.*, 1996; Petersson and Al-Laham, 1991). The values of highest occupied molecular orbital (HOMO), lowest unoccupied molecular orbital (LUMO), E_g levels, dihedral angles, bond lengths and energies of the minima of the compounds were determined from these optimized geometries. In the same way the charge quantities were determined at the same level and on the same optimized structures. For the ultraviolet-visible (UV-vis) spectrum as well as the oscillator power (f), excitation energies and wavelengths of the oligomers, has been chosen the TD-BP86/6-31G (d,p) method (Becke *et al.*, 1988; Burke *et al.*, 1996) for its reliability in such evaluations.

3. Results and discussion

The 9-(4-octyloxyphenyl)-2,7-divinylcarbazole (CrV-H) (Leclerc *et al.*, 2006) is the basic molecule, (Fig. 1), in which we substituted the vinyl hydrogen with heterocyclic groups (R). Figure 2 presents the different R groups studied by the DFT method to investigate the substitution effects on the electronic and optoelectronic properties of the CrV-R system (Jabha *et al.*, 2022).

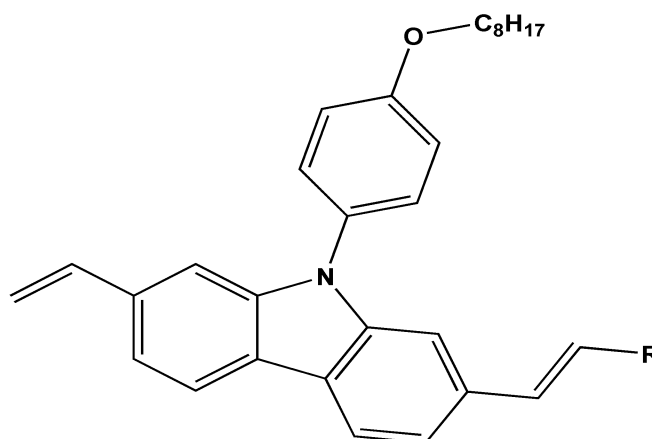


Figure 1. Structure of 9-(4-octyloxyphenyl)-2,7-divinylcarbazole (CrV-H); R=H.

Source: Adapted from Jabha *et al.* (2022).

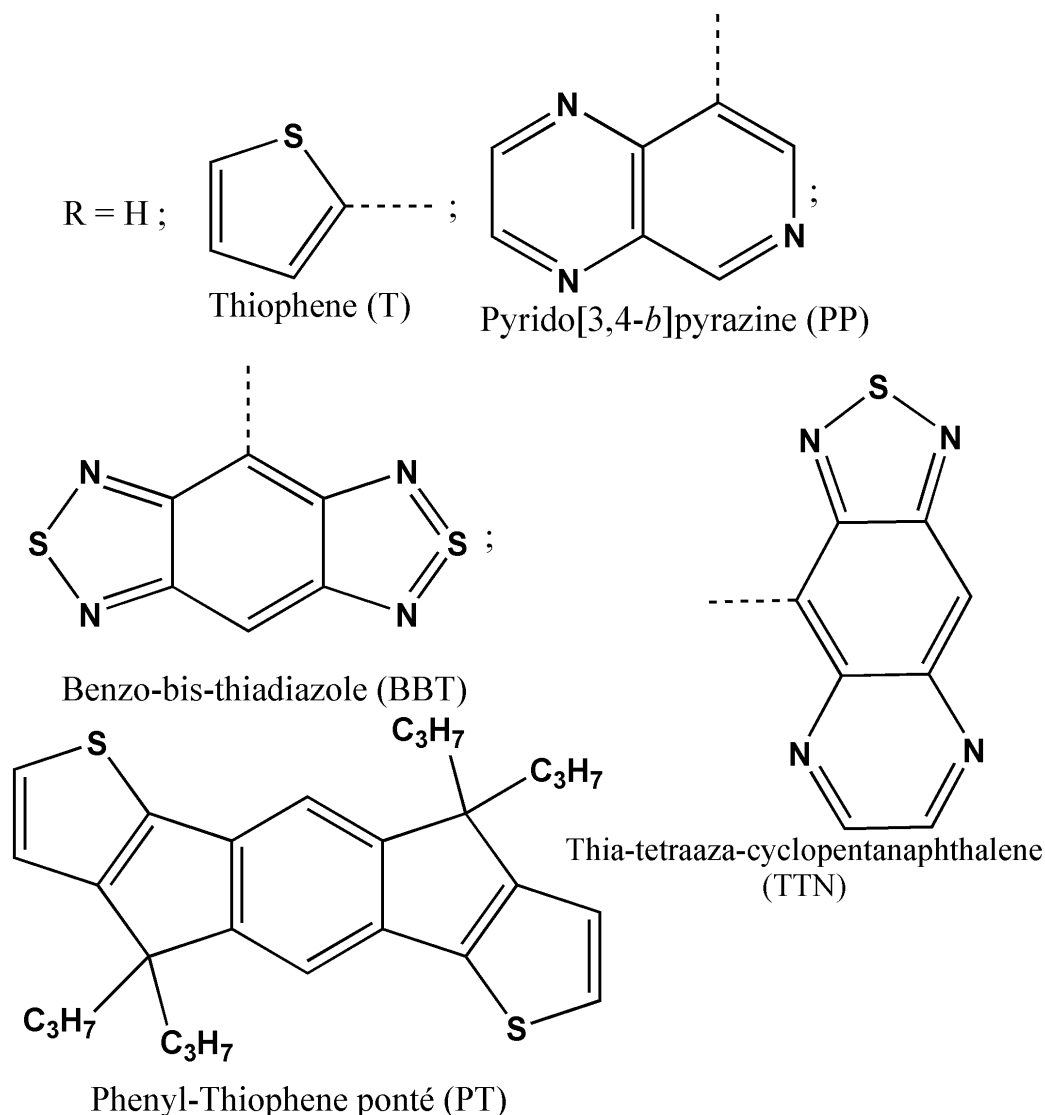


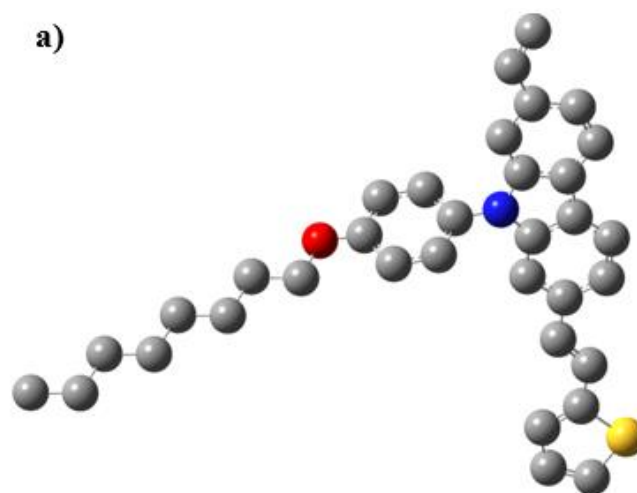
Figure 2. Schema and symbol of R groups.

Source: Adapted from Jabha *et al.* (2022).

3.1 Structural properties

All oligomers were optimized at the B3LYP/6-31G (d,p) level, and Fig. 3 represents the most stable conformations. For a credible study of the structural properties, extractions of the main structural parameters are necessary.

Based on the optimization of the systems by the DFT method at the level of the B3LYP functional under the atomic basis 6-31G (d,p), the geometrical study of the oligomers neutral and charged is completed by the calculation of the various structural parameters which depend on the geometry of the molecules, mainly the dihedral angles, the lengths of the primordial bonds between the base unit note CrV and the adjacent groups R (Fig. 4).



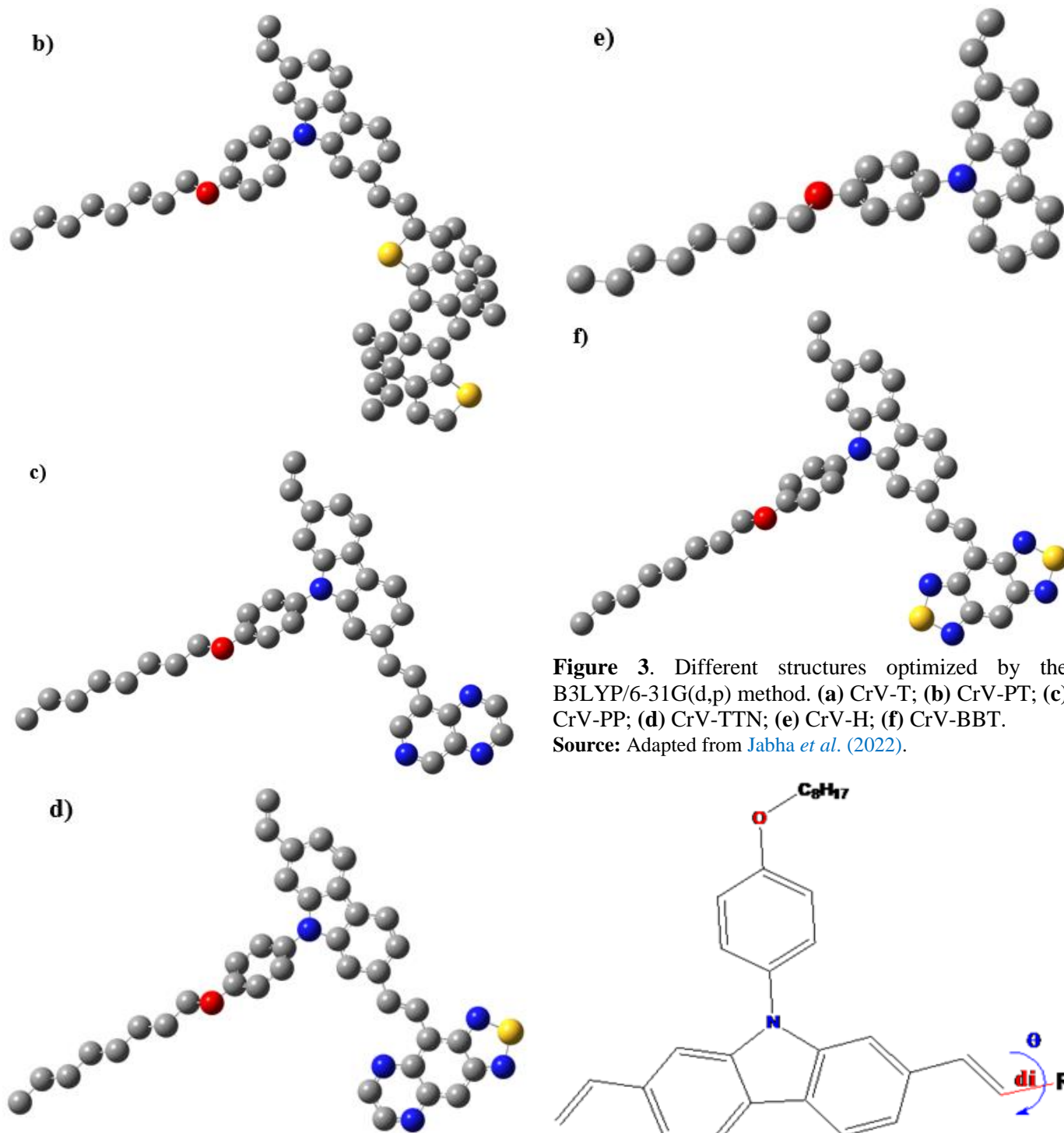


Figure 3. Different structures optimized by the B3LYP/6-31G(d,p) method. (a) CrV-T; (b) CrV-PT; (c) CrV-PP; (d) CrV-TTN; (e) CrV-H; (f) CrV-BBT.
Source: Adapted from Jabha *et al.* (2022).

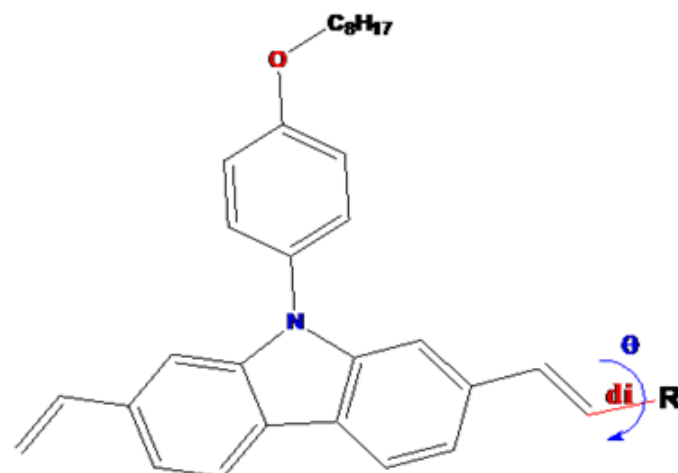


Figure 4. Position of the dihedral angles, and the studied bonds.
Source: Adapted from Jabha *et al.* (2022).

In the theory of Marcus *et al.* (1989), the charge transfer integral is important for electron transfer because it is one of the factors for calculating the mobility of a material. The other factor is the reorganization energy. The higher the charge transfer

integral and the lower the reorganization energy, the higher the charge transfer rate and mobility. The charge transfer integral represents for exchange electrons between molecules, and strongly affected by the intermolecular and/or intramolecular (interatomic) distance, the shorter the distance, the stronger the orbital overlaps. Figures 5 and 6 illustrate the main structural parameters, especially the intramolecular distances and the dihedral angles of the studied systems.

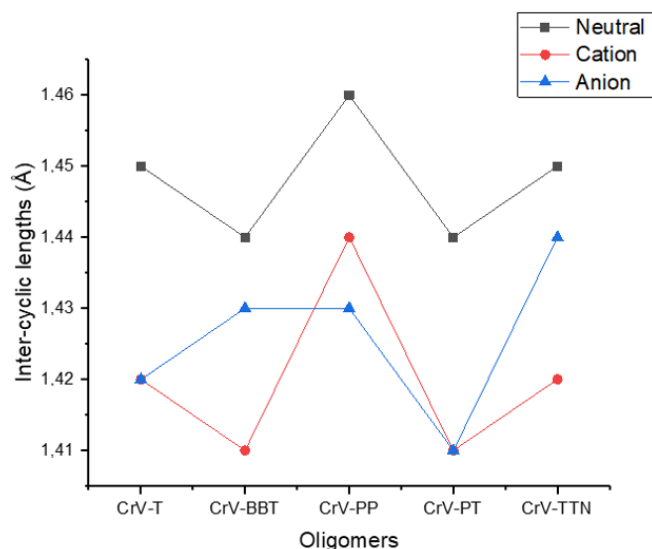


Figure 5. Inter-cyclic lengths (Å) obtained by the B3LYP/6-31G method (d,p).

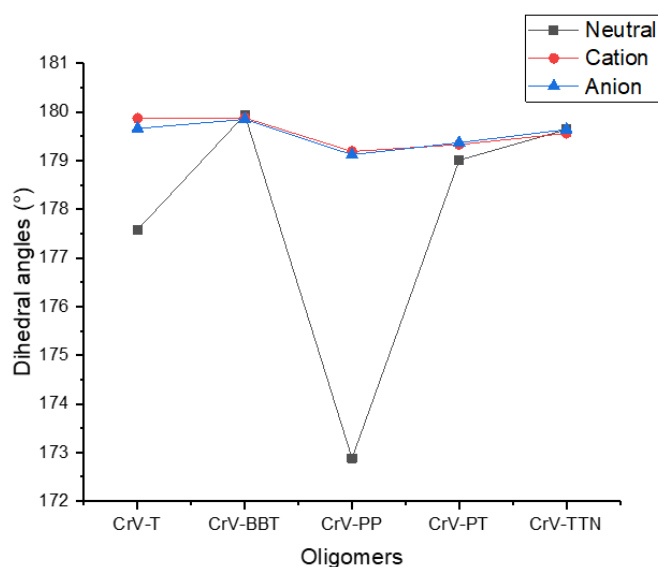


Figure 6. Dihedral angles obtained by the B3LYP/6-31G method (d,p).

The dihedral angles between the blocks of conjugated oligomers contribute significantly to the determination of the reorganization energy (λ_{tot}) and the charge

transport process. Thus, comparison of the dihedral angles between charged and neutral counterparts is crucial in the optoelectronic study of these oligomers. The values of the dihedral angles of the neutral and charged forms of all the studied oligomers (Fig. 6) are generally close to 180° , which would allow to conclude that the structures are nearly planar, especially the CrV-BBT based compounds, whose values are 179.94° , 179.88° , and 179.85° for the neutral, cationic and anionic structure, respectively. It is concluded that the neutral states tend towards flat and rigid structures.

In addition, a dramatic reduction of the bond length from the neutral to the anionic or cationic state was observed in Fig. 5. As well as the introduction of the groups containing nitrogen atoms at the terminal of the vinyl, would give more flatness to the molecular skeleton, so all the bonds are kept short of about 1.44 \AA between oligomer CrV-BBT and the vinyl unit. This shortening is attributed to the size and electronegativity of the nitrogen atom, as well as influencing the electron density distribution.

Dipole moments can explain charge transport properties. Thus, Fig. 7 indicates that the dipole moment of oligomers with planar structures is higher than that of other oligomers in the neutral state. This means that CrV-BBT and CrV-TTN, which show high dipole moments, indicate the presence of significant charge transfer.

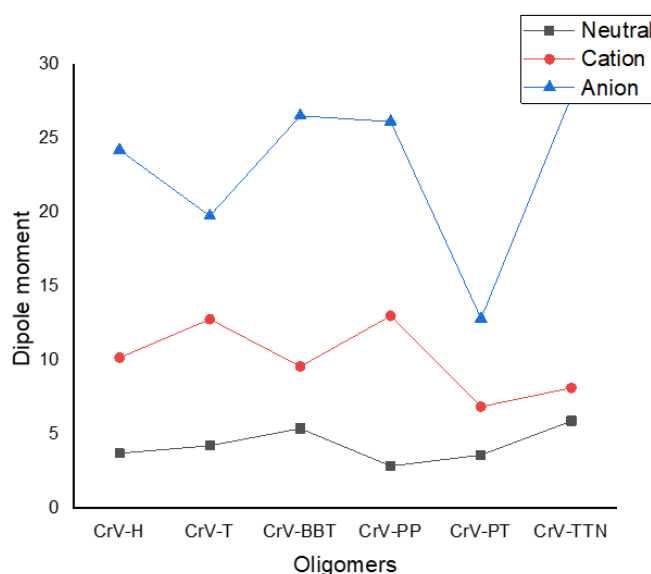


Figure 7. Dipole moment of oligomers in the neutral and charged state obtained by B3LYP/6-31G (d,p).

When the ground states are excited a sharp change in dipole moment takes place which would have a change in the degree of intermolecular charge transfer. The dipole moment of the oligomers in the neutral and charged states were calculated. The values are presented

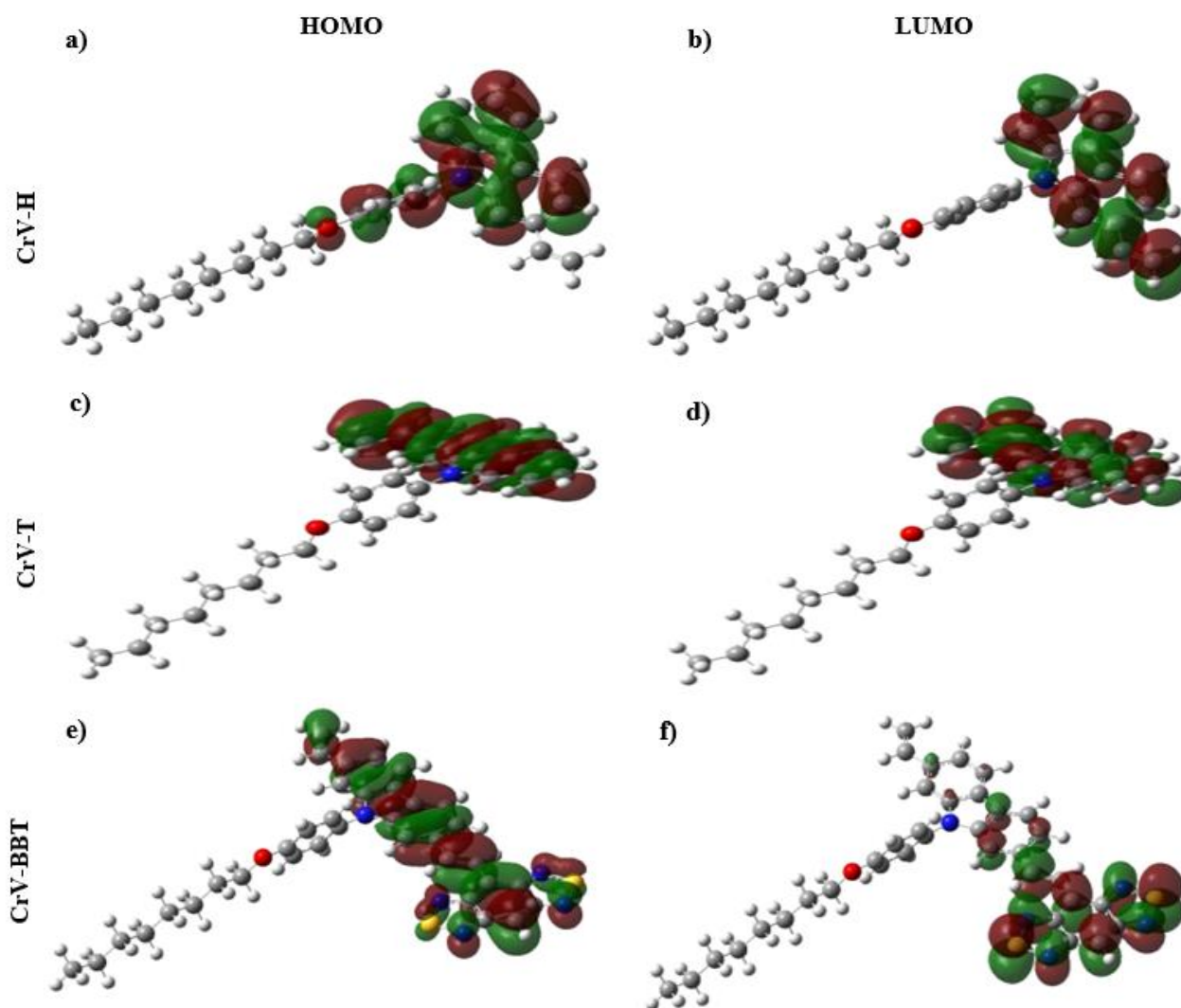
in Fig. 7. It is clear that CrV-BBT and CrV-TTN have the highest values of the dipole moments, which make their excited states highly polarized and facilitate the charge transport. These results agree with the reorganization energy. In the excited state, the negative charge tends to localize on the acceptor unit (A) while the positive charge tends to localize on the donor (D). The large separation between the negative and positive charges after excitation reduces the D-A binding energy which facilitates exciton dissociation and transport.

Conversely, the recombination rate is high and fast in compounds with low dipole moment, which indicates

that electrons and holes are more bound in compounds with high dipole moment value namely CrV-BBT and CrV-TTN than in other compounds with low dipole moment.

3.2 The boundary orbitals

Figure 8 presents the electronic density of the HOMO and LUMO orbitals of the studied oligomers, which give a qualitative and rational indication of the electronic properties of the studied oligomers.



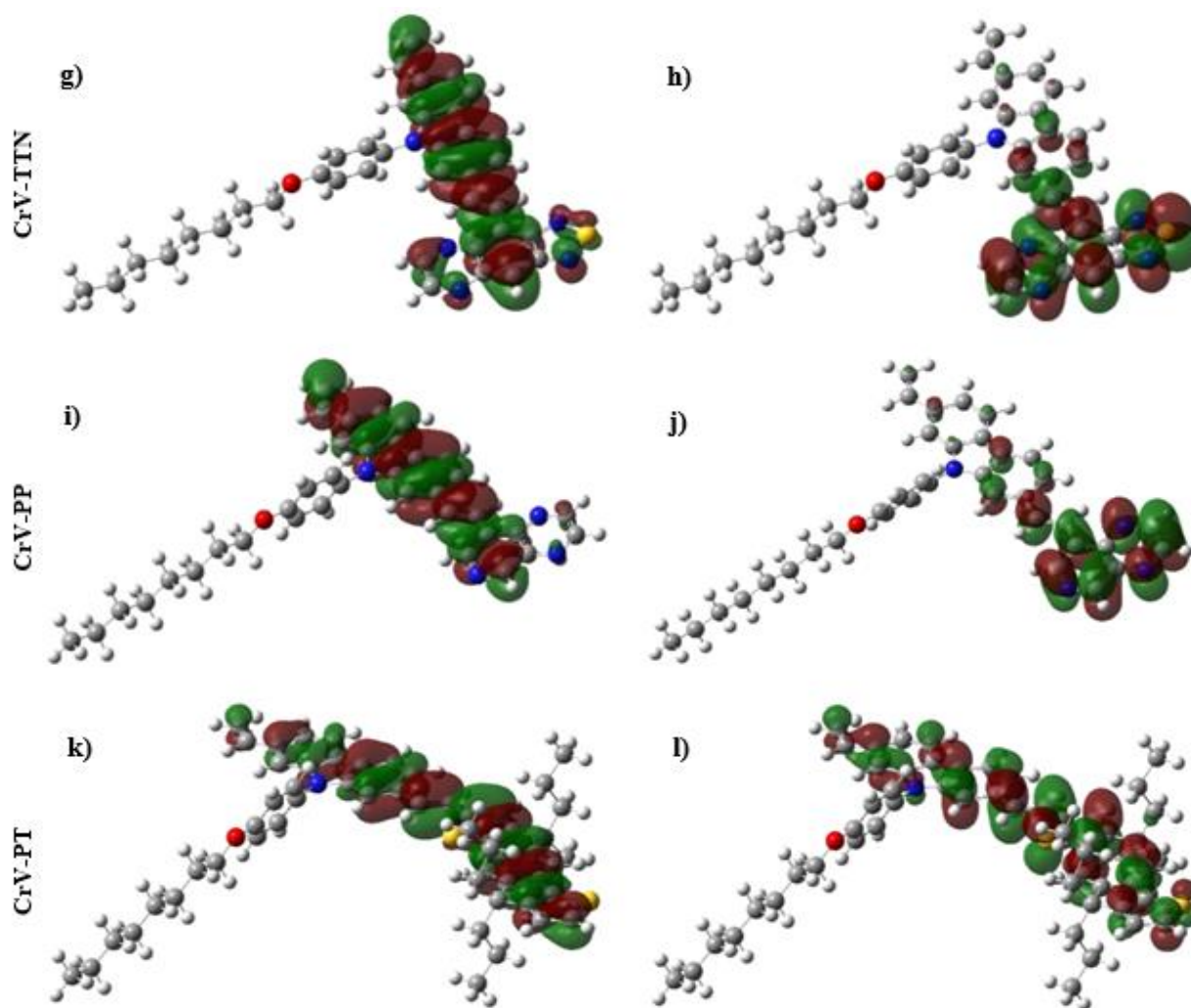


Figure 8. The contour plots of HOMO (a, c, e, g, i, k) and LUMO (b, d, f, h, j, l) orbitals of the studied oligomers by DFT/B3LYP 6-31G (d,p).

Source: Adapted from [Jabha *et al.* \(2022\)](#).

The propagation of the electron density appears very clearly in [Fig. 8](#). The electron density of the LUMO is stronger around the nitrogenous group, on the other hand the systems related to groups possessing the thiophene are characterized by electron densities spread out on the whole carbon skeleton. Thus, at the HOMO level, the electron density is spread over the whole skeleton of the system. It is important to notice the absence of electron density on the chain linked to the carbazole nitrogen (N). Thus, this chain does not present any optical effect. It plays, perhaps, a role of solubilization and stability of the system.

3.3 Electronic properties

The electronic properties are of fundamental importance for the study of this type of molecules. Thus, the knowledge of the energy levels of the HOMO and

LUMO orbitals is fundamental for the study of the properties and feasibility of these oligomers to be used as base materials of the active layer of organic solar cells ([Dufil *et al.*, 2018](#); [Jabha *et al.*, 2018](#)).

[Figure 9](#) groups the energy levels of the systems optimized by the DFT method at the level of the B3LYP functional with the base 6-31G (d,p). The values of E_g show that the oligomers having a group different from hydrogen, has a semiconductor character, mainly the CrV-BBT by the smallest value of gap energy ($E_g = 1.75$). This value allows a good exciton creation, i.e., excitation of the electrons from the HOMO to the LUMO, thus the recombination rate decreases.

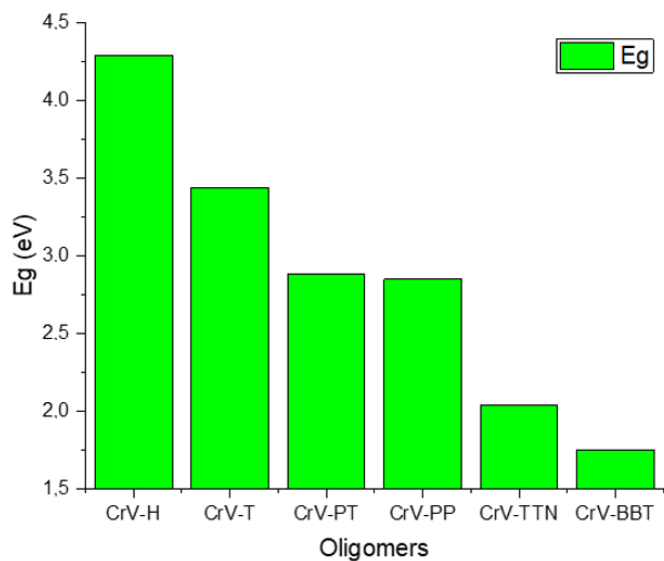


Figure 9. Gap energies (E_g) calculated by the DFT/B3LYP/6-31G(d,p) method.

Figure 10 shows that the LUMO values become lower when moving from CrV-H to CrV-BBT while the HOMO varies slightly and remains stable. The decrease in energy of the LUMO of CrV-BBT (donor) approaches that of the acceptor unit here Bis-PCBM as shown in Fig. 11.

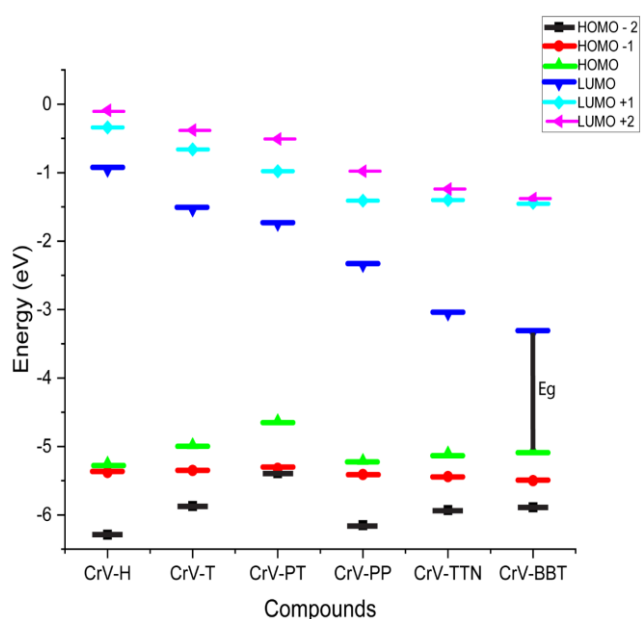


Figure 10. Evolution of energy levels with respect to the added R group.

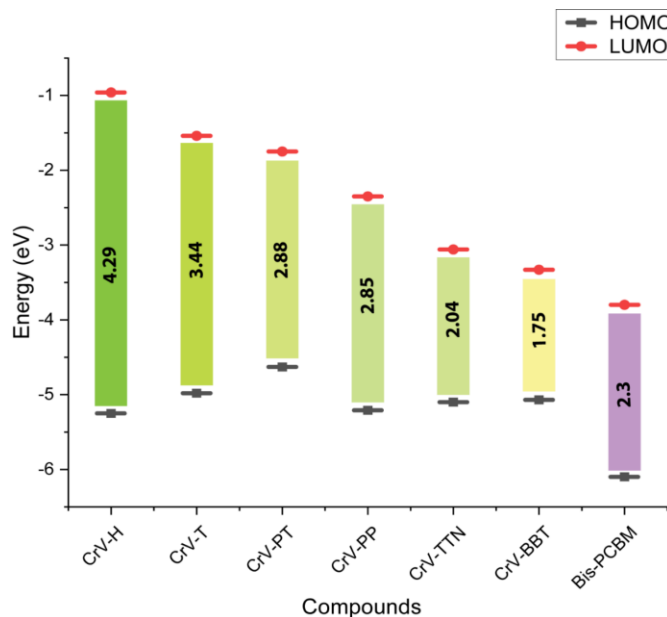


Figure 11. Position of the energy levels of oligomers (D) relative to oligomer A (Bis-PCBM) studied at the B3LYP level.

The HOMO energy of CrV-BBT is high compared to the other oligomers, with the lowest band gap energy indicating that the BBT groups in this molecule have significantly improved the properties of the hole carrier, thus the better stability of the LUMO level gives this oligomer a lower HOMO-LUMO gap. As a result, there should be higher carrier mobility and low kinetic stability. As well as the hole acceptor character accompanied by the decrease of the ionization potential (IP) increases. This phenomenon is accompanied by an increase in the conjugation length and the flatness of the structure. These findings are confirmed by the structural parameters (Figs. 5 and 6).

3.4 Reorganization energy

In general, conjugated organic oligomers and polymers undergo charge transfer phenomena via a jump-type mechanism. However, organic oligomers are mainly p-type. Therefore, in this case, the charge transfer process is essentially a hole transfer process. The hole transport in organic semiconductor materials between adjacent molecules depended on the reorganization energy. The rate of hole transfer mainly depends on the reorganization energy (λ) due to the geometric relaxation accompanying the charge transfer and the electronic coupling matrix element (V) between the two D-A semiconductors. However, V is related to the bandwidth in conventional solid-state descriptions (Camara, 2011;

Khoudir *et al.*, 2000; Koh *et al.*, 2008; Liu *et al.*, 2019; Provencher *et al.*, 2014).

The hole/electron transfer rate for higher temperature mainly depends on the reorganization energy (λ) due to geometric relaxation (Camara, 2011). The importance of λ in charge transfer processes has been widely studied in the context of Marcus *et al.* (1989) and Baran *et al.* (2017) theories.

Some reorganization energy studies have been performed on isolated molecules (Khoudir *et al.*, 2000; Marcus *et al.*, 1989). The reorganization energy is usually expressed as the sum of the internal and external contributions. The internal contribution consists of two terms related to the relaxation of the geometry from the neutral to the charged state and from the charged to the neutral state (Liu *et al.*, 2019). On the other hand, the external reorganization energy represents the effect of the external environment on the charge transfer. The calculated values of the external reorganization in pure organic phases are negligible in front of the internal reorganization energy values (Camara, 2011). Therefore, an estimate of the internal reorganization energy can give accurate and important information about the charge mobility in organic semiconductor materials (Koh *et al.*, 2008). Internal reorganization energies for hole (λ^+) and electron (λ^-) transfer, adiabatic electron affinity, and potential are also discussed.

The reorganization energy for electron (λ^-) and hole (λ^+) of the oligomers was predicted from energetic calculations at the B3LYP/6-31G(d,p) level based on the optimized neutral, cationic, and anionic geometries at the B3LYP/6-31G(d) level. Thus, the reorganization energies for λ^+ and λ^- transfer are determined by Eqs. 1 and 2 (Berlin *et al.*, 2003; Cheung *et al.*, 2010; Sun *et al.*, 2017):

$$\lambda^+ = [E^+(M) - E^+(M^+)] + [E(M^+) - E(M)] = IP_v - HEP \quad (1)$$

$$\lambda^- = [E^-(M) - E^-(M^-)] + [E(M^-) - E(M)] = EA_v - EEP \quad (2)$$

where $E(M)$, $E^-(M^-)$, and $E^+(M^+)$ are the energy of the neutral state, anion, and cation in their optimized structures, respectively. $E^+(M)$ is the total energy of the cation in the neutral geometry, $E(M^+)$ is the total energy of the neutral state in the cation geometry, $E^-(M)$ is the total energy of the anion in the neutral geometry, and $E(M^-)$ is the total energy of the neutral in anion geometry.

The values of the adiabatic (EAa) and vertical (EA_v) electron affinity and the adiabatic (IPa) and vertical (IP_v) ionization potential of the molecules are calculated from according to Eqs. 3–6:

- **Electronic affinity:**

$$EA_a = E(M) - E^-(M^-) \quad (3)$$

$$EA_v = E(M) - E^-(M) \quad (4)$$

- **Ionization potential:**

$$IP_a = E^+(M^+) - E(M) \quad (5)$$

$$IP_v = E^+(M) - E(M) \quad (6)$$

The electron extraction potential (EEP) and hole extraction potential (HEP) are calculated by the Eq. 7 and 8:

$$EEP = E(M^-) - E^-(M^-) \quad (7)$$

$$HEP = E^+(M^+) - E(M^+) \quad (8)$$

Figures 12–14 show several parameters related to the studied oligomers: the adiabatic ionization potential, vertical ionization potential and hole extraction potential (Fig. 12), adiabatic electron affinity, vertical electron affinity and electron extraction potential (Fig. 13) and oligomer hole/electron reorganization energy (Fig. 14).

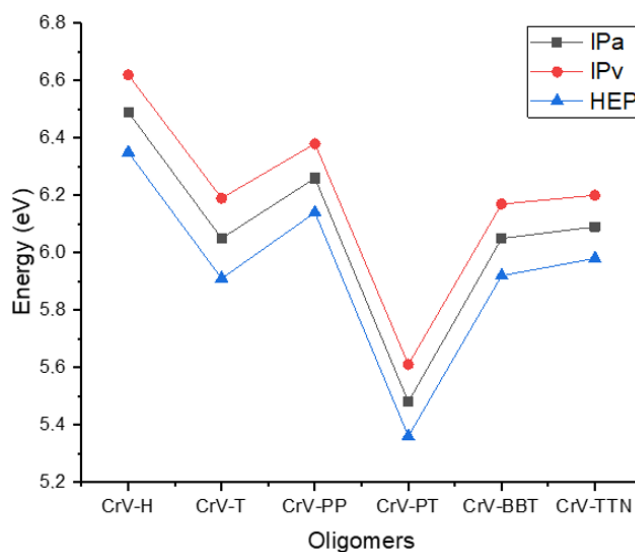


Figure 12. Adiabatic ionization potential (IPa), vertical ionization potential (IPv), hole extraction potential (HEP) of oligomers (eV) calculated by B3LYP/6-31G(d,p).

Figure 12 shows the lowest value of ionization potential carried by the CrV-PT molecule, which gives this molecule the character of an electron donor, as well as the values of the CrV-BBT molecule are also slightly small, i.e., this oligomer has an electron donor character.

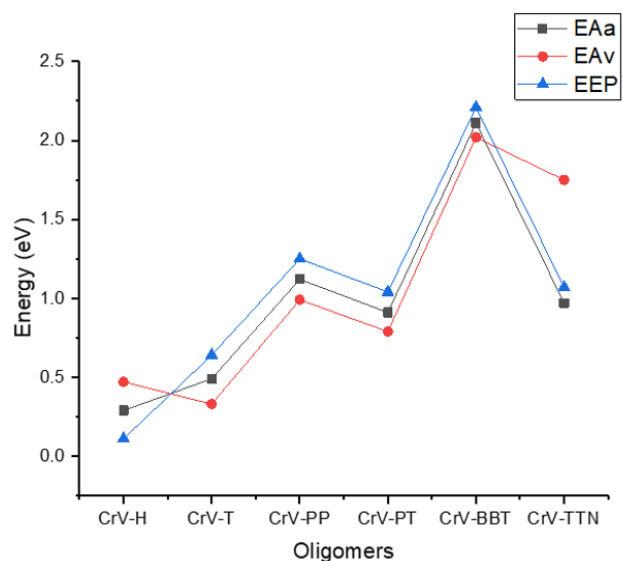


Figure 13. Adiabatic electron affinity (EAa), vertical electron affinity (EAν), electron extraction potential (EEP) of oligomers (eV) calculated by B3LYP/6-31G (d,p).

In Fig. 13, the higher value of electron affinity of the CrV-BBT molecule makes this molecule more stable and electron rich, which confirms that this molecule is a strong electron donor.

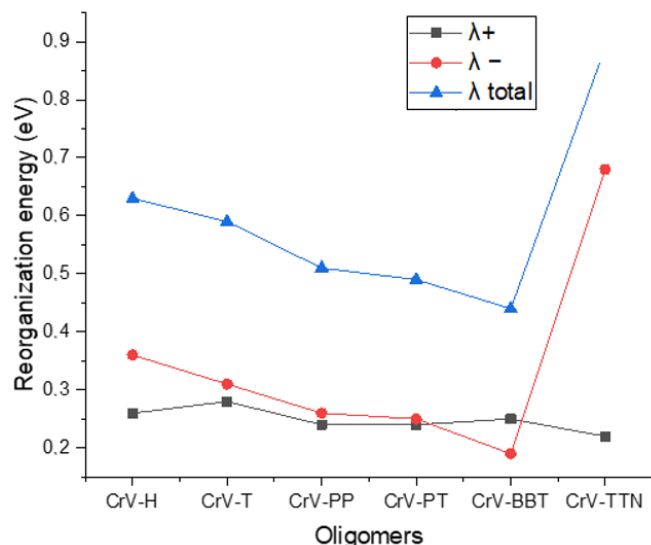


Figure 14. Oligomer hole/electron reorganization energy (eV) calculated by B3LYP/6-31G(d,p).

The oligomer with the BBT moiety has at the lowest value of λ reorganization energy (0.4431 eV). This indicates that the transport of electrons gives the materials based on this compound is favored, likewise this compound to the greatest value of EAa. Therefore, the greater the electron affinity the better the electron capture ability.

The IP values for the molecules with R groups are all lower than the value of the CrV-H oligomer, which can be attributed to the inductive and negative resonance effects of R groups.

From the values of EA and IP, it is believed that the systems with R groups can be used as a better organic semiconductor material, for D- π -A-A type devices.

As shown in Fig. 14, the λ^+ of all the studied oligomers was lower than their λ^- , except for the CrV-BBT oligomer, indicating a lower hole transfer cost than electron transfer cost with changes in molecular geometry during this charge transfer.

3.5 Excitation state calculation

The OSC (oligomer semi-conductor) coefficient of the studied molecules was obtained by DFT-B3LYP/6-31G (d,p) method and the maximum absorption wavelength (λ_{\max}), oscillator strengths (f) and excitation energy values Eex (eV) were obtained. The knowledge of the UV-visible absorptions of the studied oligomers contributes to their evaluation as potential materials in photovoltaic applications.

Taking the optimized structures at the level B3LYP/6-31G (d,p), we calculated the UV-Visible spectra of the oligomers at the level TD-DFT-BP86/6-31G(d,p) (Burke *et al.*, 1996).

3.5.1 Electronic transition, excitation energy and oscillation strength

The calculated electronic absorption spectra of the studied oligomers are shown in Fig. 15. Table 1 presents the λ_{\max} , oscillation strengths (f), and excitation energy values Eex (eV).

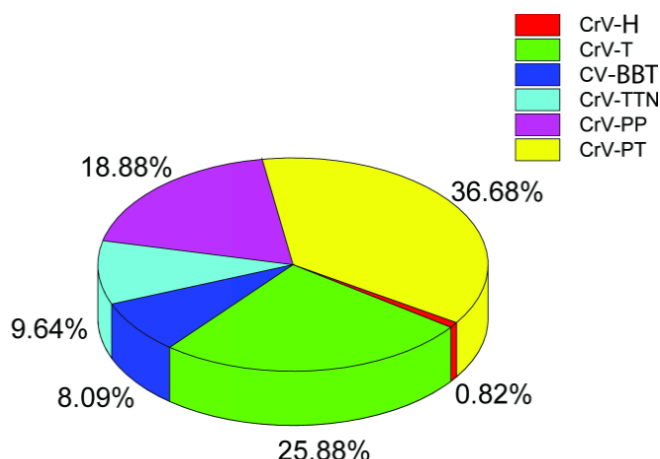


Figure 15. Percent of OSC of the molecules studied by the DFT-B3LYP/6-3G method (d,p).

Table 1. Electronic transition data obtained by TD-DFT-BP86/6-31G (d, p) calculation for all oligomers models.

Compound	DFT-BP86/6-31G (d,p)			λ_{\max} 'exp' (nm)*
	E _{ex} (eV)	f	λ_{\max} (nm)	
CrV-H	3.1182	0.0354	397.62	436
	3.5174	0.0051	352.49	
	3.6101	0.0006	343.44	
CrV-T	2.6142	0.0222	474.28	466
	2.8195	1.2246	439.74	
	3.0152	0.0061	411.20	
CV-BBT	1.1671	0.0027	1062.34	
	1.3509	0.3658	917.77	
	1.8504	0.0098	670.04	
CrV-TTN	1.2660	0.0028	979.37	
	1.4403	0.3549	860.84	
	2.0194	0.0317	613.96	
CrV-PP	1.7405	0.0036	712.35	
	1.8352	0.2258	675.59	
	2.5562	0.0051	485.02	
CrV-PT	2.2100	1.9128	561.02	
	2.3550	0.0102	526.47	
	2.4545	0.0408	505.13	

*Leclerc *et al.* (2006)

As presented in Tab. 1, the maximum absorption wavelength λ_{\max} of the reference oligomers (CrV-H, CrV-T) (397.62 and 474.28 nm) correlates perfectly with the available experimental values (of 436 and 466 nm, respectively) (Leclerc *et al.*, 2006), suggesting that TD-BP86/6-31G (d,p) was a suitable level to predict the evolution of the optoelectronic properties of the oligomers.

Molecules with gap energies below 2.87 eV absorb light in the visible range and CrV-TTN and CrV-BBT oligomers absorb in the infrared, so with low excitation

energy (1.16–1.26 eV) one can excite electrons from HOMO to LUMO.

Figure 15 shows that all the substituted molecules have an important proportion of OSC, compared to that of the basic oligomer (CrV-H), which implies an increase of the rate of excitation in these molecules, as well as the transfer of charge from the HOMO level to LUMO will be easier, with a low energy of excitation.

3.5.2 Absorption spectrum

Figure 16 shows UV-vis spectra of all oligomers calculated at DFT-B3LYP/6-31G(d,p) level.

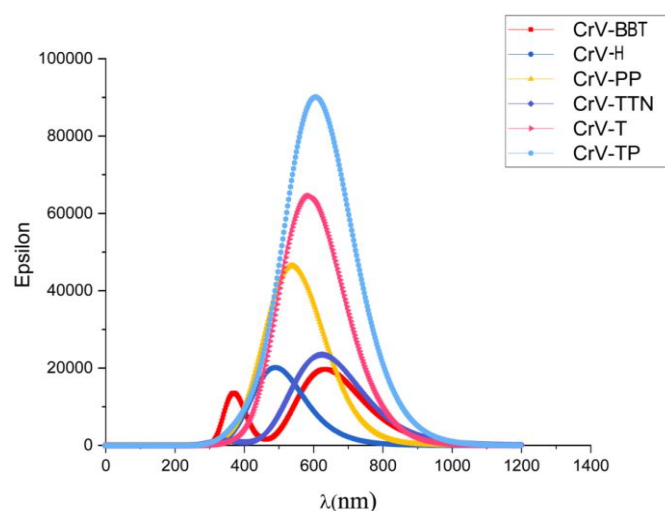


Figure 16. Data of UV-vis spectra of all oligomers calculated at DFT-B3LYP/6-31G(d,p) level.

Source: Adapted from Jabha *et al.* (2022).

All the studied oligomers have absorption spectral bands obtained by DFT method that can be attributed to the intermolecular transfer charge in the structures of these molecules. This indicates that these organic materials could absorb the maximum incident light radiation. The energy range for all the structures studied is generally in the visible and near infrared, however the CrV-BBT oligomer has a dual excitation band, one of which is broad like that of the reference oligomer (CrV-H).

3.5.3 Photovoltaic properties

Theoretically the open circuit voltage (V_{oc}) and α were calculated from Eqs. 9 and 10 (Jabha *et al.*, 2018):

$$V_{oc} = |E_{HOMO}(\text{Donor})| - |E_{LUMO}(\text{Acceptor})| - 0.3 \quad (9)$$

$$\alpha = |E_{\text{LUMO}}(\text{Acceptor})| - |E_{\text{LUMO}}(\text{Donor})| \quad (10)$$

The Voc is obtained when the current through the cell is zero. In the case of organic solar cells, the Voc is linearly dependent on the HOMO level of the donor material and the LUMO level of the acceptor material (Brabec *et al.*, 2001). In addition, charge losses at the material-electrode interfaces can also affect the Voc value (Günes *et al.*, 2007). Finally, this value decreases with temperature and varies little with light intensity (Oukachmih, 2003). The energy levels, Voc and α of the studied systems obtained by the DFT method are shown in Fig. 17.

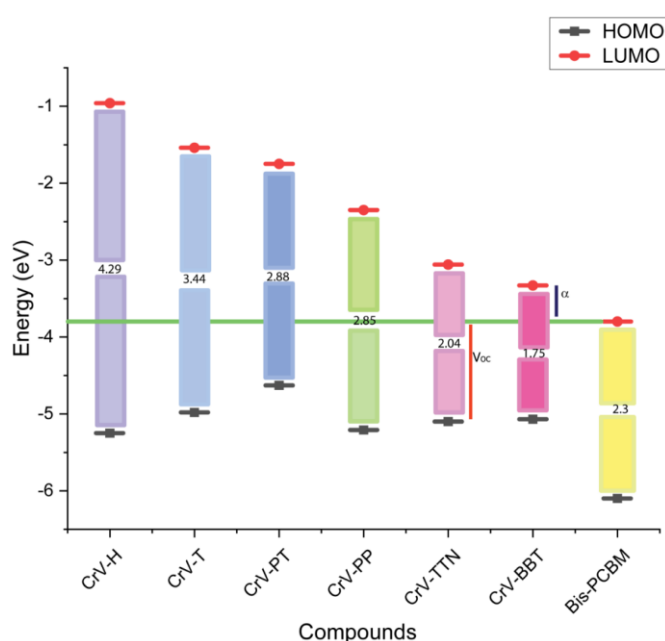


Figure 17. Illustration of the energy levels and Voc and α of the studied systems obtained by the DFT method.

The theoretical values of the Voc of the studied systems are ranked from 0.53 to 1.15 eV taking Bis-PCBM within the solar cell as the semiconductor acceptor. The CrV-PP, CrV-TTN, and CrV-BBT systems exhibit large open-circuit voltage values and low α values. Consequently, the lower the α values the greater the electron transfer from the donor LUMO levels to the acceptor LUMO levels.

4. Conclusions

In this work, the addition of R = T, PT, PP, TTN, and BBT radical to CrV to improve the electronic properties for uses in solar energy conversion devices was analyzed. Thus, the result of long conjugated chain structures, a decrease in gap energy and a high dipole

moment, has a considerable influence on a charge transfer which is the main link of this conversion.

However, this study shows that systems with a smaller energy gap, precisely for the oligomers CrV-BBT, CrV-TTN, are able to absorb sunlight in the visible range and the conversion into electricity is thus ensured. This property allows these systems (CrV-BBT, CrV-TTN) to be used to produce and manufacture electronic devices such as photovoltaic cells. Considering the EA – (electron affinity) and IP (ionization potential) values, it is believed that the systems with R = BBT, TTN groupings can be used as better organic semiconductor materials, for donor- π -acceptor-acceptor (D- π -A) type devices.

Authors' contribution

Conceptualization: Jabha, M.; Elalaoui, A.; Jarid A.

Data curation: Jabha, M.

Formal Analysis: Jabha, M.

Funding acquisition: Not applicable

Investigation: Jabha, M.; Mabrouk, E. H.

Methodology: Jabha, M.; Elalaoui, A.; Jarid, A.

Project administration: Elalaoui, A.

Resources: Not applicable

Software: Not applicable

Supervision: Elalaoui A.; Jarid A.

Validation: Elalaoui, A.; Jarid A.; Mabrouk, E. H.

Visualization: Elalaoui, A.; Jarid, A.

Writing – original draft: Jabha, M.

Writing – review & editing: Jabha, M.; Jarid, A.

Data availability statement

All data sets were generated and analyzed in the current study.

Funding

Not applicable

Acknowledgments

The authors are grateful to the “Association Marocaine des Chimistes Théoriciens” (AMCT) for its pertinent help concerning the programs.

References

- Aly, S. M. B. Transfert D'électron Et D'énergie Photo-induits Dans Les Polyads, Oligomères Et Polymères Organiques Et Organométalliques. Ph.D. Thesis, University of Sherbrooke, 2009. <https://library-archives.canada.ca/eng/services/services-libraries/theses/Pages/item.aspx?idNumber=648383653> (accessed 2022-06-15)
- André, J.-M.; Brédas, J.-L. Transfert d'électrons: des polymères conducteurs d'électricité aux diodes organiques électroluminescentes ou une avalanche de Prix Nobel. *Bull. Acad. R. Belg.* **2002**, *13* (7), 273–289. <https://doi.org/10.3406/barb.2002.28296>
- Baker, J.; Andzelm, J.; Muir, M.; Taylor, P. R. $\text{OH} + \text{H}_2 \rightarrow \text{H}_2\text{O} + \text{H}$. The importance of 'exact exchange' in density functional theory. *Chem. Phys. Lett.* **1995**, *237* (1–2), 53–60. [https://doi.org/10.1016/0009-2614\(95\)00299-J](https://doi.org/10.1016/0009-2614(95)00299-J)
- Bally, T.; Carrupt, P.-A.; Weber, J. Comparison of the Performances of the Gaussian and Cadpac ab initio Program Packages on Different Computers. *Chimia.* **1991**, *45* (11), 352–356. <https://doi.org/10.2533/chimia.1991.352>
- Baran, D.; Ashraf, R. S.; Hanifi, D. A.; Abdelsamie, M.; Gasparini, N.; Röhr, J. A.; Holliday, S.; Wadsworth, A.; Lockett, S.; Neophytou, M.; Emmott, J. M.; Nelson, J.; Brabec, C. J.; Amassian, A.; Salleo, A.; Kirchartz, T.; James R. Durrant, J. R.; McCulloch, I. Reducing the efficiency–stability–cost gap of organic photovoltaics with highly efficient and stable small molecule acceptor ternary solar cells. *Nature Mater.* **2017**, *16* (3), 363–369. <https://doi.org/10.1038/nmat4797>
- Becke, A. D. Density-functional exchange-energy approximation with correct asymptotic behavior. *Phys. Rev. A* **1988**, *38* (6), 3098. <https://doi.org/10.1103/PhysRevA.38.3098>
- Berlin, Y. A.; Hutchison, G. R.; Rempala, P.; Ratner, M. A.; Michl, J. Charge Hopping in Molecular Wires as a Sequence of Electron-Transfer Reactions. *J. Phys. Chem. A* **2003**, *107* (19), 3970–3980. <https://doi.org/10.1021/jp034225i>
- Brabec, C. J.; Cravino, A.; Meissner, D.; Sariciftci, N. S.; Fromherz, T.; Rispen, M. T.; Sanchez, L.; Hummelen, J. C. Origin of the Open Circuit Voltage of Plastic Solar Cells. *Adv. Funct. Mater.* **2001**, *11* (5), 374–380. <https://doi.org/10.1002/1616-3028>
- Burke, K.; Perdew, J. P.; Levy, M. Improving energies by using exact electron densities. *Phys. Rev. A* **1996**, *53* (5), R2915. <https://doi.org/10.1103/PhysRevA.53.R2915>
- Camara, M. A. Modélisation du stockage de l'énergie photovoltaïque par supercondensateurs. Ph.D. Thesis, University of Paris-Est, France, 2011. <https://tel.archives-ouvertes.fr/tel-00673218/> (accessed 2022-04-20)
- Cheung, D. L.; Troisi, A. Theoretical Study of the Organic Photovoltaic Electron Acceptor PCBM: Morphology, Electronic Structure, and Charge Localization. *J. Phys. Chem. C* **2010**, *114* (48), 20479–20488. <https://doi.org/10.1021/jp1049167>
- Dufil, Y. Monocouches auto-assemblées et nanostructures de métaux nobles: Préparation et application au photovoltaïque. Ph.D. Dissertation, Queen's University and University of Aix-Marseille, 2018.
- Frisch, M. J.; Pople, J. A.; Binkley, J. S. Self-consistent molecular orbital methods 25. Supplementary functions for Gaussian basis sets. *J. Chem. Phys.* **1984**, *80* (7), 3265. <https://doi.org/10.1063/1.447079>
- Green, M. A.; Emery, K.; King, D. L.; Igari, S.; Warta, W. SHORT COMMUNICATION: Solar cell efficiency tables (version 25). *Prog. Photovol.* **2005**, *13* (1), 49–54. <https://doi.org/10.1002/pip.598>
- Günes, S.; Neugebauer, H.; Sariciftci, N. S. Conjugated Polymer-Based Organic Solar Cells. *Chem. Rev.* **2007**, *107* (4), 1324–1338. <https://doi.org/10.1021/cr050149z>
- Huixia, X.; Fang, W.; Kexiang, W.; Peng, S.; Jie, L.; Tingting, Y.; Hua, W.; Bingshe, X. Two novel bipolar Ir (III) complexes based on 9-(4-(pyridin-2-yl) phenyl)-9H-carbazole and N-heterocyclic ligand. *Dyes Pigm.* **2017**, *146*, 316–322. <https://doi.org/10.1016/j.dyepig.2017.07.012>
- Jabha, M.; Abdelah, A. Study Optoelectronic and Geometric Properties of New compounds Based on Carbazole-thiophene Bridged for Solar Cells. *Orbital: Electron. J. Chem.* **2018**, *10* (7), 552–560. <https://doi.org/10.17807/orbital.v10i7.1322>
- Jabha, M.; El Alaoui, A.; Jarid, A.; Mabrouk, E. H. The Effect of Substitution and Polymerization of 2, 7-Divinylcarbazole-benzo-bis-thiadiazole on Optoelectronic Properties: A DFT Study. *Orbital: Electron. J. Chem.* **2021**, *13* (4), 291–300. <https://doi.org/10.17807/orbital.v13i4.1580>
- Jabha, M.; El Alaoui, A.; Jarid, A.; Mabrouk, E. H. Theoretically studying the optoelectronic properties of oligomers based on 2,7-divinyl-cabazole. *Eclét. Quim. J.* **2022**, *47* (1), 40–54. <https://doi.org/10.26850/1678-4618eqj.v47.1.2022.p40-54>
- Khoudir, A.; Maruani, J.; Tronc, M. SCF, CI and DFT Charge Transfers and XPS Chemical Shifts in Fluorinated Compounds. In *Quantum Systems in Chemistry and Physics*; Hernández-Laguna, A., Maruani, J., McWeeny, R., Wilson, S., Eds., Vol. 2; Springer, 2000; pp 57–89. https://doi.org/10.1007/0-306-48145-6_5
- Koh, S. E.; Risko, C.; Silva Filho, D. A.; Kwon, O.; Facchetti, A.; Brédas, J.-L.; Marks, T. J.; Ratner, M. A. Modeling Electron and Hole Transport in Fluoroarene-Oligothiophene Semiconductors: Investigation of Geometric and Electronic

- Structure Properties. *Adv. Funct. Mater.* **2008**, *18* (2), 332–340. <https://doi.org/10.1002/adfm.200700713>
- Leclerc, N.; Michaud, A.; Sirois, K.; Morin, J.-F.; Leclerc, M. Synthesis of 2,7-Carbazolenevinylene-Based Copolymers and Characterization of Their Photovoltaic Properties. *Adv. Funct. Mater.* **2006**, *16* (13), 1694–1704. <https://doi.org/10.1002/adfm.200600171>
- Liu, X.; Rand, B. P.; Forrest, S. R. Engineering Charge-Transfer States for Efficient, Low-Energy-Loss Organic Photovoltaics. *Trends Chem.* **2019**, *1* (9), 815–829. <https://doi.org/10.1016/j.trechm.2019.08.001>
- Marcus, R. A. Relation between charge transfer absorption and fluorescence spectra and the inverted region. *J. Phys. Chem.* **1989**, *93* (8), 3078–3086. <https://doi.org/10.1021/j100345a040>
- Muth, M.-A.; Mitchell, W.; Tierney, S.; Lada, T. A.; Xue, X.; Richter, H.; Carrasco-Orozco, M.; Thelakkat, M. Influence of charge carrier mobility and morphology on solar cell parameters in devices of mono-and bis-fullerene adducts. *J. Nanotechnol.* **2013**, *24* (48), 484001. <https://doi.org/10.1088/0957-4484/24/48/484001>
- Ochterski, J. W.; Petersson, G. A.; Montgomery Junior, J. A. A complete basis set model chemistry. V. Extensions to six or more heavy atoms. *J. Chem. Phys.* **1996**, *104* (7), 2598. <https://doi.org/10.1063/1.470985>
- Oukachmih, M. *Université Toulouse-Paul Sabatier, France*. 2003. (Doctoral Theses).
- Petersson, G. A.; Al-Laham, M. A. A complete basis set model chemistry. II. Open-shell systems and the total energies of the first-row atoms. *J. Chem. Phys.* **1991**, *94* (9), 6081. <https://doi.org/10.1063/1.460447>
- Provencher, F. Dynamique de séparation de charges à l'hétérojonction de semi-conducteurs organiques. Ph.D. Thesis, University of Montreal, 2014. <http://hdl.handle.net/1866/10654> (accessed 2022-02-24)
- Rassolov, V. A.; Ratner, M. A.; Pople, J. A.; Redfern, P. C.; Curtiss, L. A. 6-31G* basis set for third-row atoms. *J. Comput. Chem.* **2001**, *22* (9), 976–984. <https://doi.org/10.1002/jcc.1058>
- Rodríguez-Monge, L.; Larsson, S. Conductivity in polyacetylene. I. *Ab initio* calculation of charge localization, bond distances, and reorganization energy in model molecules. *J. Chem. Phys.* **1995**, *102* (18), 7106. <https://doi.org/10.1063/1.469104>
- Schwenn, P. E.; Burn, P. L.; Powell, B. J. Calculation of solid state molecular ionisation energies and electron affinities for organic semiconductors. *Org. Electron.* **2011**, *12* (2), 394–403. <https://doi.org/10.1016/j.orgel.2010.11.025>
- Sun, F.; Jin, R. DFT and TD-DFT study on the optical and electronic properties of derivatives of 1, 4-bis (2-substituted-1, 3, 4-oxadiazole) benzene. *Arab. J. Chem.* 2017, *10* (Suppl. 2), S2988–S2993. <https://doi.org/10.1016/j.arabjc.2013.11.037>